GAMMA - GAMMA COINCIDENCE AND DIRECTIONAL CORRELATION STUDIES

A Dissertation

Presented to

the Faculty of the Graduate School

University of Manitoba

In Partial Fulfilment

of the Requirements for the Degree

Doctor of Philosophy

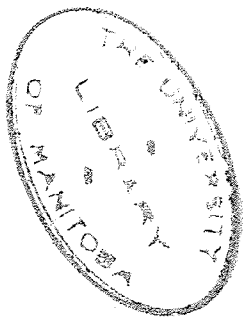

by

H.W. Taylor

September, 1954.

TABLE OF CONTENTS

LIST OF PLATES AND FIGURES

PLATES

FIGURES

ABSTRACT

A coincidence spectrometer suitable for directional correlation measurements has been used to investigate the decay schemes of several radioisotopes. High energy selectivity was secured through the use of two differential discriminators and conventional scintillation counters. The resolving time of the coincidence stage was about 1.1×10^{-7} seconds.

Reports of additional positron and gamma ray components accompanying the decay of Zn^{65} have been discounted by coincidence experiments carried out with the above spectrometer. Instrumental effects have been shown to give rise to asymmetrical time resolution curves.

The directional correlation between the two strong lines in the gamma ray spectrum of Se^{75} has been studied. The observed correlation is consistent with the spin assignment 5/2 (99.12% M1; .88% E2) 7/2 (E2) 3/2 for the levels concerned, if it is assumed that an interfering cascade is weak. Possible re-interpretations of the present data will have to await more accurate intensity measurements for the transitions involved.

The gamma ray spectrum of Sb^{124} was investigated, using a single channel spectrometer. Two new gamma rays with energies of 965 and 1365 kev were found during the course of the investigation. It was confirmed that the 1690 and 2090 kev gamma radiations were in coincidence with the 600 kev transition. The directional correlation of the 1690 - 600 kev cascade was studied and found to be consistent with a spin sequence 3 (D) 2 (E2) 0 for the levels concerned. The E1 assignment for the first transition, which has appeared in the literature, was discussed.

The directional correlation of the combined 67 - 1122 kev and 67 - 1222 kev cascades in W^{182} has been investigated. The results were discussed in the light of two independent spin assignments which have appeared in the literature. The results obtained favor one of these assignments slightly, but they are not conclusive.

Spins have been assigned to five states of the Pt^{192} level scheme on the basis of directional correlation studies undertaken with the 468 - 316 kev and 308 - 296 - 316 kev cascades. The net spin assignment 4 - 4 - 2 - 2 - 0 seems to be consistent with all the known details of the decay scheme of Ir^{192}. The expected correlation function for the triple gamma ray cascade was calculated and found to agree with experiment if the $2 \rightarrow 2$ (296 kev) transition is a 2.5% M1 - 97.5% E2 multipole mixture.

CHAPTER I.

THEORETICAL CONSIDERATIONS

a) Introduction

One of the principal aims of modern experimental nuclear physics is to supply a foundation of measurement upon which a theory of nuclear forces may be erected. To this end, a variety of techniques have been developed to determine the properties of nuclear energy levels. One of the most recent of these is the study of the angular correlation between particles or gamma rays emitted in cascade by an excited nucleus. Theoretical considerations show that when two radiations are emitted in this way, the directions of emission are not oriented randomly but are spatially correlated. Furthermore, the character of this correlation is determined solely by the spins or the spin-parity assignments of the nuclear states involved in the emission process. It is apparent, then, that by a careful study of the spatial correlation between nuclear radiations, one can learn something about the spins and parities of nuclear energy levels. Of course, this is not the only technique by which they may be determined. The shape of a β-ray spectrum, or the conversion coefficient of a gamma ray may yield the same information. It has been found, however, that angular correlation studies lead to less ambiguous results than either of the above techniques. This is particularly evident for gamma ray transitions involving mixed multipolarities. In this case the observed conversion coefficient will have a value lying somewhere between the theoretical values corresponding to pure multipole transitions. The relative intensities of the two types of radiation present in the transition cannot be unambiguously determined from these data. However, the angular correlation between this mixed radiation and some other radiation associated with it, might well be

expected to yield the mixing ratios with a fair degree of accuracy. This will be demonstrated in later sections of this thesis.

As mentioned above, the angular correlation between nuclear radiations is determined by the spins and parities of the nuclear states concerned. It is important to distinguish between two kinds of angular correlation experiment, however. Suppose, for example, we consider a simple two-component gamma ray cascade. If the spatial correlation between the two radiations is measured, a "directional" correlation experiment has been performed. On the other hand, if the polarization of one of the radiations is measured also, then a "polarization-direction" experiment has been performed. The former is dependent only on the spins of the nuclear levels, while the latter determines the relative parities of nuclear states. Hence it has become customary to refer to an experiment as a directional correlation investigation if the detectors are polarization insensitive, and as a polarization-direction experiment if the detectors are polarization sensitive. The term 'angular correlation' embraces both cases. This terminology will be used throughout the remainder of this treatise.

The purpose of the present work is to present gamma-gamma directional correlation and coincidence data for several selected radioisotopes. Since the experiments have been restricted to the study of radiative transitions, theoretical discussions will not be presented in their most general form, but rather in that form which pertains to radiative processes only. Before proceeding with this discussion, however, a brief outline of the history of the phenomenon will be given. This will be followed by the theoretical aspects of the subject mentioned above,

and an outline of the coincidence technique, errors, angular corrections, etc. A discussion of the apparatus, and the experimental results will be reserved for Chapters II and III respectively. A brief summary in Chapter IV will complete the work.

b) Historical Note

The theory of the angular correlation of nuclear radiations is one of the better developed physical theories. However, until recently, the experimental techniques had lagged behind their theoretical counterpart to a considerable extent. This was due to 1) a lack of sensitive detection equipment and 2) an unawareness of the care with which correlation measurements should be made. The first defect has been overcome by the wide use of scintillation spectrometers; the second deficiency still persists to some extent, although in recent months it has become evident from the literature on the subject that more attention is now being paid to the collection and correction of experimental data. However, much of the early work must now be regarded as ambiguous due to faulty technique. Some examples of this will be discussed in the later sections of this thesis. They will indicate clearly how much progress has been made in the last year or two.

Prior to 1940 there existed neither experimental evidence of, nor theoretical reason to expect, a spatial correlation between nuclear radiations emitted in cascade. In the subsequent thirteen years, however, the theoretical aspects of the subject have been developed to a high degree of perfection. The first substantial contribution in this regard came in 1940 when Hamilton (1) presented a theoretical paper on the

gamma-gamma directional correlation. In the same year, Dunworth (2) mentioned the possibility of directional experiments in his classic paper on coincidence techniques. After a lapse of some six years, a generalization of Hamilton's results was given by Goertzel (3) who, in discussing the effect of a magnetic field on a directional correlation, laid the foundation for the group-theoretic methods currently in vogue. The next important steps on the experimental scene were taken in 1942-43 by Kikuchi et al., and Beringer (4). Of the isotopes studied by these authors, only one - Cl^{38} - gave a result which indicated the existence of a directional correlation. For the others, any existing correlation was smaller in magnitude than the experimental errors. In 1947-48, however, Brady and Deutsch (5), using Geiger counters, finally confirmed the theoretical predictions for Co^{60}, Sc^{46}, Y^{86}, Cs^{134}, Na^{24} and Rh^{106}. In 1950, these authors (6) repeated their experiments using the newly-developed scintillation counters. Once again, the results were in good agreement with theory and the way was at last opened to the securing of reliable data. By this time, largely through the efforts of Racah, Lloyd, Falkoff and others, the theoretical aspects of the subject were finally consolidated using the techniques of group theory. In 1953, Biedenharn and Rose (7) published a long review article on the mathematical formulation, which was intended to be a source book for the experimentalist. On the experimental side, however, the picture was less promising. In the same year, the interpretation of the gamma-gamma directional correlation in Ni^{60} was again in doubt, and had to be settled once for all by an excellent experiment performed by Klema and McGowan (8) at Oak Ridge. Since the Ni^{60} cascade was the best known and most extensively studied gamma-ray cascade as far as correlation measurements were concerned, it

was apparent, prior to Klema's paper, that the experimentalists had a long way to go to equal the accomplishments of the theorists. At the present time the experimental picture is considerably brighter, however. The quality of the work done in the last year indicates that substantial progress has been made toward attaining the precision necessary for the elucidation of complex decay schemes.

Although brief, the above outline of the historical development of the subject should give the reader some perspective on the subject as a whole; that, at least, was its intention. Several of the remarks made regarding the inaccuracy of early experiments will come up for further elaboration in later sections. We shall now consider the theory proper.

c) The Method of D. R. Hamilton (1)

Before proceeding with the formulation due to Hamilton, it will be profitable to consider in qualitative terms why there should be a directional correlation between nuclear radiations. In addition, a tabulation of the characteristics of nuclear radiative transitions will be given.

Consider a large number of nuclei, all of which are in the same state. This state is characterized by a total angular momentum j, whose component along a reference axis is m. All the nuclei are eventually to undergo radiative transitions to a final state with arbitrary spin. Due to the $(2j + 1)$-fold degeneracy of the initial state, there will be a set of substates characterized by values of m. Since each substate is associated with the same energy, and if there are no external magnetic or electric fields present, then the substates will be equally populated. If transitions occur from the state j, the radiation from the ensemble will be isotropic,

since, although the radiation from a single transition is emitted anisotropically, the equal population of the substates leads to a net intensity independent of angle. If there is a magnetic field present, however, the degeneracy is removed (Zeeman effect) and the m substates in the ensemble become populated according to the Boltzmann distribution law. When transitions occur, the net effect is an anisotropy with respect to the magnetic field axis, since the substates are now unequally populated.

In the case of a coincidence measurement involving two correlated gamma rays, the selection of a definite direction in space by means of one detector means that only a particular set of transitions from the substates can be studied, viz. those whose emission directions pass through the detector. The situation is similar to that with the magnetic field mentioned above. In the coincidence experiment, the selection of a particular direction introduces an anisotropy into space, which prevents the substates from contributing equally to the radiation field detected experimentally, even though the substates are equally populated. Thus the Zeeman effect is strongly analogous to the directional correlation phenomenon.

The presentation of the above analogy is intended to give the reader an intuitive feeling for the phenomenon. This is most desirable. A purely mathematical argument is often less satisfying to the experimentalist, who invariably thinks in terms of a model. We pass now to a brief review of the selection rules for radiative processes in general.

When a nuclear state undergoes a radiative transition, the total

angular momentum (referred to as 'spin' hereinafter; denoted by $\underline{j}$) and the parity (π) of the resultant state are in general different from those of the former. Mathematical analysis of the expression for the transition probability indicates that both magnetic and electric multipole radiations may occur; the order of the multipole being determined by the spin change, and the character of the radiation by the parity change. The multipole order and parity of the radiations are not completely independent, as will be seen later.

If $\underline{j}_i$ and $\underline{j}_f$ are the spin vectors of the initial and final states respectively, and if the gamma ray carries away $\underline{L}$ units of angular momentum, the following selection rules can be shown to hold (9):

$$|j_i - j_f| \leq L \leq j_i + j_f$$

$$\pi_i = \pi_f \quad \text{for even parity radiation}$$

$$\pi_i = -\pi_f \quad \text{for odd parity radiation.}$$

where $|\underline{j}_i| = \hbar\sqrt{j_i(j_i + 1)}$ etc. and the transition $j_i = 0 \rightarrow j_f = 0$ is absolutely forbidden. The lowest order of multipole radiation consistent with these selection rules has been assumed for the transition. The following table summarizes the results in a convenient form.

Lowest Order of Multipole Radiation in a Transition j_i, π_i to j_f, π_f.

a) $j_i \neq j_f$

	Electric (E) radiation	Magnetic (M) radiation
Parity favored, $\pi_i \pi_f = (-1)^{j_i - j_f}$	$L = \lvert j_i - j_f \rvert$	$L = \lvert j_i - j_f \rvert + 1$ except $j_i = j_f = 0$
Parity unfavored, $\pi_i \pi_f = (-1)^{j_i - j_f + 1}$	$L = \lvert j_i - j_f \rvert + 1$ except j_i or $j_f = 0$	$L = \lvert j_i - j_f \rvert$

b) $j_i = j_f \neq 0$

$\pi_i = \pi_f$	$L = 2$ except $j_i = j_f = 1/2$	$L = 1$
$\pi_i = -\pi_f$	$L = 1$	$L = 2$ except $j_i = j_f = 1/2$

Since frequent use will be made of this table in discussing experimental results, it was felt necessary to reproduce it here. A full discussion of radiative processes cannot be given, however. For further details, the reader is referred to reference (9). We now proceed with the discussion of the main topic of this section.

Hamilton's approach to the correlation problem involves the standard techniques of time-dependent perturbation theory. The clarity of his calculations permits the experimentalist to follow the arguments without the necessity of first reading extensively of the literature on group theory. For this reason alone, it will be profitable to present Hamilton's arguments here. Following that, a summary of the results obtainable using group-theoretic methods will be given.

Throughout this thesis, the following notation will be used:

j_1, j, and j_2 are the angular momentum quantum numbers corresponding to nuclear states A, B and C respectively; m_1, m and m_2 are the quantum numbers for the z-components of $\underline{j}_1$, $\underline{j}$ and $\underline{j}_2$. The states A, B and C will describe not only the nucleus but the radiation field as well. When the nucleus is coupled to the field, a radiative transition is assumed to occur yielding a photon of a given type. The further coupling of the resultant nuclear state to the radiation field then results in another transition and the appearance of a photon of a second given type. In the final state C, the nucleus and the radiation field are assumed to be decoupled.

In carrying out his calculations, Hamilton assumes that
a) the intermediate state is unperturbed by external influences,
b) the substates of A and C are uniformly populated,
c) the emitted gamma radiations have pure multipolarities, and that
d) the detection equipment is to be polarization insensitive.
With the exception of the 'postulate of purity', these conditions are usually fulfilled in a normal case. However, for a triple gamma ray cascade, (b) does not hold since the sublevels of the second state are populated according to the transition probabilities for the different components of the first gamma ray.

Hamilton starts his solution by writing down the differential equations for the probability amplitudes of the three states A, B and C. He assumes a series solution for each amplitude and by direct substitution finds those series parameters which are consistent with the initial equations. The matrix elements for the entire process are then written down formally, and expressed in terms of the above parameters. The probability of the de-excitation of the nucleus through radiative transitions yielding two photons is written as

$$W(\underline{k}'_o\ \underline{e}'\ ,\ \underline{k}''_o\ \underline{e}'') = \sum_{m_2\ \underline{e}'\underline{e}''} \left\langle |C_{m_2}|^2 \right\rangle_{av} \qquad (1)$$

where C_{m_2} is the probability amplitude corresponding to state C, $\underline{k}'_o$ $\underline{k}''_o$ are propagation vectors for the first and second photons respectively, and $\underline{e}'$, $\underline{e}''$ are their corresponding polarization vectors. The summation extends over all the final magnetic substates and polarization directions. By using the definition of C_{m_2} as given by Hamilton, equation (1) can be rewritten in the form:

$$W = \sum_{m_1 m_2 \underline{e}'\underline{e}''} \left| \sum_m (A_{m_1} | H(\underline{k}'_o\ \underline{e}') | B_m)^* (B_m | H(\underline{k}''_o\ \underline{e}'') | C_{m_2})^* \right|^2 \qquad (2)$$

where H is the interaction term in the Hamiltonian operator, and the brackets (| |) are matrix elements describing transitions between adjacent states. It is apparent from equation (2) that the summation over m produces a number of interference terms, i.e. terms which contain a product of two matrix elements, each of which refers to a different transition. These interference terms can be removed by taking the direction of emission of the first gamma ray along the z-axis. Hamilton proves this as a theorem, the statement of which is: If the z-axis of quantization is along the emission direction of the first gamma ray, the probability of the double transition is given by the product of the probabilities of the separate single transitions. The reader is referred to Hamilton's paper (1) for the mathematical proof. Lippman (10) has given the following qualitative proof: The interference terms arising in a transition involving an intermediate state are due to a lack of information concerning that state. If, however, the first gamma ray moves along the z-axis, then its z-component of angular momentum can be measured without disturbing the system. Since the initial state is known in detail, it is possible to determine the pertinent characteristics of the intermediate state, and hence, for this case, no interference can occur.

Making use of this theorem, W can be written as:

$$W = \sum_{\substack{m_1 m\, m_2 \\ \underline{e}'\underline{e}''}} \left|(A_{m_1} \mid H(0) \mid B_m)\right|^2 \left|(B_m \mid H(\theta) \mid C_{m_2})\right|^2 \qquad (3)$$

where $\underline{k}_o'$ has been taken along the z-axis and θ is the angle between this axis and $\underline{k}_o''$. Thus any angular dependence in W comes from the matrix element for the second transition. It is convenient to define

$$P_{m_1 m}(0) = \sum_{\underline{e}'} \left|(A_{m_1} \mid H(0) \mid B_m)\right|^2$$

and

$$P_{m\, m_2}(\theta) = \sum_{\underline{e}''} \left|(B_m \mid H(\theta) \mid C_{m_2})\right|^2$$

then W becomes

$$W = \sum_{m_1 m\, m_2} P_{m_1 m}(0)\; P_{m\, m_2}(\theta) \qquad (4)$$

The P's are the probabilities for the transitions concerned. It can be shown (1) that

$$P_{m\, m_2}(\theta) = C(j\, L_2 j_2;\; m\; m_2 - m)\; F^M_{L_2} \quad , \; etc.$$

where $\underline{L}_1$, $\underline{L}_2$ are the angular momenta for the first and second photons respectively, $M = m_2 - m$, and the C's are the vector addition coefficients. $F^M_{L_2}$ is a function of (θ) only. The notation for the C's given above is related to that of Condon and Shortley (11) by: $C(a\ b\ c;\ d\ e) \equiv (a\ b\ d\ e \mid a\ b\ c\ d+e)$. The F-function in $P_{m_1 m}(0)$ is unity because we have chosen the z-axis as the direction of emission of the first photon.

Hamilton was able to carry out the summations indicated in equation (4), and tabulate the following results:

second transition dipole: $$W(\theta) = 1 + \frac{R'}{Q'} \cos^2 \theta \qquad (5)$$

second transition quadrupole: $$W(\theta) = 1 + \frac{R}{Q} \cos^2 \theta + \frac{S}{Q} \cos^4 \theta \qquad (6)$$

(Since only the dependence of W on θ is important for a directional correlation measurement, several common factors have been dropped from (5) and (6) in order to reduce them to simple forms.) In subsequent

sections the coefficients R/Q and S/Q will be denoted by a_2 and a_4 respectively. They were tabulated by Hamilton in his original paper (1) as functions of j .

It turns out that the summations carried out by Hamilton cannot be extended to multipoles of order higher than quadrupole if the form of equation (6) is taken as the correlation function. The summations involve products of vector addition coefficients, however, which play an important role in group theory as applied to physical problems. Thus it is natural to expect that a group-theoretic formalism will yield equivalent results, and this has indeed been found to be the case.

d) The Results of Group-Theoretic Analysis of the Directional Correlation of Associated Gamma Rays.

i) Double Correlation Formulae

It can be shown (7) that if the expansion of $W(\theta)$ is carried out in terms of Legendre polynomials of even order, the generalization to higher multipolarities follows immediately. The maximum order, k_m, of the polynomials involved is determined by the inequality $k_m \leqslant$ lowest multipole order of the radiations concerned. Furthermore, the case of mixed radiative transitions can be handled with the same formalism. These statements are given without proof. The reader is once again referred to the review article by Biedenharn and Rose (7) for the details.

Using the same notation as before, $W(\theta)$, as determined by the more general technique mentioned above, can be written (7) as:

$$W(\theta) = (j_1|L_1|j)^2 W_I + (j_1|L_1'|j)^2 W_{II} + 2(j_1|L_1|j)(j_1|L_1'|j) W_{III} \quad (7)$$

This equation is the most general form of the directional correlation function for an unpolarized two-component gamma ray cascade and involves

what we shall refer to as "quadratic" multipole mixing. It has been assumed that the first radiation is a mixture of 2^{L_1} and $2^{L_1'}$-pole radiations, and that the second radiation is pure 2^{L_2}-pole. Obviously there is no loss in generality involved in this assumption. For completeness, the W_I, W_{II} and W_{III} are tabulated below.

$$W_I = (2L_1+1)(2L_2+1) \sum_{k \geq 0} C(L_1 L_1 k;\ 1\ -1)\ C\ (L_2 L_2 k;\ 1\ -1)$$
$$\times\ W(jjL_1L_2;\ kj_1)\ W(jjL_2L_2\ ;\ kj_2\ )\ P_k\ (\cos\theta) \qquad (8)$$

$$W_{II} = (2L_1'+1)(2L_2+1) \sum_{k \geq 0} C(L_1' L_1' k\ ;\ 1\ -1)\ C\ (L_2 L_2 k\ ;\ 1\ -1)$$
$$\times\ W(jjL_1'L_2\ ;kj_1)\ W(jjL_2L_2\ ;\ kj_2\ )\ P_k\ (\cos\theta) \qquad (9)$$

$$W_{III} = \sqrt{(2L_1+1)(2L_1'+1)}(2L_2+1) \sum_{k \geq 2} C(L_1 L_1' k;\ 1\ -1)\ C\ (L_2 L_2 k\ ;\ 1\ -1)$$
$$\times\ W(jjL_1L_1'\ ;\ kj_1)\ W(jjL_2L_2\ ;\ kj_2\ )\ P_k\ (\cos\theta) \qquad (10)$$

k is an even integer in all the summations. The C's are the vector addition coefficients, the W(a b c d ; e f) the Racah coefficients. (The latter have been tabulated by Biedenharn et al (12).) The $(j_1 \| L_1 \| j)$ etc. are the matrix elements of the transitions concerned, and the P_k are the Legendre polynomials.

From a consideration of the transition probabilities for electric and magnetic radiations (9), it can be shown that any multipole-mixing will involve 2^{L_1}- and 2^{L_1+1}-pole radiations, i.e. M1 and E2, M2 and E3, etc. Assuming this to be the case, and normalizing the coefficient of W_I in equation (7) to unity we get

$$W(\theta) = W_I + \delta^2 W_{II} + 2\delta W_{III} \qquad (11)$$

where $$\delta^2 = \frac{(j_1 \| L_1+1 \| j)^2}{(j_1 \| L_1 \| j)^2} \qquad (12)$$

is the 2^{L_1+1}- to 2^{L_1}-pole intensity ratio for the mixed transition. By convention, it is assumed that if δ is positive the phase angle between the radiations is zero; if δ is negative, the phase angle is 180°.

If the first transition involves only pure radiation, the correlation function $W(\theta)$ is just W_I. Thus

$$W(\theta) = W_I = \sum_k A_k P_k(\cos\theta) \qquad (13)$$

The coefficients A_k are evaluated by means of tables in a practical case. There are at present three independent sets of these, which can be used by research workers. They are equivalent to some extent but important differences exist between them. We shall tabulate the principal results for each set below and illustrate their range of applicability. This will be done under author headings.

a) Biedenharn and Rose (7)

For a pure-multipole cascade, we had

$$W_I(\theta) = \sum_{k \geqslant 0} A_k P_k(\cos\theta) \qquad (13)$$

where

$$A_k = F_k(L_1 j_1 j) \cdot F_k(L_2 j_2 j) ,$$

$$F_k(a\ b\ c) = (-1)^{b-c-1} \sqrt{2c+1}\ (2a+1)\ C(a\ a\ k;\ 1\ -1)\ W(c\ c\ a\ a;\ k\ b), \qquad (14)$$

and $F_o = 0$. The coefficients F_k have been tabulated for $a = 1,2,3,4$ and all necessary values of k, and for $b = 0, 1, 2, 3, 4$ and $c \leqslant 5$ in integral steps. Values for all half-integer values of b in the range 1/2 to 13/2, and $c \leqslant 13/2$ are also available.

For mixed radiations, W_I and W_{II} are defined as in equation (13) but W_{III} is given by

$$W_{III}(\theta) = (-1)^{j-j_1-1} \sqrt{(2j+1)(2L_1+1)(2L_1'+1)} \sum_k G_k F_k P_k(\cos\theta) \qquad (15)$$

where $G_k(a\ b\ c\ d) = C(a\ b\ k;\ 1\ -1)\ W(d\ d\ a\ b;\ k\ c)$ (16)

The G_k have also been tabulated for the same range of values mentioned for F_k.

b) Sharp, Kennedy, Sears and Hoyle (13)

Assuming that the first component of the cascade is mixed, Sharp et al write the correlation function $W(\theta)$ as:

$$W(\theta) = \sum_k (-1)^{j_1-j} \left\{ Z_1(L_1 j L_1 j'; j_2 k) + \delta^2 Z_1(L_1' j L_1' j'; j_2 k) + 2\delta Z_1(L_1 j L_1' j'; j_2 k) \right\} \times Z_1(L_2 j L_2 j; j_2 k) P_k(\cos\theta) \quad (17)$$

If the correlation involves pure multipoles only, this equation becomes

$$W(\theta) = \sum_k (-1)^{j_1-j} Z_1(L_1 j L_1 j; j_1 k) Z_1(L_2 j L_2 j; j_2 k) P_k(\cos\theta) \quad (18)$$

The primed L and j in equation (17) take account of the different multipolarity of the second component of the mixed transition. $W(\theta)$ is not normalized in either of these equations. To carry this out (i.e. to get $A_o = 1$) one must divide the terms for $k \geqslant 2$ by the term for $k = 0$. The Z_1 coefficients are defined in reference (13) and tabulated values of Z_1^2 given. These tables are quite extensive and will be mentioned again in connection with triple correlation functions.

c) Lloyd (14)

Lloyd has introduced the idea of the basic correlation. If $W(\theta)$ is written in the normalized form

$$W(\theta) = 1 + \sum_k A_k^{(b)} P_k(\cos\theta) \quad (19)$$

then this is a basic correlation function if either of the following spin assignments yields equation (19):

$$j - L_1(L_1)\, j\, (L_2)\, j + L_2 \quad \underline{\text{or}} \quad j + L_1(L_1)\, j\, (L_2)\, j - L_2 .$$

The $A_k^{(b)}$ are given by

$$A_k^{(b)} = (2k+1)\, b_k(L_1)\, b_k(L_2)$$

where $b_k(L) = \left[1 - \frac{k(k+1)}{2L(L+1)}\right] \frac{(2L+1)!\, k!\, (L+\frac{k}{2})!}{(2L+k+1)! \left[(\frac{k}{2})!\right]^2 (L-\frac{k}{2})!}$

For non-basic correlations, the coefficients A_k are obtained from the equation $A_k = \upsilon_k A_k^{(b)}$ where the υ_k are the 'attenuation' factors. Of course, the correlation for $j_2(L_2)\, j\, (L_1)\, j_1$ is the same as for

$j_1(L_1)\ j\ (L_2)\ j_2$. In the tabulating of the A_k and $A_k^{(b)}$, Lloyd has assumed that the multipolarities of the emitted radiations are the minima permitted by the selection rules given on Page 8. The reader is referred to Lloyd's paper (14) for the form of the ν_k.

In the case of multipole mixing, this author has given the form of $W(\theta)$ when "linear" multipole mixing is present, i.e. when δ is small enough so that δ^2 can be neglected. We get then

$$W(\theta) = 1 + \sum_k A_k P_k(\cos\theta) + x\delta \sum_k y_k(L_1) A_k P_k(\cos\theta) \qquad (21)$$

As usual the mixing has been assumed to occur in the first transition. δ is defined as the ratio of the electric 2^{L+1} intensity to the magnetic 2^L intensity in a given parity forbidden transition. The factors x and $y_k(L_1)$ have been given in closed form (14).

Lloyd's numerical tables are more convenient than those due to Sharp and Biedenharn, because no computation has to be done to arrive at the correlation coefficients. This is particularly useful when the correlation coefficients have been determined experimentally and a spin assignment has to be found. On the other hand, Lloyd's tables cannot be used directly for quadratic mixing of radiations, which occurs when δ^2 is comparable in magnitude to δ.

Mention should be made concerning the interrelations among the three formulations mentioned above. The $(Z_1)^2$ coefficients have been tabulated extensively by Sharp et al. It is not difficult to show that the A_k of Lloyd's paper are simply of the form

$$\left(\frac{Z_1^2\ (L_1 j L_1' j';\ j_1 k)\ Z_1^2\ (L_2 j L_2' j';\ j_2 k)}{Z_1^2\ (L_1 j L_1' j';\ j_1 o)\ Z_1^2\ (L_2 j L_2' j';\ j_2 0)} \right)^{1/2}$$

for pure transitions. The coefficients F_k and G_k (7) are related to

the Z_l coefficients by

$$F_k\,(Lj_1j) = (-1)^{j_1 - j - \frac{k}{2}}\,(2j+1)^{1/2}\,Z_l\,(LjLj;\ j_1k) \qquad (22)$$

$$G_k\,(LL'j_1j) = (-1)^{L+L'+\frac{k}{2}}\,(2j+1)^{-1}(2L+1)^{-1/2}\,Z_l(LjL'j;\ j_1k)\,(2L'+1)^{-1/2} \qquad (23)$$

In spite of these interrelations, the author has found that no single set of tables of correlation coefficients is completely satisfactory; each set has its limitations. Lloyd's tables are suitable for quick identification of spin assignments in double correlations, but they are limited to linear mixing, and have no value in triple correlation calculations. Biedenharn's tables can be used for all double correlations and both types of mixing, but some numerical work must be done before the coefficients are obtained. The coefficients for triple correlations are limited to the case where the intermediate transition is not observed. The tabulation by Sharp et al is excellent from the point of view of scope. Coefficients for all double and triple correlations can be calculated using these tables, but a fair amount of numerical work must be done. In the case of triple correlations, the computation becomes exceedingly arduous. The author has found it necessary to use all the tabulations mentioned here in the analysis of experimental data. For that reason, the formalism for each has been set down in some detail, as an aid to those who are faced with similar tasks.

Before passing to a discussion of triple correlations, we shall record without derivation the transformations which enable one to express the coefficients a_k of the Hamilton formalism in terms of the A_k of the group-theoretic formalism, and vice versa. The correlation function can be expressed in either of the equivalent forms

$$\begin{aligned} W(\theta) &= Q + R\ \cos^2\theta + S\cos^4\theta \\ &= A_0' + A_2'\ P_2\,(\cos\theta) + A_4'\ P_4\,(\cos\theta) \end{aligned} \qquad (24)$$

The coefficients are then related by the equations:

$$A_o' = Q + \frac{1}{3} R + \frac{1}{5} S \quad ; \quad A_2' = \frac{2}{3} R + \frac{4}{7} S \quad ; \quad A_4' = \frac{8}{35} S \qquad (25)$$

$$Q = A_o' - \frac{1}{2} A_2' + \frac{3}{8} A_4' \quad ; \quad R = \frac{3}{2} A_2' - \frac{30}{8} A_4' \quad ; \quad S = \frac{35}{8} A_4' \qquad (26)$$

and, of course, $a_2 = R/Q$; $a_4 = S/Q$

and $A_2 = \frac{A_2'}{A_o'}$; $A_4 = \frac{A_4'}{A_o'}$.

Both sets of coefficients are used in analysing the results of an experiment -- the a's for graphical analysis, and the A's for numerical analysis.

ii) Triple Correlation Formulae

Biedenharn et al. (7) have outlined a few special cases of the triple correlation problem but their work is rather limited, as was mentioned above. On the other hand, Sharp et al (13) have presented the complete formalism. Their results will be tabulated here - again without proof.

A triple gamma ray cascade can be displayed in schematic form as below

$$j_o \xrightarrow{L_1} j_1 \xrightarrow{L_{12}\ \pi_{12}} j_2 \xrightarrow{L_2} j_3$$

where the j's are the spins of the nuclear states, the L's are angular momenta of the radiations, and π_{12} is the parity of the intermediate state (π_{12} = 0 for electric radiation, = 1 for magnetic radiation). If $\theta_1\ \phi_1$, $\theta_{12}\ \phi_{12}$, and $\theta_2\ \phi_2$ are the angles between the reference axes and the three emission directions, then the directional correlation function $W(\theta_1\ \theta_{12}\ \theta_2)$ is given by:

$$W(\theta_1\theta_{12}\theta_2) = 2\sum_{k_1k_{12}k_2} (-1)^{j_0+j_3+L_1+L_1'+L_{12}+L_{12}'+L_2+L_2'+j_1+j_2}$$

$$\times Z_1(L_1 j_1 L_1' j_1'; j_0 k_1)\, G_1\begin{pmatrix} j_1 L_{12} j_2 \\ k_1 k_{12} k_2 \\ j_1' L_{12}' j_2' \end{pmatrix} \times Z_1(L_2 j_2 L_2' j_2'; j_3 k_2)\, \Lambda_{k_1k_2k_{12}} \tag{27}$$

where

$$G_1\begin{pmatrix} j_1 L_{12} j_2 \\ k_1 k_{12} k_2 \\ j_1' L_{12}' j_2' \end{pmatrix} = \text{Real part of } \Big\{ (i)^{-L_{12}+\pi_{12}-L_{12}'-\pi_{12}'-k_1-k_2+2} \times (2L_{12}+1)^{1/2}(2L_{12}'+1)^{1/2}(2k_1+1)^{1/2}(2k_2+1)^{1/2}$$

$$\times (L_{12}L_{12}'\,-1,\,1 \mid k_{12}\,0)\, X\begin{pmatrix} j_1 L_{12} j_2 \\ k_1 k_{12} k_2 \\ j_1' L_{12}' j_2' \end{pmatrix} \Big\} \tag{28}$$

$$\text{and } \Lambda_{k_1k_2k_{12}} = \sum_{\mu_1\mu_2} (k_1k_2\mu_1\mu_2 \mid k_{12}\,\mu_1+\mu_2)\left[\frac{(4\pi)^3}{(2k_1+1)(2k_2+1)(2k_{12}+1)}\right]^{1/2}$$

$$\times Y_{k_1}^{\mu_1}(\theta_1\phi_1) \cdot Y_{k_2}^{\mu_2}(\theta_2\phi_2) \cdot Y_{k_{12}}^{\mu_1+\mu_2\,*}(\theta_{12}\phi_{12}) \tag{29}$$

The Y_k^{μ} are the usual normalized spherical harmonics:

$$Y_L^M(\theta\,\phi) = (-1)^{\frac{1}{2}(M+|M|)}\sqrt{\frac{(L-|M|)!}{(L+|M|)!}}\; e^{iM\phi}\sqrt{\frac{2L+1}{4\pi}}\; P_L^{|M|}(\cos\theta).$$

We have used Sharp's notation for the vector addition coefficients because they are tabulated in his report using this form. It is apparent, however, that $(k_1k_2\mu_1\mu_2 \mid k_{12}\,\mu_1+\mu_2) \equiv C(k_1k_2k_{12};\mu_2\mu_1)$. If the radiations are pure, the primed indices can be replaced by unprimed ones as in the case of equation (17). From the form of equation (27) it is obvious that the first and third components of the cascade are described by the Z_1 coefficients, while the intermediate transition is characterized by the G_1 coefficient (i.e. by the X coefficient).

The above equations are simplified to a considerable extent if two of the radiations are parallel and their emission direction is taken to be the z axis. For definiteness, we shall assume the first two gamma

rays are parallel; then

$$\theta_1 = \theta_{12} = 0 \qquad Y_{k_1}^{\mu_1}(\theta_1\phi_1) = Y_{k_{12}}^{\mu_1+\mu_2}(\theta_{12}\phi_{12}) = 1 \text{ and } \theta_2 = \theta,\ \phi_2 = 0.$$

Equation (29) becomes, with these substitutions

$$\Lambda_{k_1 k_2 k_{12}} = (k_1 k_2 0\ 0 \mid k_{12}\ 0)\ P_{k_2}(\cos\theta) \tag{30}$$

The limitations on k_2 are 1) that it be an even integer and 2) that its maximum value k_m be determined by the equality

$$k_m = 2 \text{ min.} \left\{ \min \left[(L_1, j_1) + L_{12} \right],\ j_2,\ L_2 \right\} \tag{31}$$

It can be shown that the values of k_2 must be consistent with the definition of the X coefficients. The latter satisfy the following conditions:

1) the parameters of each row (each column) must sum to an integer,
2) the sum of any two parameters of a row (column) must be greater than or equal to the third parameter,
3) if two rows (columns) are equal, the third must have an even integral sum.

A special case of the triple correlation arises when the intermediate transition (no matter what its nature) is unobserved. This case will be of particular interest in later sections of this thesis. If the intermediate transition only involves mixed multipoles, then the form of the first-third correlation function is given by

$$W = W(L_{12}) + \delta^2\ W(L'_{12}) \tag{31a}$$

where L_{12} and L'_{12} are the multipole orders of the radiations concerned, and δ^2 is the ratio of the intensity of L'_{12} radiation to L_{12} radiation, and

$$W(L_{12}) = \sum_k (-1)^{j_o+j_3-L_{12}+j_2-j_2'+L_2+L_2'}$$

$$Z_1 (L_1 j_1 L_1 j_1,\ j_o k)\ W (j_1 j_2 j_1' j_2' L_{12} k)\ Z_1 (L_2 j_2 L_2 j_2,\ j_3 k)$$

$$\times\ P_k (\cos\theta) \qquad (31b)$$

It is interesting to note that interfering multipoles of the intermediate transition make no contribution to the correlation since they are not observed (13).

The coefficients $(L_{12} L_{12}' - 1\ \ 1 \mid k_{12}\ 0)^2$, X^2, Z_1^2 and W^2 have been tabulated in the report by Sharp. These tables greatly facilitate the evaluation of both first-third and triple correlations.

In the preceding section (d) those mathematical results have been tabulated which are necessary for the analysis of both double and triple correlation data. The three tabulations which are available have been discussed briefly; results have been quoted only in so far as they are necessary for the use of the tabulations of coefficients. The interrelations between the different sets of tables have been indicated, as

have the limitations of each. The author has found that the equations given above are sufficient for the needs of the experimentalist; no apology is made for the pragmatic nature of this review nor for the lack of mathematical justification for the formulae quoted. This task lies in the province of the theorist. The reader is referred to the admirable review article of Biedenharn and Rose (7) for further details on the theoretical aspects of the subject.

e) The Coincidence Technique; Errors

Dunworth (2) pointed out in 1940, in a valuable review article, how coincidence measurements could be used to elucidate nuclear level schemes. The scintillation counter has been largely responsible for the precision of the technique at the present time. Only through this precision has it been possible to perform directional correlation experiments which yield unambiguous results. Since correlation investigations involve basic coincidence techniques, a brief review of the essential features of the latter will be given here.

Consider a radioactive source which is decaying by particle emission followed by a simple two component gamma ray cascade. The decay scheme is being studied by means of two scintillation counters which feed a coincidence mixer. One counter detects the first gamma ray only, and the other the second gamma ray. If the single counting rates of the first and second counters are N_1 and N_2 respectively, then the 'accidental' coincidence rate N_{12} is given by

$$N_{12} = 2\tau N_1 N_2 \qquad (32)$$

where τ is the resolving time of the coincidence mixer. (The above result is readily obtained from a simple statistical study of the single

counting rates of the two counters.) The genuine coincidence rate N' is given by the formula

$$N' = N \omega_1 \omega_2 \epsilon_1 \epsilon_2 \qquad (33)$$

where N is the number of disintegrations per unit time leading to the gamma ray cascade, ω_1, ω_2 are the solid angles subtended at the source by the first and second counters respectively and $\epsilon_1 \epsilon_2$ are the corresponding detection efficiencies.

The solid angles and detection efficiencies can be determined either by measurement or calculation, whereas τ is determined entirely by measurement as will be discussed later. With a complex decay scheme, the value of N must be determined with some care, for it will vary for a given source depending on what part of the decay scheme is under observation. For this reason, it is customary to refer to N as the effective source strength for an experiment.

Equations (32) and (33) are the basic results quoted by Dunworth.

As with any counting rate determination, a coincidence measurement possesses an intrinsic statistical error. However, the statistics of counting experiments cannot be discussed at length here. For an elementary discussion of the subject the reader is referred to standard textbooks (15); a more advanced exposition has been published by the Atomic Energy Commission (16). The problems encountered in this regard have also been reviewed by Chatterjee and Saha (17), whose paper contains, in addition, a discussion of angular resolution corrections, which forms the subject of the following section.

f) Angular Resolution Corrections

Consider a point source mounted equidistant from, and along the axes of two scintillation counters, one of which is free to rotate in the plane of the source and the two counters. The source-to-crystal distance is a few centimetres and the crystals are right circular cylinders. The source is assumed to emit two gamma rays which are correlated spatially. It is desired to study this directional correlation. If each counter detects a gamma ray of one energy only, the coincidence rate as a function of the angle between the counter axes will give the desired correlation function. Since the counters are not point-detectors but subtend a finite solid angle at the source, the variation in the coincidence rate with angle will be masked to some extent. The resulting correlation function will exhibit a smaller asymmetry than would be realized with point-detectors. In order to obtain the true correlation function from the observed one, a correction factor must be applied to the experimental data to compensate for the effect of the finite solid angles.

Several authors have discussed the problem outlined above but in the experimental work to be described later only the results of Church and Kraushaar (18) and Lawson and Frauenfelder (19) have been used; they will be outlined in some detail. Calculations have also been carried out by Rose (20), Chatterjee and Saha (17) and Breitenberger (21), but their results were either not applicable to the present apparatus, or not in a convenient mathematical form.

Consider the directional correlation function $W(\theta)$ to be expanded in a series of Legendre polynomials:

$$W(\theta) = \sum_k A_{2k} \; P_{2k} (\cos \theta) \qquad (34)$$

where $k = 0, 1, 2$, etc. Church et al (18) define the resolution curve $f(\alpha)$

as the spectrum of coincidences between annihilation-radiation quanta expressed as a function of the angle α between the counters. If $f(\alpha)$ be written in the form

$$f(\alpha) = \sum_{k'} \left(\frac{2k' + 1}{4}\right) Q_{2k'} P_{2k'} (\cos \alpha) \qquad (35)$$

then it can be shown (18) that the observed correlation function is given by

$$W(\theta) = \sum_{k} A'_{2k} P_{2k} (\cos \theta) \qquad (36)$$

where $A'_{2k} = Q_{2k} A_{2k}$

and $$Q_{2k} = \int f(\cos \alpha) P_{2k} (\cos \alpha) \, d(\cos \alpha) \qquad (37)$$

For $f(\alpha)$ a Gaussian distribution, the correction factors Q_{2k} can be expressed as series in ascending powers of α_o - the half-width at half height of the resolution curve $f(\alpha)$. (α_o is expressed in degrees.) The numerical results are given below:

$$\begin{aligned} Q_o &= 1 - 7.325 \times 10^{-5} \alpha_o^2 + \ldots\ldots \\ Q_2 &= 1 - 7.325 \times 10^{-4} \alpha_o^2 + 2.930 \times 10^{-7} \alpha_o^4 + \ldots\ldots \qquad (38) \\ Q_4 &= 1 - 2.271 \times 10^{-3} \alpha_o^2 + 2.659 \times 10^{-6} \alpha_o^4 - 2.133 \times 10^{-9} \alpha_o^6 + \ldots \end{aligned}$$

It should be noted that if A_{2k} is normalized to unity, the corrections are applied to A_{2k} for $k > 0$ only; they are then of the form Q_{2k}/Q_o.

Although it might appear obvious to the reader at this stage, the dependence of the angular resolution curve on energy was not fully appreciated by experimentalists until recently. Lawson and Frauenfelder (19) in 1953 observed that some of the discrepancies in the early experimental work might be due to the use of correction terms (equation (38)) which were suitable only for gamma rays of 510 kev energy. Consequently, they re-examined the entire problem as given below.

If θ' is the angle between the counter axes, then once again the observed correlation function can be written as

$$W(\theta') = \sum_{k \geq 0} Q_{2k} A_{2k} P_{2k} (\cos \theta') = \sum_{k \geq 0} A'_{2k} P_{2k} (\cos \theta')$$

If A_o is normalized to unity then $A_{2k} = \frac{Q_o}{Q_{2k}} A'_{2k}$. In this formulation, however, the correction factors must be obtained from a different type of angular resolution curve. These curves are determined by sweeping each counter separately across a highly collimated beam of the gamma-radiation to be studied. (If this is not appropriate, gamma radiation having an energy close to the radiation in the experiment may be used.) The practical details of the technique need not concern us at this point; they will be outlined in detail later.

Using superscipts I and II to denote the first and second counters respectively, the Q_{2k} are defined by

$$Q_{2k} = \tfrac{1}{2} \left[J^{I}_{2k}(\gamma_1)\, J^{II}_{2k}(\gamma_2) + J^{I}_{2k}(\gamma_2)\, J^{II}_{2k}(\gamma_1) \right] \qquad (39)$$

provided that the gamma rays have essentially different energies and each counter detects both. If the experiment is so arranged that each counter detects a gamma ray of one energy only, equation (39) simplifies to

$$Q_{2k} = J^{I}_{2k}(\gamma_1)\, J^{II}_{2k}(\gamma_2) \qquad k = 0,1,2.... \qquad (40)$$

In the last two equations the J's are given by:

$$J_{2k} = \int \epsilon(\alpha)\, P_{2k}(\cos\alpha)\, |\sin\alpha|\, d\alpha \qquad k = 0,1,2.... \qquad (41)$$

where $\epsilon(\alpha)$ is the angular resolution curve for the counter concerned and α is the angle between the counter axis and the gamma ray beam. The above integrals must be evaluated numerically from the resolution curves obtained in the laboratory, and the appropriate Q's calculated.

In practice it turns out that the angular resolution corrections are the most important corrections to be applied to the experimental data. It is particularly important to recognize the dependence of $\epsilon(\alpha)$ on energy and the need to use the correction factors appropriate to the radiations being studied.

g) Least Squares Analysis of the Data

The 'raw' experimental data from correlation measurements are usually analysed by the method of least squares, in order to determine the correlation coefficients A_{2k} and the shape of the correlation function. The use of least squares fitting is standard practice in the physical sciences and will not be discussed here. Of the many treatises on the subject, the author found the treatment given by Sokolnikoff (22) to be both lucid and to the point.

One cannot stress too strongly the necessity for careful numerical analysis of correlation data when determining the correlation coefficients. Only in this way can correlation functions be expected to yield results of physical significance.

h) Time Resolution Measurements

In the study of one of the isotopes investigated in the present work, it was necessary to perform several time resolution (delayed coincidence) experiments. Consequently it was felt that a brief explanation of the technique in general terms was desirable at this stage of the thesis.

Suppose we have a two-counter coincidence system with the facility that pulses from one counter may be delayed by an arbitrary time interval before entering the mixing stage of the coincidence unit. This time interval is referred to as the delay; it is usually limited to the range 0 $\rightarrow$ a few microseconds. If a single nuclear radiation (either a particle or a gamma ray) traverses both counters, the resulting time resolution curve (coincidence rate vs. artificial delay) can be

shown to be Gaussian in shape (23, 24). Now suppose it is necessary to find the time resolution curve for two distinct coincident radiations which are emitted in cascade by a given nucleus. This problem has been investigated mathematically by Bay (25) and Newton (26), who conclude that the 'long-delay' tail of the resolution curve will no longer have a Gaussian shape but rather that of a pure exponential. If the coincidence rate vs. delay curve is plotted on semi-logarithmic paper, this portion will appear as a straight line whose slope gives a measure of the half-life of the intermediate state between the two emissions. In practice, however, this asymmetry is present only if the lifetime of the state is greater than τ (see equation (32)). If this condition is not met, the mean life of the state may be determined from the shift in the centroid of the resolution curve -- now symmetric -- when compared to a prompt resolution curve (25,26). (A prompt curve is one obtained from a cascade whose intermediate state has a lifetime very much shorter than τ .)

The above techniques have been used with success by many workers in the study of isomeric states. In this regard the reader is referred to an excellent experimental paper by Graham and Bell (27).

CHAPTER II

THE APPARATUS

a) General Description

The coincidence scintillation spectrometer is rapidly becoming standard equipment in the nuclear physics laboratory. In spite of its rather poor energy resolution, its high degree of versatility makes it an important tool in the study of nuclear level schemes. In this chapter the coincidence spectrometer used in the present investigations will be described. Circuit diagrams of the component parts of the device will be omitted since they have been presented elsewhere (28). However, brief mention will be made of the mode of functioning of the differential discriminators.

In Plate I, the complete spectrometer is illustrated, while a close-up of the detectors and their associated amplifiers is given in Plate II. The units in the former illustration are the following. To the left are the scintillation counters; they are mounted on aluminum brackets which are fastened to the bench of an ordinary optical spectroscope. The graduated circle on the bench permits the determination of the position of the movable counter to the nearest 0.5 degree. (See Plate II). To the right of the counters are the pulse amplifiers and their power supplies. The latter supply plate and filament voltage to the amplifiers and to the cathode followers, which are mounted at the bases of the photomultiplier tubes. The table rack contains two single-channel differential discriminators and a single power supply. The floor rack supports the following units: at the bottom, the stabilized high voltage power supply for the photomultiplier tubes; second from the bottom, the Harwell-type 1036A coincidence unit; at the center, two Atomic Instrument scalers; at the top, a series of precision potentiometer

PLATE I.

The Coincidence Spectrometer. See P. 28 for identification of the units shown.

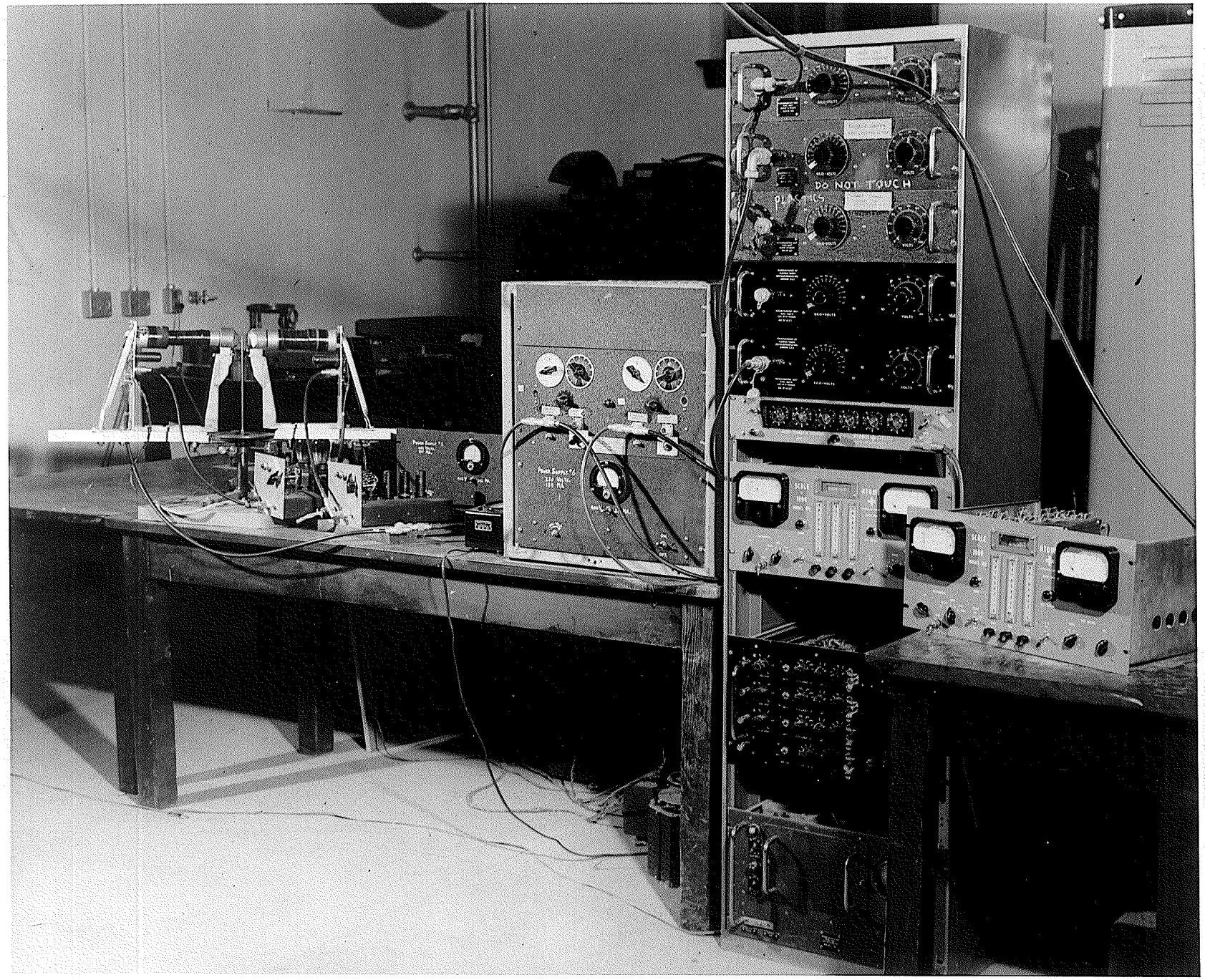
DO NOT TOUCH

PLATE II.

Close-up of the scintillation counters, the spectrometer bench and the pulse amplifiers.

PLATE III.

The detectors: The photomultiplier tube on the left is the Dumont 6292 mentioned in the text. Below it is one of the conical lead shields. At the bottom, a 1" cylindrical packaged crystal is shown on the left, and an aluminum cap on the right. The Dumont K 1185 photomultiplier is exhibited also, together with its supporting bracket and cathode follower. The lead shield in this case has been removed from the aluminum cap.

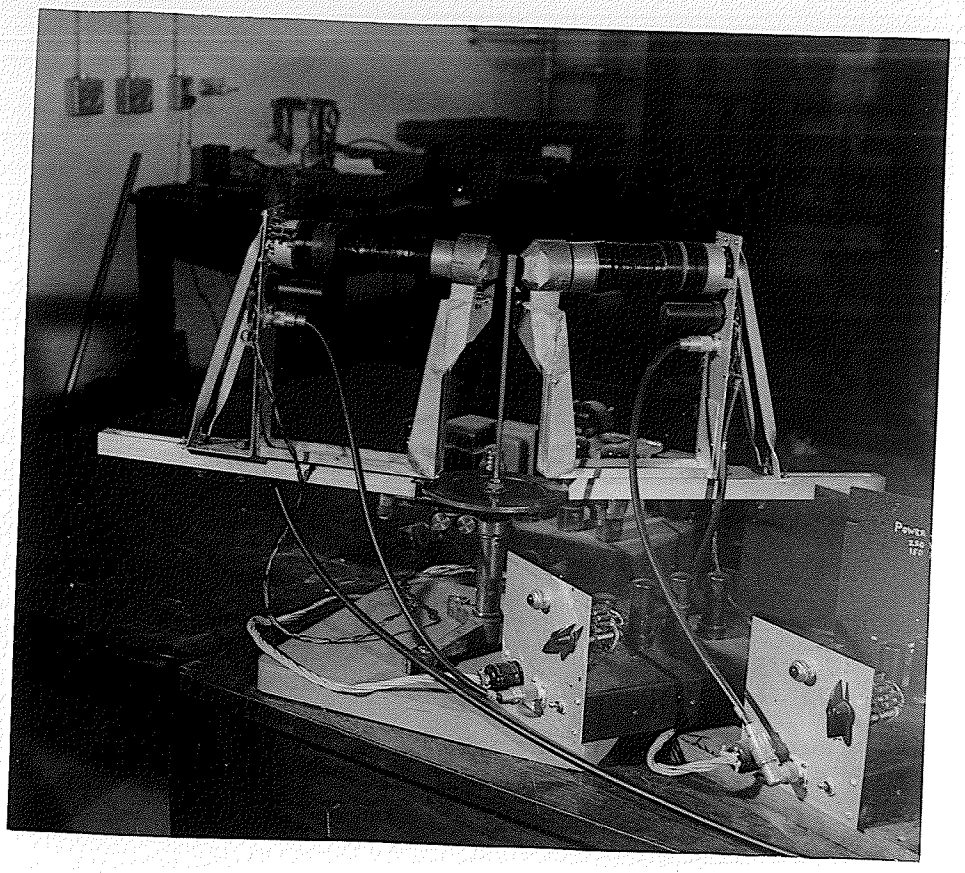

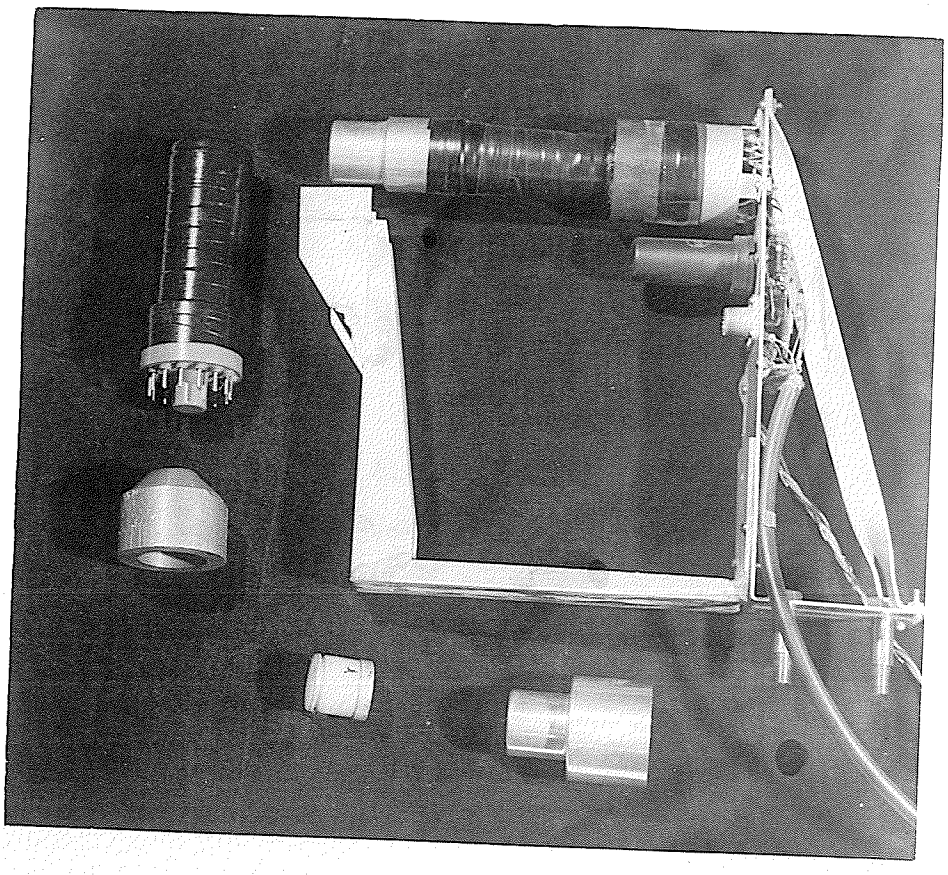

boxes, one of which was used to distribute high voltage to the photomultiplier tubes. The Atomic Instrument scaler on the table on the right completes the apparatus.

The functioning of the spectrometer can best be understood from a consideration of the block diagram of Fig. 1. For definiteness let us consider a source which emits two gamma rays in a simple cascade. The quanta coming from the source excite the sodium iodide phosphors which are mounted on the windows of the photomultiplier tubes. The light emitted by the phosphors upon de-excitation is converted into voltage pulses by the photomultipliers. The pulses are then transmitted to the pulse amplifiers by cathode followers (C.F.). These amplified signals are fed into differential discriminators, each of which can be set to accept only those pulses which lie in the voltage range V to $V + dV$, where dV is the gate width. (If the pulse height corresponding to a given gamma ray energy is known, it is obvious that the discriminators can be set to accept pulses due to gamma rays of a predetermined energy.) The fixed amplitude output pulses of the discriminators are fed into a coincidence mixer. If the pulses coming from the two counters are associated in time, the coincidence mixer delivers a fixed amplitude pulse for each coincidence detected. These are recorded by a scaler as shown. The numbers of pulses having the predetermined sizes coming from the two counters are recorded by means of two additional scalers which are fed by the discriminators. The spectrometer thus permits the simultaneous determination of the coincidence counting rate and the single counting rate from each discriminator. If τ is known, equation (32) permits an estimate of the accidental rate to be made; subtraction of the accidental rate from the measured coincidence rate gives the number of genuine coincidences per unit time.

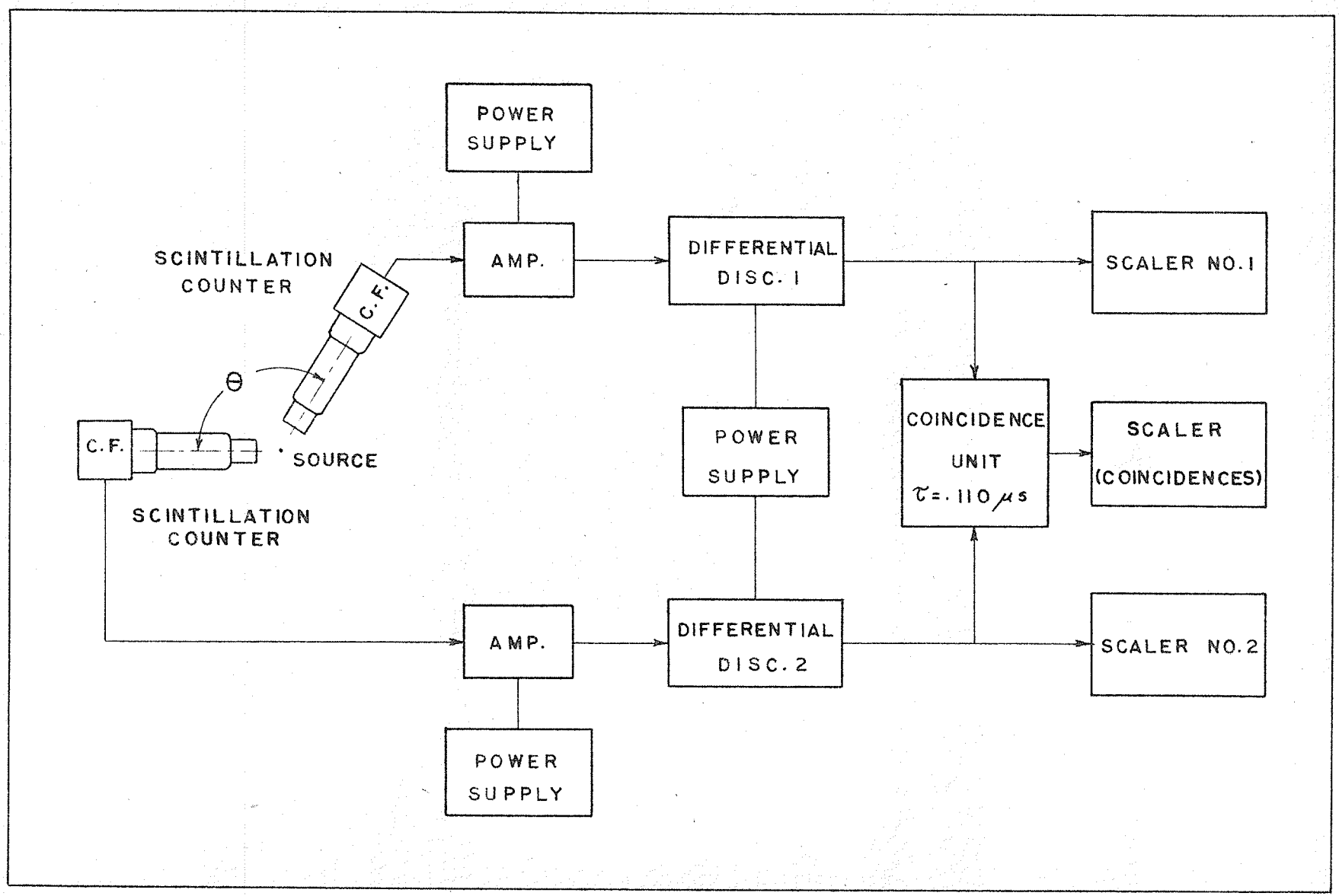

Fig. 1. Schematic diagram of the coincidence spectrometer. The high voltage power supply for the photomultipliers is not shown.

The various parts of the spectrometer will now be considered individually.

b) The Detectors

The components of the two scintillation counters used are shown in Plate III. The caption identifies each part. The photomultipliers used were a Dumont 6292 (2" photocathode) and a Dumont K 1185 ($1\frac{1}{2}$" photocathode). The glass portions of the tubes, with the exception of the end 'windows', were covered in black electrical tape in order to eliminate the necessity for having light-tight containers for the tubes. The aluminum spinnings shown in Plate III fitted snugly over both the crystals and end windows of the tubes. When taped in position, they provided excellent light-tight covering for the light sensitive portions of the photomultipliers.

The crystals, obtained from the Harshaw Chemical Co. and mounted by them, were 1" x 1" right circular cylinders of thallium-activated sodium iodide (NaI-Tl). The crystal containers were made of thin aluminum. The gaps between the crystals and the containers were filled with magnesium oxide which acted as a diffuse reflector. Glass end windows completed the mounts. Small springs were inserted in the closed ends of the spinnings, against which the metal ends of the crystal mountings butted. These springs kept the crystals firmly in place against the photomultiplier windows. Heavy Dow Corning silicone grease (60,000 c. s.) was used as an optical bond between the crystals and the windows. With the arrangement described above, it was found that both counters maintained a constant performance over a period of approximately eight months.

The photomultipliers were mounted on aluminum brackets (see Plate II) which were free to move along the aluminum arms attached to the spectrometer bench. The 6AG7 pentodes which served as cathode followers were also mounted on these brackets. The cathode follower and photomultiplier circuitry was identical with that due to Roulston (28) except for a change in the size of dynode resistors from 10 megohms to 680 K. An additional support was fastened to each bracket to bear the lead shields which were placed around the crystal for the correlation experiments. These supports were made removable in order that the counters might also be used for ordinary coincidence studies. The shielding for each crystal consisted of a lead block which had been recessed to fit snugly over the aluminum spinning. The thickness of lead protecting the 'sides' of the crystal was 0.44 in., the front face was covered by a 0.62 in. thickness of lead through which a tapered hole was cut. The inner end of this hole had a diameter of 0.90 in., the outer end 0.70 in. For correlation studies, 2 mm thick circular lead plates were inserted in the tapered holes to reduce the effects of backscattering from the surrounding equipment.

From the center of the graduated disk of the spectrometer bench there extended vertically a $\frac{1}{4}$" diam. brass rod which supported the sources. Its length was such that when the source was in position, it was just on the horizontal axes of the counters. Each source was mounted in a plastic holder and sealed in with paraffin (see Fig. 7(a)). This arrangement was found to be ideally suited to a speedy interchange of sources.

The negative stabilized high voltage supply used for the

photomultiplier tubes was the A.E.R.E. Model 1007, supplying -2000 volts with a possible variation of $\pm$ 0.1% for a 10% fluctuation in line voltage. Of course, only a portion of the full voltage was applied to the tubes; a precision potentiometer was used for this, as mentioned previously.

Before proceeding with the description of the other parts of the coincidence spectrometer, a few words should be said regarding the detection and effective photo-peak efficiencies of the counters used. If a scintillation spectrometer is to be used to determine gamma ray intensities, the detection and photo-peak efficiencies for the crystal concerned must be known as functions of the gamma ray energy. These are determined solely by the dimensions and linear absorption coefficient of the crystal. The detection efficiency T for a cylindrical crystal, as given by McGowan (29), can be expressed as:

$$T = \frac{\int_o^{\alpha 2} \sin \alpha \left[1 - e^{-\tau x(\alpha)}\right] d\alpha}{\int_o^{\alpha 2} \sin \alpha \cdot d\alpha} \qquad (42)$$

where $x(\alpha) = t \sec \alpha \qquad o \leq \alpha \leq \alpha_1 \left(= \tan^{-1} \frac{r}{h+t} \right)$

$= r \operatorname{cosec} \alpha - h \sec \alpha \;, \alpha_1 \leq \alpha \leq \alpha_2 \left(= \tan^{-1} \frac{r}{h} \right)$

t is the length of the crystal, r its radius, and h the source-to-crystal distance - all in cm. (The source is assumed to be located on the axis of the crystal.) τ is the total linear absorption coefficient for the crystal material. This definition of T assumes that the portion of an incident beam which is absorbed by the crystal is proportional to $1 - e^{-\tau x}$ where x is the distance in cm. travelled in the crystal by the radiation. The correctness of equation (42) has been verified experimentally by Klema and McGowan (30). Unfortunately, lengthy numerical calculations must be carried out before T can be determined

for even one energy. Such calculations constitute, quite properly, the work of a computational laboratory. For this reason an approximation to equation (42) was used here.

The result is due to Maeder et al (31) and is shown in Fig. 2(a) for a 1" x 1" cylindrical NaI-Tl crystal. In this case one considers a beam of gamma rays normally incident on an infinite slab of crystal of constant and finite thickness (this is equivalent to allowing h to approach ∞). The calculations are then carried out without considering the effects of solid angle. In order to test the validity of the approximation, a comparison between the Oak Ridge data (32) and Maeder's result was made for cylindrical $1\frac{1}{2}$" diam. x 1" NaI-Tl crystals. Assuming h = 10 cm., say, the value of T given by equation (42) was found to be 15% lower than that given by Fig. 2(a) for E_γ = 300 kev. Errors of the same order of magnitude were exhibited right out to 1500 kev. However, when the ratio $T_{E'}/T_E$, where E' and E are two different energies, was determined first from equation (42) and then from Fig. 2(a), the two values were found to agree to within 1% over the range 300 - 1500 kev. Since it was necessary in the present experiments to know relative values of T only, it was concluded that Maeder's approximate result could be used for the present investigation. For absolute intensity measurements, however, equation (42) is the more appropriate theoretical form.

Fig. 2(b) shows the effective photo-peak efficiency for a 1" x 1" cylinder of sodium iodide. (The effective photo-peak efficiency for a scintillation counter is defined as the ratio of the number of quanta giving pulses whose amplitudes are proportional to the full gamma ray energy, to the total number of quanta detected by the crystal.)

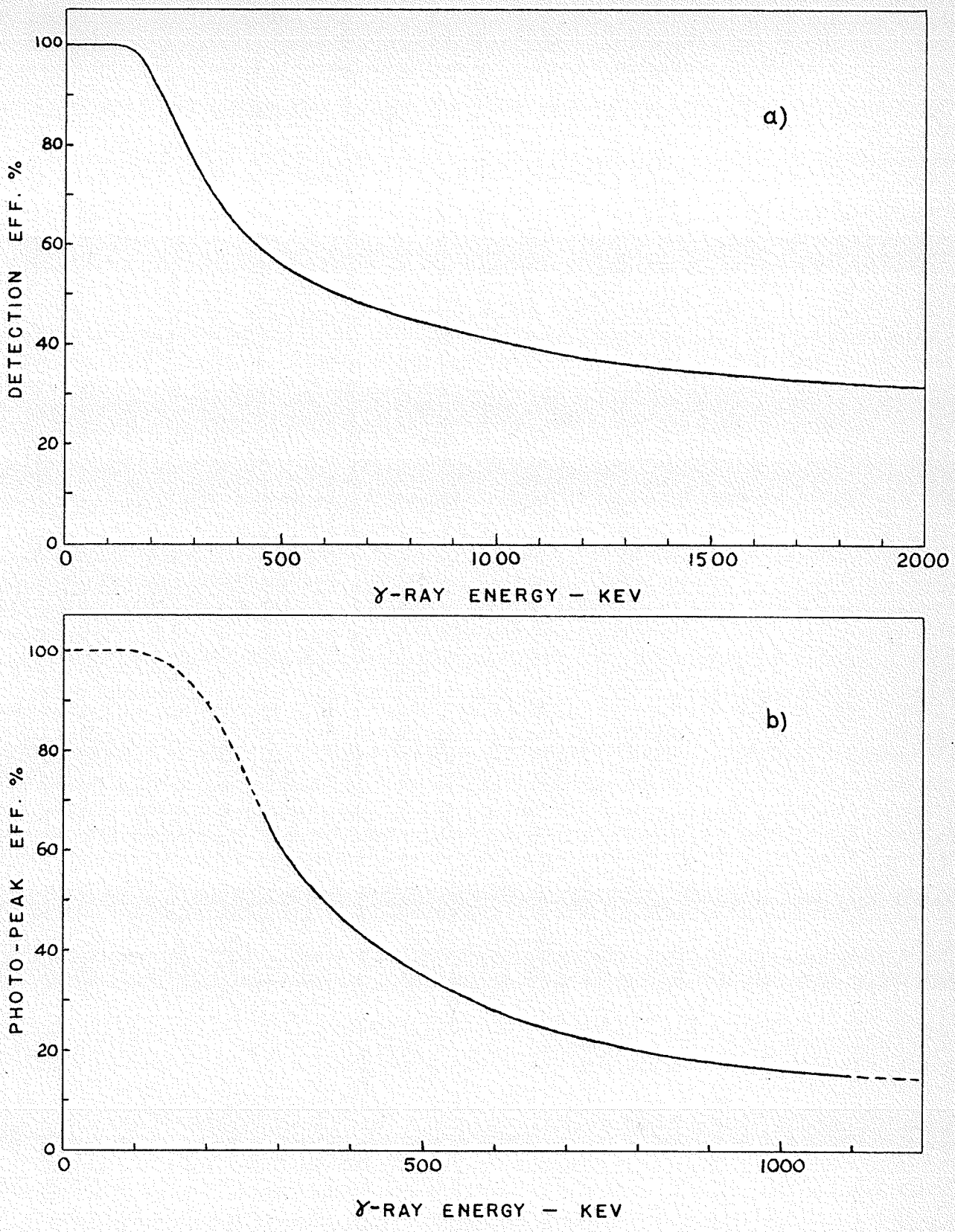

Fig. 2 (a) Detection efficiency as function of gamma ray energy for a 1" cylindrical NaI-Tl crystal.
(b) Effective photo-peak efficiency as function of energy for same crystal size as above.
The dashed sections are theoretical extrapolations of the solid experimental curve.

The solid portion of the curve is an experimental result due to Kreger (33); the points in this region have an estimated accuracy of ± 3%. The dashed portions of the curve represent an attempt by the author to extrapolate into the low and high energy regions. Theoretical curves given by Maeder (31) were used for this. The results are believed to be as accurate as the experimental portion of the curve.

As mentioned above, Figs. 2(a) and (b) permit relative intensity measurements to be made with the scintillation spectrometer. For such measurements, of course, it is necessary to have the spectrum of the gamma radiation concerned. This is most accurately determined by the use of a differential discriminator. Several examples of such measurements will be given in later sections of this thesis.

c) Pulse Amplifiers

The amplifiers used in the coincidence spectrometer were patterned after the Atomic Amplifier Model 204-C. Two extra stages of gain contained in the 204-C were omitted, resulting in an overall gain of about 80 times. The circuit diagram of the amplifiers has been given by Roulston (28) and will not be repeated here. The amplifiers were designed to accept either positive or negative pulses, and could deliver an output pulse of up to 40 volts without distortion or overloading.

The power for the amplifiers was supplied by a positive voltage power supply which gave + 250 volts as a plate supply and 6.3 volts A.C. for filaments. The same power supplies were used for the cathode followers and discriminators (28).

d) The Differential Discriminators

The differential discriminators were designed and built in this laboratory (34). Each level of the 'gate' consists of a modified Schmitt trigger circuit followed by pulse shaping circuitry. The pulse from the upper level is inverted by means of a triode and fed onto one end of a precision resistance chain; the uninverted pulse from the lower level is fed onto the other end of the chain. A suitable point near the center of the chain is connected to the grid of a cathode follower. If both levels are triggered by a pulse, cancellation occurs in the chain and no pulse appears at the grid of the cathode follower. On the other hand, if the lower level only is triggered, a positive pulse appears on this grid and is transmitted to the next unit of the spectrometer. Due to imperfect cancellation when both levels are triggered, a residual 5 volt positive pulse is usually present at the output. However, when the lower level only is triggered, the output pulse has an amplitude of about 15 volts, so that discrimination against the 'cancelled' pulses is relatively simple.

In practice, it was found that due to overloading in the photomultipliers, the pulses from the amplifiers had to be kept less than 40 volts in height. The discriminators were thus used over the range 5 - 40 volts only. The width of the gate was found to vary by about 10% over this range. For coincidence measurements this was not important. When intensity measurements were being made, however, the necessary corrections were determined to compensate for this variation.

For details of the circuitry, references (28) and (34) are cited.

e) Coincidence Mixer

Modern coincidence techniques demand coincidence mixers possessing both short resolving times and versatility. Both features are present in the Harwell Type 1036A unit used here. It consists of three identical input trays, each of which contains a discriminator, a paralysis circuit, a variable delay line and a pulse limiter. The fourth tray is a mixing stage which permits the use of the unit either as a double or a triple coincidence mixer; a double coincidence - anticoincidence arrangement is also possible.

The input trays will accept positive pulses from 2 to 50 volts in magnitude. The position of the discrimination level on a tray affects the delay between the time of triggering and the arrival of the pulse at the mixing stage. Thus once the discriminators are set for an experiment, they cannot be altered without affecting the coincidence rate.

The paralysis time of each tray (i.e. the time interval during which the tray is inoperative after passing a pulse) is variable in coarse steps from 5 to 500 microseconds. The smallest value was used in all the experiments to be described. The delay line in each tray gave a variable delay from 0 to 1 microsecond in .05 microsecond steps. This permits one to carry out time resolution experiments in the 10^{-6} - 10^{-7} sec. region.

Nominal resolving times (τ) of .1, .2, .3, .4, .5, 1, 2 and 4 microseconds were available. In practice only the 0.1 μs setting was used. It was found to vary by as much as 25% from day to day but by less than 10% during the course of any single day. The technique used for measuring τ with some precision will be discussed later.

When a pulse from a single tray arrives at the mixing stage, no output pulse is delivered by the unit. When a coincidence occurs between two (or three) trays, the mixer delivers a 15 volt positive pulse which can be used to activate either a scaler or another unit.

f) Scalers

For the determination of the single counting rates of each counter, Atomic Model 1005 scalers were used. They are reasonably fast (dead time $\sim 10\,\mu s$), and were found to be quite adequate for all the counting rates encountered. The coincidence rate, being considerably smaller than either single rate, was recorded by the slower Atomic Glow Transfer scaler. Since both types of scalers are quite standard, we shall omit any discussion of their performances and operation here.

Before terminating this discussion of the spectrometer, the overall stability of the apparatus should be mentioned. Day-to-day drifts were detected throughout the course of the investigations; photoelectron lines were found to change position by as much as 5% during a 24-hour period. It was not possible to isolate the cause of this drifting to any one unit, however. It seemed to be a characteristic of the spectrometer as a whole, due, probably, to the superposition of minor drifts in several units. The installation of a single, central stabilizer for the line voltages employed might well eliminate much of this observed instability, and is recommended by the author for future experiments. Some attention should also be paid to the stabilization of the filament voltages for the various units.

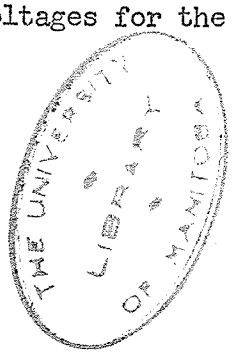

CHAPTER III

EXPERIMENTAL RESULTS

a) Calibration of the Spectrometer

(i) Resolution

When a gamma ray of less than one Mev energy interacts with the atoms of the NaI-Tl crystal in a scintillation counter, it does so by one of two processes:- 1) the photoelectric effect, or 2) the Compton effect. If the phosphor has dimensions several times larger than the range of a one Mev photoelectron in the phosphor, a photoelectric interaction results in a voltage pulse from the counter, with an amplitude proportional to the full energy of the incident gamma ray. A pulse of the same size can result from a Compton interaction also, if both the Compton electron and the scattered quantum are absorbed by the phosphor. If the scattered quantum escapes from the crystal, however, a voltage pulse with amplitude proportional to the energy of the Compton electron results. (At energies greater than one Mev the pair-production process becomes important; this will not be discussed here, however, since the effect was not encountered in the experimental work carried out.) The proportionality between pulse height and gamma ray energy mentioned above is responsible for much of the success of the scintillation counter as a tool in nuclear physics. Without it, the device would lose much of its present convenience.

If a differential discriminator is used to scan the pulses coming from a counter which is excited by monoenergetic gamma rays, the pulse height spectrum (counting rate vs. pulse height) will be found to consist of a sharp photoelectron line located at a certain pulse height, and a broad Compton distribution on the low energy side. The photoelectron line

results from a superposition of pulses arising from primary photoelectric and Compton interactions which result in the liberation of the full energy of the gamma ray in the crystal. The line is Gaussian in shape. This leads to the definition of the energy resolution of the spectrometer at this energy as:

$$\text{Energy Resolution} = \frac{\text{full width at half-height on photoelectron line (volts)}}{\text{pulse height corresponding to center of line (volts)}}$$

Hereinafter, we shall refer to this ratio as simply the "resolution". The dependence of the resolution (R) on gamma ray energy is a result of statistical fluctuations in the number of photoelectrons emitted by the cathode and first few dynodes of the photomultiplier. In practice, one can express R as a function of energy E (in kev) in the form

$$R = \frac{A}{\sqrt{E}} \quad (\%) \qquad (43)$$

where A is a constant. For the statistical arguments leading to equation (43), the reader is referred to textbooks on scintillation counters (35).

A knowledge of R is required if intensity measurements are to be made. The finite width of the discriminator gate results in photoelectron lines which are unduly broad. Since an intensity measurement involves determining the areas of photoelectron lines, corrections must be applied to the lines to compensate for the effect of gate width. If R' is the observed resolution on a line, then R is the limit of R' as the gate width approaches zero.

Pringle, Taylor and Roulston (36) in 1952 gave the resolution vs. energy curve for a scintillation spectrometer employing an EMI 5311 photomultiplier and a sodium iodide crystal. Since that time the resolution

of the spectrometer has been greatly improved through the use of Dumont photomultiplier tubes and commercially-packaged crystals. In view of this, new data were collected using a Dumont 6292 tube and a 1" x 1" NaI-Tl crystal. The gamma rays used for this investigation extended over the range 45 - 2090 kev. In order to correct for the effect of gate width, the following technique was used. A photoelectron line was scanned using $\frac{1}{4}$, $\frac{1}{2}$, 1 and 2 volt gates on the discriminator. The resolution was calculated from the pulse height curves and plotted against the appropriate nominal gate width. The resolution R was then determined by a linear extrapolation of the resulting curves to zero gate width. Figs. 3(a) and (b) illustrate the technique for the 662 kev gamma ray of Cs^{137}. In this case, the line was placed at both 17 and 35 volts. The extrapolated value of R was found to be essentially the same for both runs, as one would expect. The shift in the position of a line as the gate was widened was noted and taken into consideration when estimating R'.

The final results of these measurements are shown in Fig. 3(c). The 'best' straight line through the experimental points has a slope of $-\frac{1}{2}$ as expected and can be represented by the equation: $R = 211/\sqrt{E}$ (%). The gamma rays used are tabulated in the figure. Most of them are mono-energetic; the exceptions usually contain extra radiations which are weaker than the main component and so do not affect the measurements to an appreciable extent. The spectrometer used for these measurements (#2) was found to be superior to the other one with regard to resolution. Consequently it alone was used in all the single counting experiments. It is of interest to note that the resolution at 662 kev (Cs^{137}) - 8.2% is somewhat inferior to a value of about 7.5% which has been obtained in this laboratory with another photomultiplier-crystal combination.

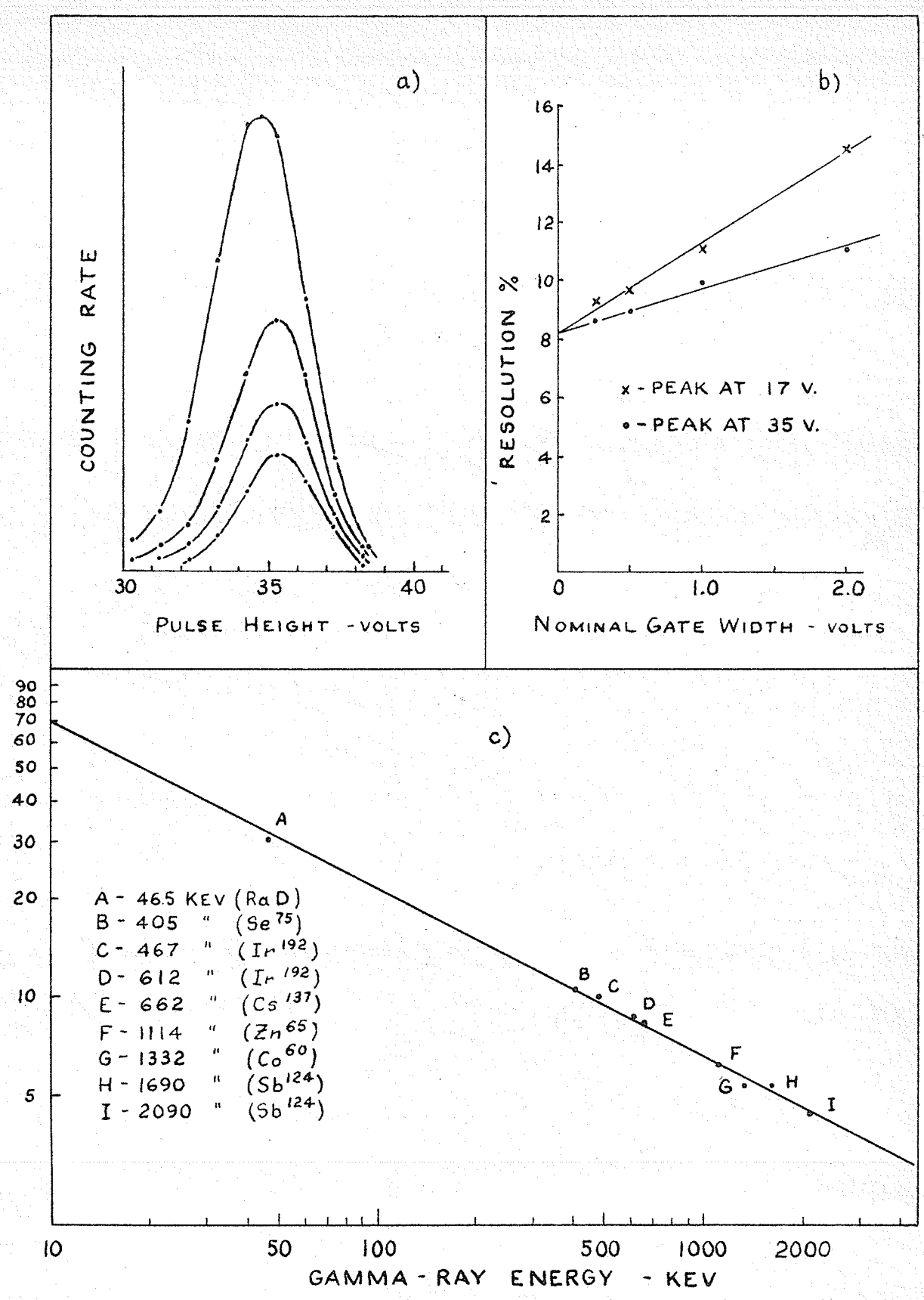

Fig. 3 (a) A set of photoelectron lines for the Cs^{137} gamma ray using gate widths 1/4, 1/2, 1 and 2 volts at 35 volts.
(b) Resolution vs. nominal gate width for Cs^{137} line at 17 and 35 volts.
(c) Resolution vs. energy curve for spectrometer #2.

(ii) Energy Measurements

As mentioned earlier, the NaI-Tl scintillation spectrometer displays a strict proportionality between pulse height and gamma ray energy. Thus if it be desired to determine the energy of a gamma ray, it is only necessary to compare the pulse height corresponding to its photoelectron line with that of a gamma ray of known energy. The method is not too precise, of course; at 662 kev the error might well be as high as ± 5 kev. This is due in part to the error involved in the location of the center of a photoelectron line.

It is desirable, though not necessary, to use monoenergetic gamma rays for the calibration of the pulse height axis in energy units. Two radiations commonly used for this purpose are the 662 kev gamma ray of Cs^{137}, and the 1114 kev gamma ray of Zn^{65}. The spectrum of the former is illustrated in Fig. 4. It was taken with a $\frac{1}{4}$-volt gate. The source was $\sim$ 5 cm. from the crystal and located on the crystal axis. The principal features are the prominent line at 662 kev, the maximum (c) of the Compton distribution and a weak line at 190 kev. This last feature is due to backscattering of the gamma rays of the primary beam. Some of these pass through the crystal and undergo Compton interactions in the tube and tube base. Those interactions which result in a recoil quantum at 180° to the direction of the incident beam, give rise to the photoelectron line at 190 kev. Needless to say, the presence of a backscattered line has led to many misinterpretations of gamma ray spectra.

The 1114 kev line due to the strong gamma ray from Zn^{65} is shown in Fig. 6. However, a discussion of the details of the spectrum will be postponed until the next section, which is concerned with the decay scheme of Zn^{65}.

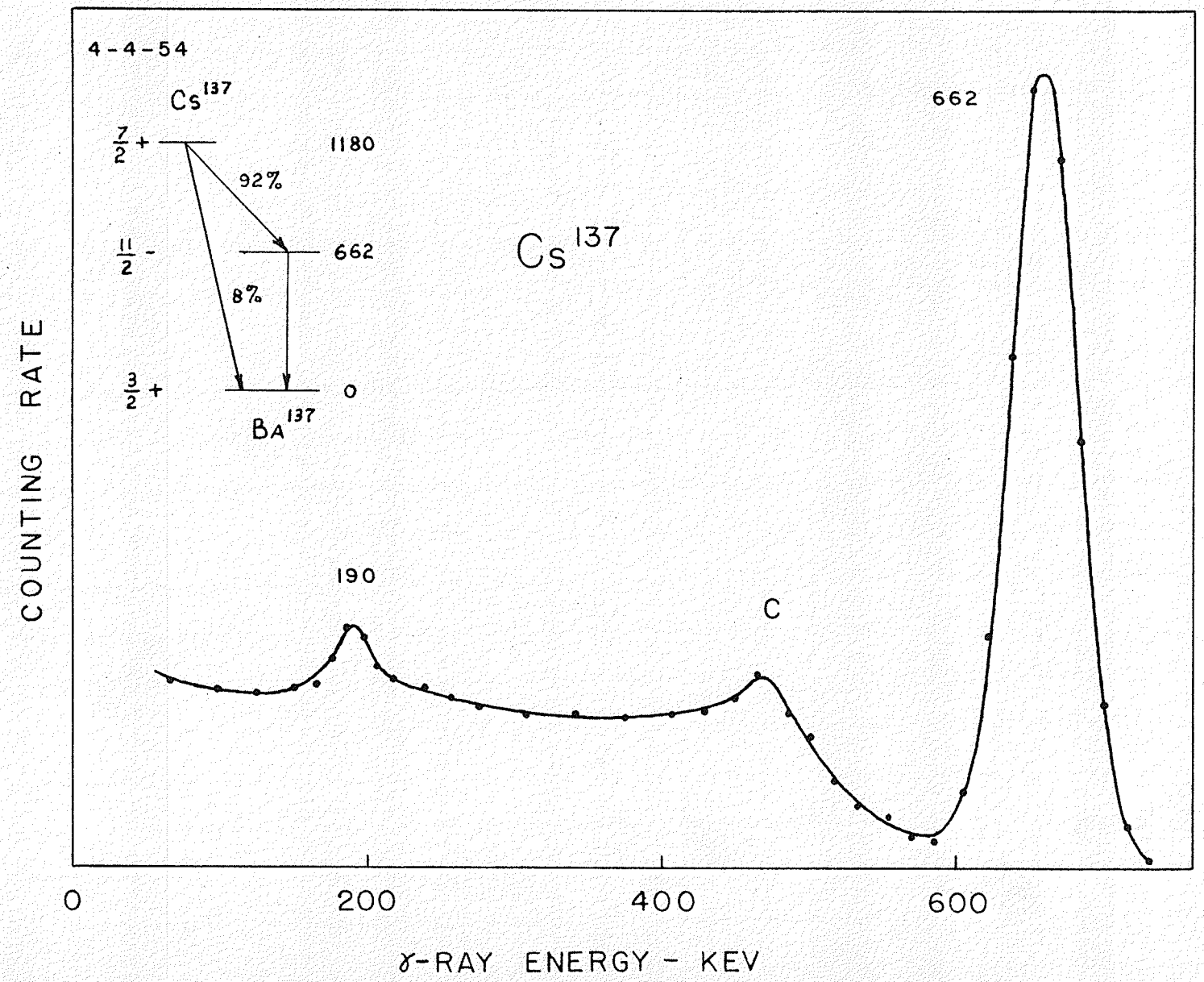

Fig. 4. Spectrum of gamma radiation following negatron emission in Cs^{137}.
Inset: The decay scheme of Cs^{137}.

In addition to the sources mentioned above, several others with prominent photoelectron lines have been used, e.g. Co^{60}, Se^{75}. The details will be given at more appropriate places in subsequent sections.

b) The Decay Scheme of Zinc - 65

In spite of its apparent simplicity, the decay of Zn^{65} has been the subject of numerous investigations in recent years. This present contribution to the literature on the subject is concerned with the gamma radiation associated with this isotope.

250-day Zn^{65} decays by both positron emission (end point energy 325 ± 3 kev) and K-capture to Cu^{65}. The former mode of decay is a ground state transition which occurs in only 1.7% of the disintegrations. About 44% of the transitions give rise to a single gamma ray at 1114 kev. However, a low energy gamma ray has been reported (37, 38, 39) at 200 kev, as well as a second positron component, with an end point energy of about 150 kev (40). These results imply the existence of a level in Cu^{65} at about 200 kev. On the other hand Sakai (41) and Perrin (42) have reported that any low energy gamma ray has an intensity $< 10^{-4}$ per 1114 kev gamma ray. Perkins and Haynes (43) have re-examined the positron spectrum using very thin sources. They report that it consists of only one component with the end point energy quoted above. The Fermi plot was found to be linear down to 50 kev. The conversion coefficient of the 1114 kev gamma ray was measured and found to be consistent with an E2 multipolarity assignment. Fig. 5 shows the decay scheme due to Perkins et al.; it contains only the well-established details.

In an effort to resolve the conflicting reports concerning the

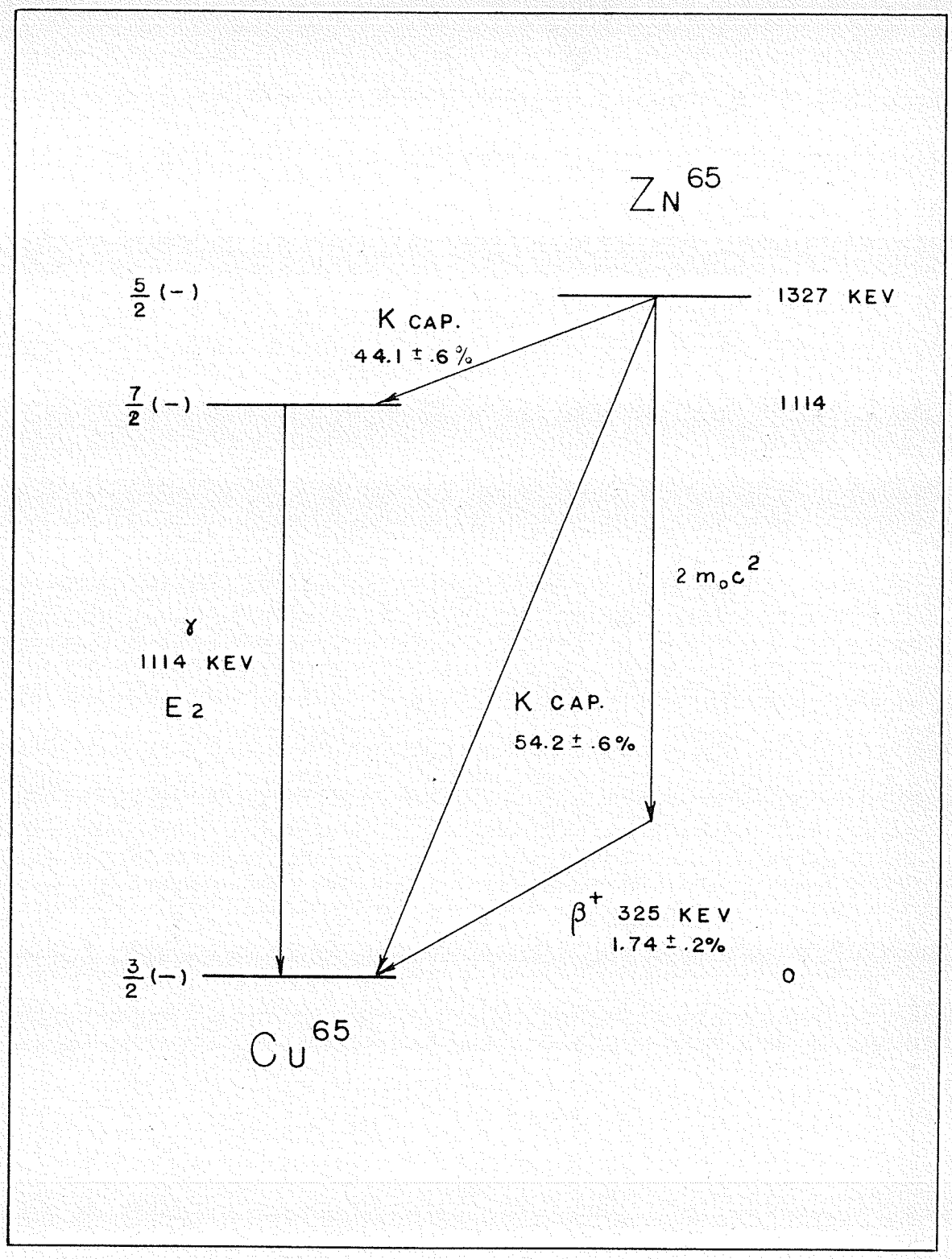

Fig. 5. Disintegration scheme of Zn^{65} (following Perkins and Haynes (43)).

200 kev gamma radiation, this isotope was studied using the coincidence spectrometer described earlier. The gamma ray spectrum was obtained with a single channel spectrometer (counter #2), using a $\frac{1}{2}$-volt gate. The pulse height distribution is shown in Fig. 6. The energy axis was calibrated using photoelectron lines from Cs^{137}(662 kev) and Co^{60}(1172, 1332 kev). The line at 1114 kev was found to be very prominent, as were lines at 511 and 210 kev. The line at 511 kev was due to the annihilation of positrons, either in the source or the source holder. The Compton maxima (C) for the two higher energy lines were in evidence also. A comparison of this spectrum with that obtained by Bouchez (38) explained immediately the false conclusions at which he had arrived. Bouchez interpreted the line at 210 kev as being due to another nuclear gamma ray which was in coincidence with the 1114 kev radiation. However, it is quite clear from the discussion of the preceding section that much of the observed radiation at this energy will be due to backscattering of the 1114 kev gamma ray. Of course, this in itself does not preclude the existence of a nuclear radiation of approximately the same energy.

The coincidence experiment was set up in rather naive fashion as shown in Fig. 7(a). The two counters were placed at 180° with respect to one another and brought up close to the source as indicated in the figure. (Some of the constructional details mentioned earlier should be noted!) A 2 mm thick lead absorber was placed over the second crystal in order to prevent backscattering from one detector to the other. A coincidence could result from this as follows. Consider a 1114 kev gamma ray to have entered one crystal and undergone a 180° Compton scattering. The recoil photon could then be absorbed by the second crystal. The first detector 'sees'

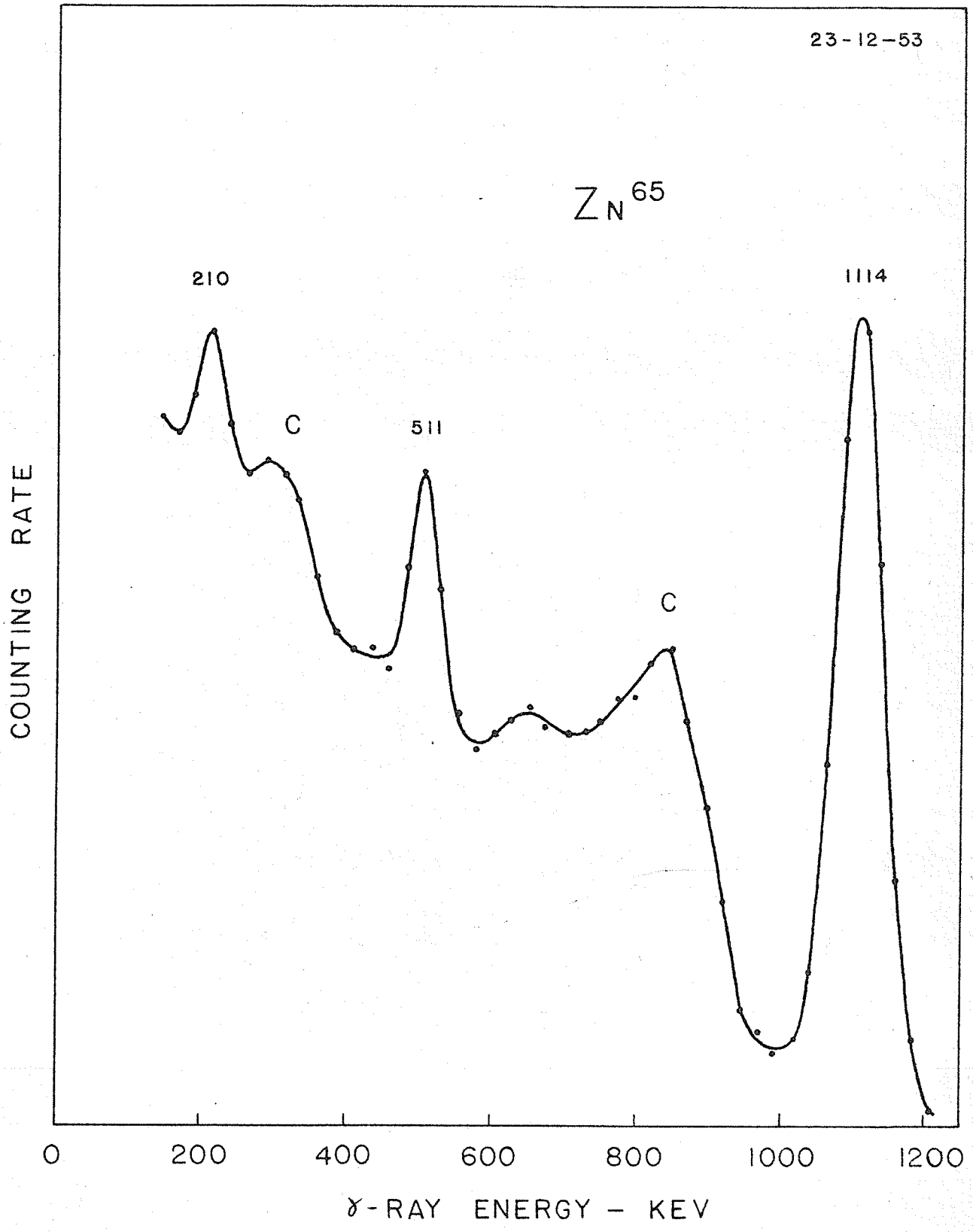

Fig. 6. Spectrum of gamma radiation following K-capture and positron emission in Zn^{65}.

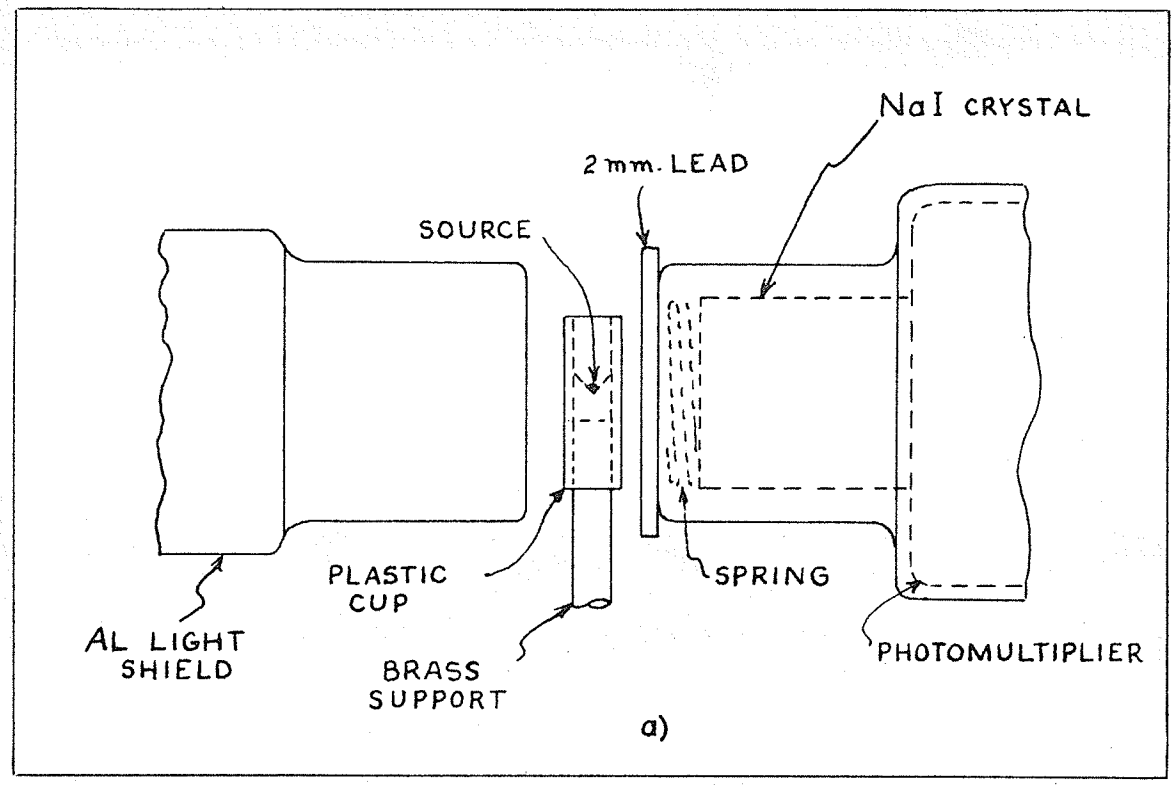

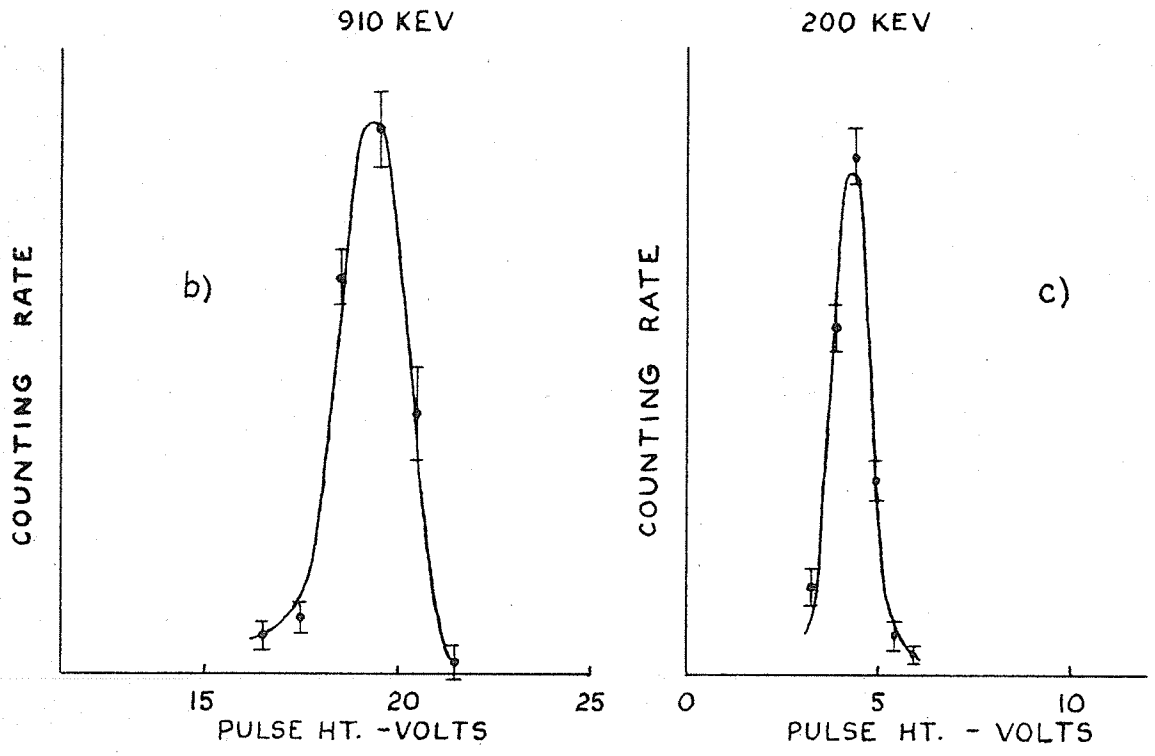

Fig. 7 (a) Side view of experimental arrangement for coincidence studies.
(b) Photoelectron line in coincidence with 'gamma' radiation at 200 kev.
(c) Photoelectron line in coincidence with '910 kev radiation'.

a 900 kev electron, while the second detects a 200 kev gamma ray in coincidence with it and a spurious coincidence count is recorded. Spectrometer #1 (on the left of Fig. 7(a)) was set to accept pulses lying in the 200 kev line, while the gate of spectrometer #2 was swept across the gamma ray spectrum (a 1-volt gate was used for this). Coincidences between annihilation quanta were detected, but in addition, a sharp line was found at 910 kev as shown in Fig. 7(b). The converse experiment was performed also; spectrometer #1 was set at the 900 kev region, and the gate of #2 swept over the low energy region. A sharp line was found in this case at about 200 kev as shown in Fig. 7(c). Two interpretations of these data are possible: 1) the 200 kev gamma exists; it is in cascade with another radiation at 910 kev and the 1114 kev gamma ray is a crossover transition, or 2) the absorber intended to eliminate backscattering was not adequate. It was felt that merely increasing the thickness of the absorber would not resolve the ambiguity. If the 910 kev radiation was very weak, the further reduction in intensity by lead absorbers might well lead to an indeterminate result.

A second series of experiments was carried out using the delayed coincidence technique (see P. 26); the radiations concerned were the 200 kev gamma ray and the proposed 150 kev positron component. One spectrometer was set on the 200 kev line in the gamma ray spectrum and the other on the 511 kev line due to annihilation quanta. The delay in the coincidence tray corresponding to the latter was varied in 0.05 microsecond steps from 0 to 1 microsecond. The coincidence rate for each delay was measured and plotted against the delay time in microseconds on semi-logarithmic paper. The resulting time resolution curve is shown in Fig. 8(a) I. The linear 'tail' of the curve appeared promising but the

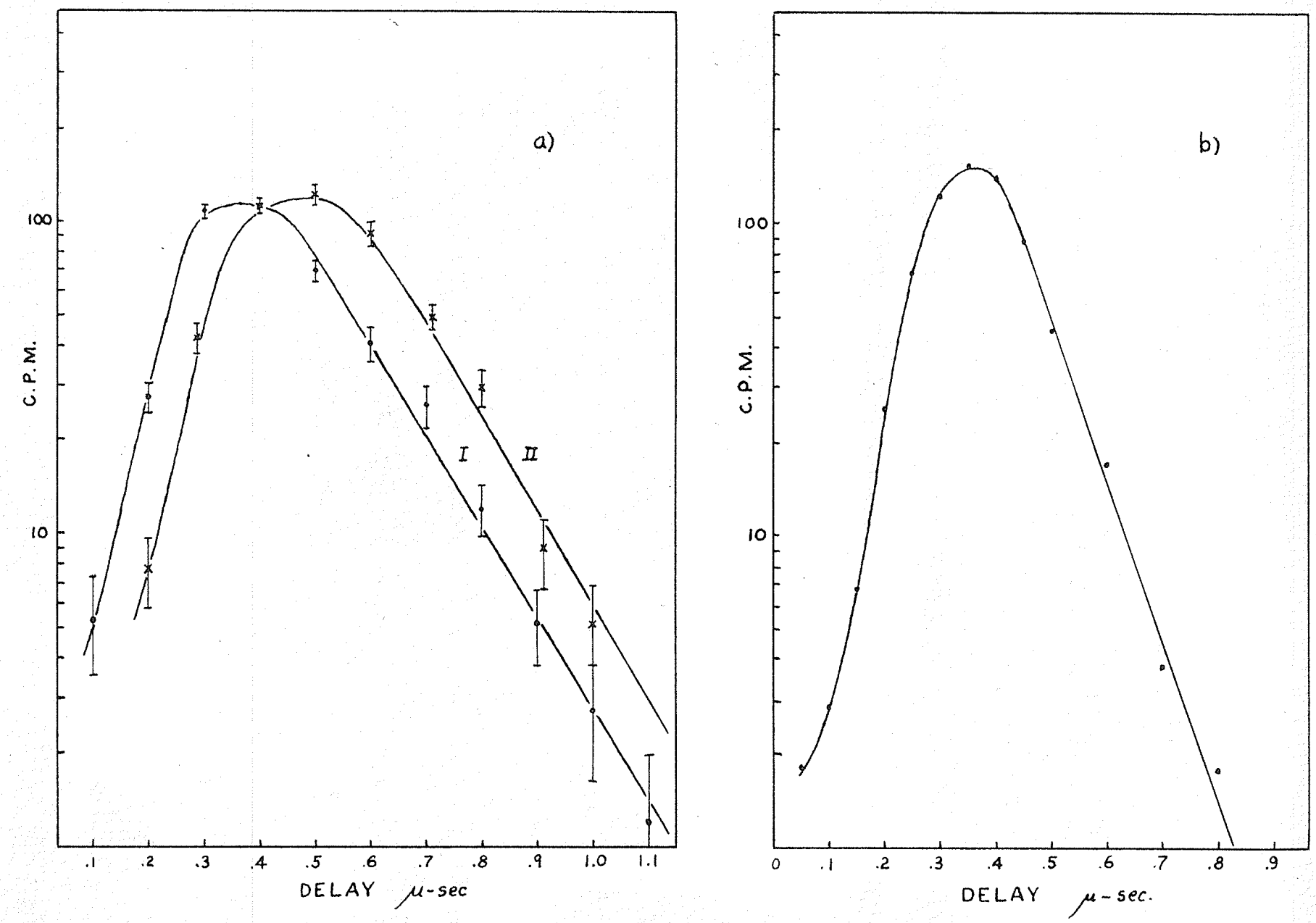

Fig. 8 (a) Time resolution curve for '200 kev gamma ray' - annihilation radiation coincidences.
(b) Time resolution curve for backscattered coincidences in Cs^{137}.

possibility of its being instrumental was not overlooked. The gate widths of both spectrometers had been the same for the experiment although the ratio of the pulse heights at the centers of the gates had been about 2.5 : 1. The experiment was repeated using gate widths which were proportional to the pulse heights at the gate centers. Curve II of Fig. 8(a) resulted. The lateral shift was thought to be due merely to the introduction of an additional delay between the two sides of the spectrometer when the relative positions of the lower levels of the gates were changed. The slope of the linear 'tail' was found to be approximately constant, however, although the errors on the experimental points were too large to establish this with certainty. The slope of the tail, if due to an isomeric level at 200 kev in Cu^{65}, corresponded to a state lifetime of 1.4×10^{-7} seconds. The results appeared to corroborate the work of Cohn and Kurbatov.

In order to check the results, however, an identical experiment was performed using Cs^{137}, which is known to emit only one gamma ray. Coincidences due to backscattering were detected; they were used in the performance of the delayed coincidence experiment. The rather unusual result is shown in Fig. 8(b). The slope of the linear portion of the curve was found to be only 0.65 times that of Fig. 8(a) I, but indicated that the Zn^{65} results may have been instrumental. The Cs^{137} result was obtained using equal gate widths and a ratio of pulse heights of about 3 : 1. A further check was carried out using annihilation radiation directly. Fig. 9 shows two time resolution curves obtained with Zn^{65}. The inner one was taken with the ratio of the pulse heights due to 511 kev gamma rays at 1 : 1. The outer curve was obtained with a ratio of 4 : 1. The interpretation of the previous results with Zn^{65} is now apparent. The time resolution curves of Fig. 8(a) and (b) were asymmetrical because

the difference in the location of the gates introduced a delay between the two sides of the spectrometer. This delay simulated an isomeric state and resulted in asymmetrical resolution curves. Any difference in the slopes of the curves could not be regarded as significant in view of the experimental errors on the points. These conclusions were substantiated using two different pulse height ratios in a further study of Cs^{137} and Zn^{65}. The results as a whole might well explain a slightly asymmetrical curve found by Roulston (28) in the study of Ce^{141}.

A final experiment was undertaken which was designed to eliminate direct coincidences due to annihilation radiation. The arrangement is shown in Fig. 10, which gives the plan view of the detectors. By placing the detectors at right angles to one another, annihilation radiation coincidences were eliminated except for those which occurred through scattering in the source or source holder. A $\frac{1}{2}$" thick lead plate was placed diagonally between the counters to prevent backscattering coincidences; the attenuation of the primary beam by this absorber, however, was negligible. The discriminators were set so that only coincidences between gamma rays at 200 and 900 kev were detected. However, after several hours of counting, no genuine coincidences could be detected above the background of accidentals. An identical result was found for 200 - 511 kev coincidences, in direct contradiction of the work of Cohn (37).

The present status of the Zn^{65} decay scheme may be summarized in the following manner. The linearity of the Fermi plot given by Perkins and Haynes seems to rule out the possibility of a second positron component. It is likely that thick sources were responsible for the earlier claims in favor of it. The results of the present investigation are consistent with this conclusion. In addition, the experiments indicate

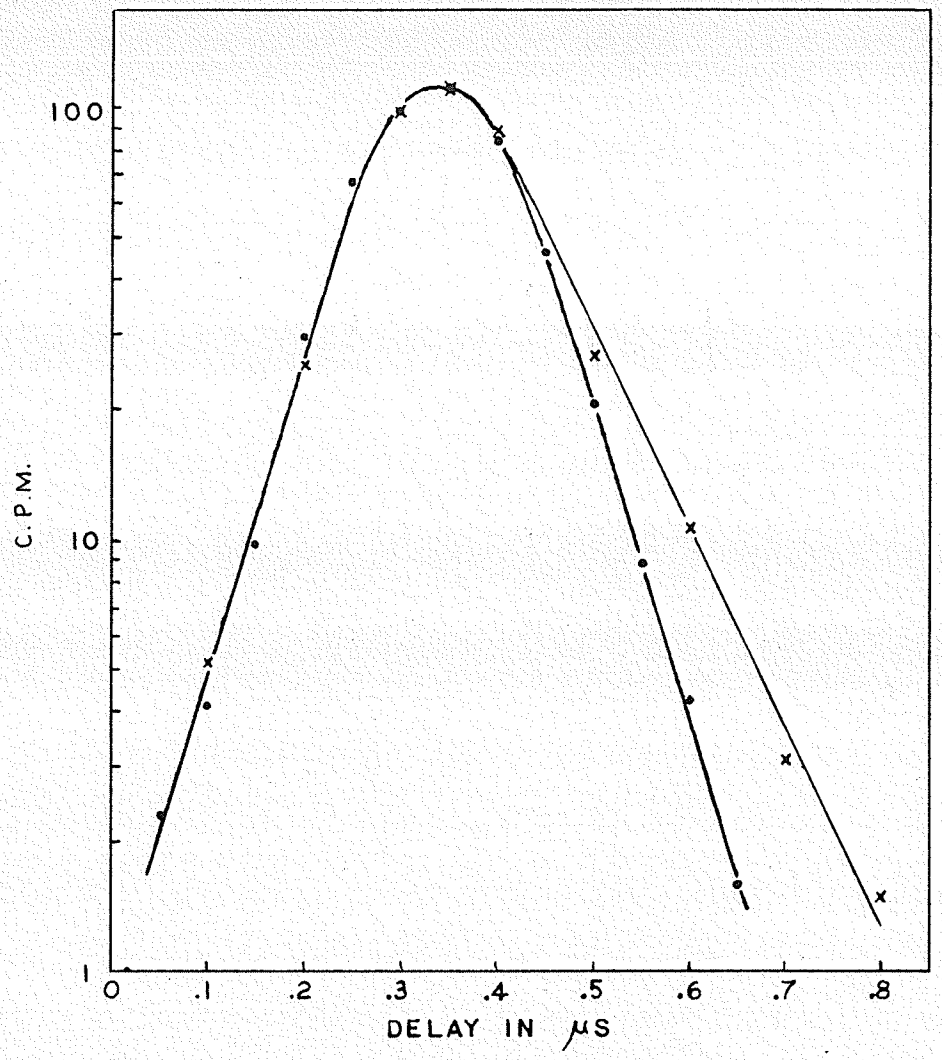

Fig. 9. Time resolution curve for annihilation radiation: • -pulse height ratio 1:1; x -pulse height ratio 4:1.

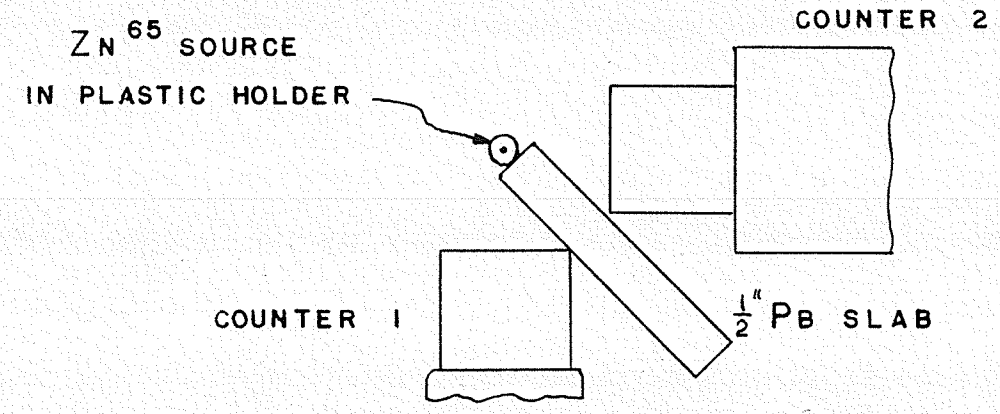

Fig. 10. Plan view of final experimental arrangement for coincidence studies with Zn^{65}.

that no genuine β^+ - 200 kev gamma ray coincidences are found if those due to annihilation radiation are avoided. M. Sakai (44) reported to the author during the final stages of this work that many of Cohn's early coincidence results were due to instrumental effects. This was gratifying in view of the present results. The decay scheme of Fig. 5 now seems to be firmly established.

In addition to the data on Zn^{65}, the experiment threw further light on the experimental techniques in current use. Two conclusions of a practical nature were drawn from the observations:

1) backscattering can give not only coincidences but also photoelectron lines in a coincidence spectrum;
2) asymmetrical time resolution curves can be caused by the positioning of triggering levels in both differential and integral discrimination equipment.

c) Angular Resolution Measurements

In Section f) of Chapter I, a discussion of angular resolution corrections was presented. In the present section, the experimental techniques used to obtain the correction factors will be described. Numerical values will be given for a number of gamma ray energies.

Brady and Deutsch (5) were the first workers to use the angular resolution curve obtained from coincidences between annihilation quanta. The technique was put on a sound theoretical basis by Church and Kraushaar (18) somewhat later (see equations (34) to (38). The corrections for 511 kev radiation were obtained here by using Brady's technique. The counters were arranged as shown in Fig. 11. A Zn^{65} pellet, mounted in a plastic cup, was used as a source of annihilation radiation. The gate

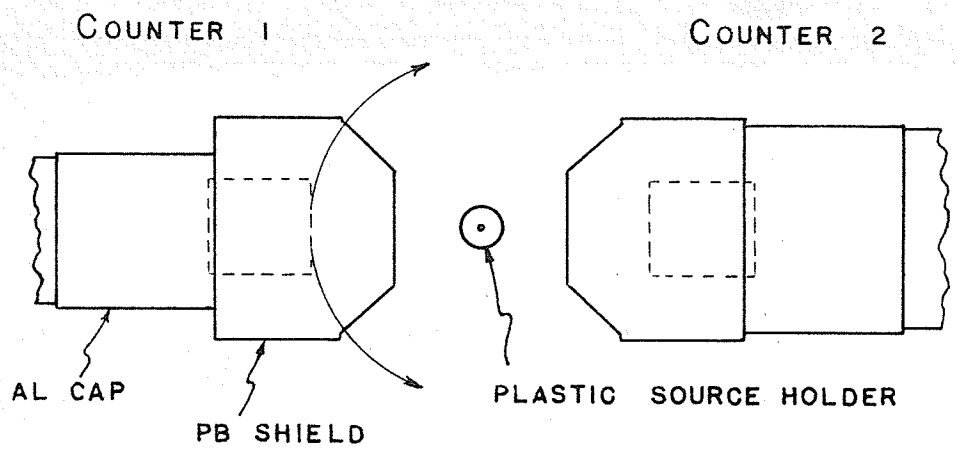

Fig. 11. Plan view of experimental arrangement used to measure angular resolution function for annihilation radiation.

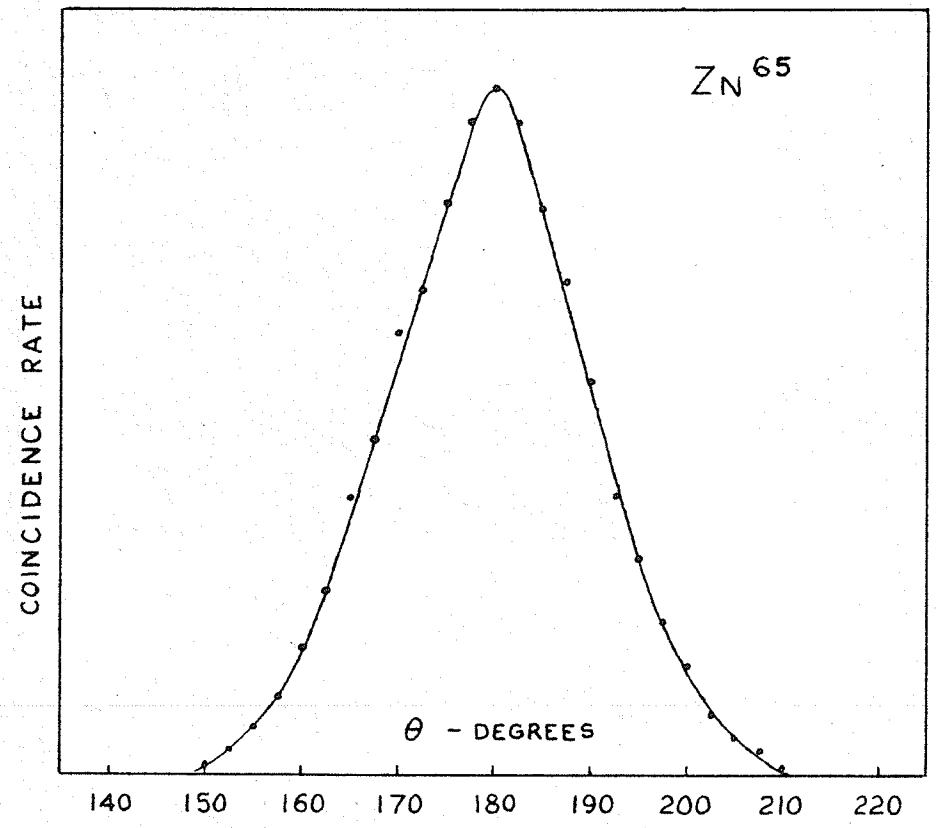

Fig. 12. Angular resolution curve for annihilation radiation. The half width (α_0) at half height is 11.5°.

of each spectrometer was set on the photoelectron line at 511 kev in the Zn^{65} spectrum (Fig. 6). With this arrangement, the genuine-to-accidental coincidence ratio was found to be better than 100 : 1. Counter #1 was moved from 145° to 215° in 2.5°steps. The coincidence rate at each angular position was recorded, then plotted against angle to yield the resolution curve of Fig. 12. The source-to-counter distance was, of course, the same as that used in an actual correlation experiment. The half-width at half-height on the resolution curve was found to be 11.5°.

Since most radiative transitions involve either dipole or quadrupole radiations, only the correction factors Q_2/Q_o and Q_4/Q_o are needed in general. These are found from Fig. 13 which shows Q_2/Q_o and Q_4/Q_o plotted as functions of α_o. For $\alpha_o = 11.5°$, the corrections were estimated to be .917 and .749 respectively. Of course, these values can be used to correct data obtained with radiations whose energies are very close to 510 kev, but they are not appropriate for radiations with energies which differ appreciably from this value.

As mentioned previously, the correction factors are energy dependent. To evaluate them for energies quite different from 510 kev, the method of Lawson and Frauenfelder (19) was used. Unfortunately, very strong sources were not available so that a rather short collimating system had to be used to define the gamma ray beam. A plan view of the arrangement is shown in Fig. 14. The collimator was a 3" x 4" x 4" lead block with a 1/16" diam. hole drilled through it as shown. It was set up so that the beam was parallel to the axis of the fixed counter and incident on the crystal of the movable counter at its center (i.e. when viewed horizontally). The distance between the movable detector and the center of the brass rod was the same as for the arrangement using

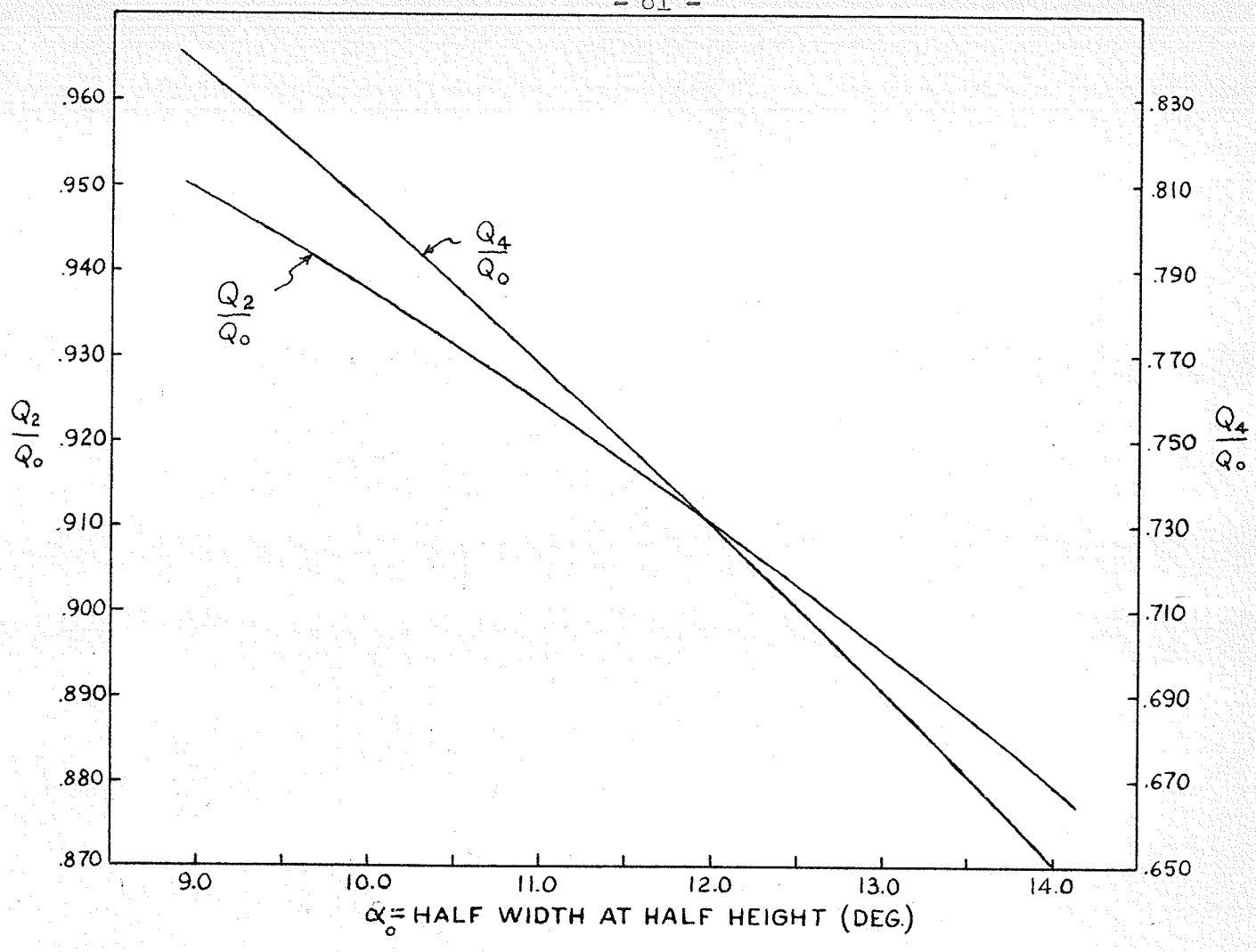

Fig. 13. Plot of Q_2/Q_o and Q_4/Q_o against α_o (Church et al.(18)), for annihilation radiation.

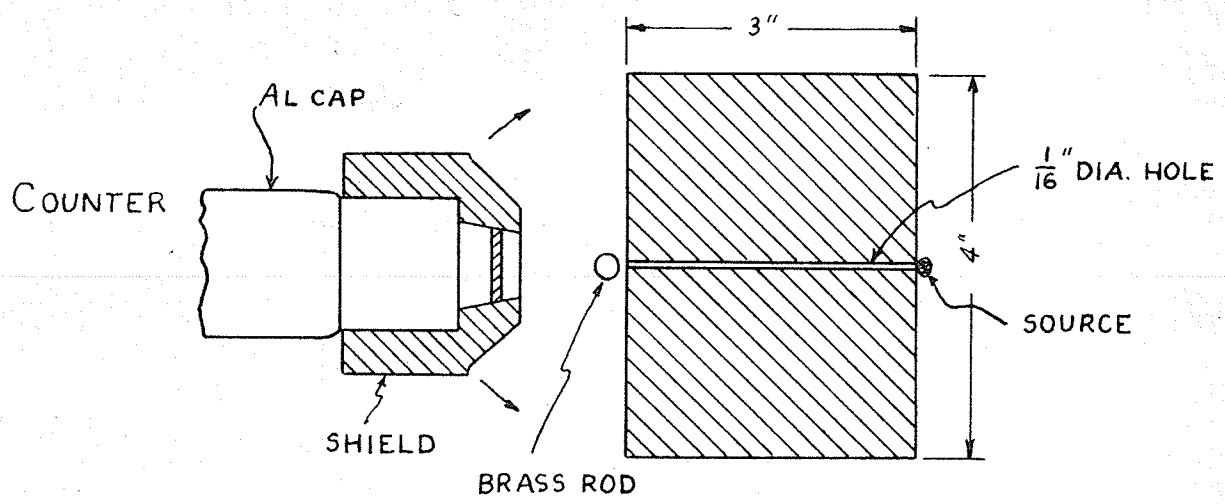

Fig. 14. Plan view of experimental arrangement for measuring angular resolution curve for different gamma ray energies.

annihilation radiation. The counter was shielded from degenerate radiation with the lead covers used during a correlation experiment. The measurements were carried out as follows. The spectrum of the gamma rays emitted by the source to be used in the measurement was scanned using spectrometer #1 (movable); the gate of the discriminator was then widened and set over the photoelectron line of the appropriate gamma ray. With the collimator replaced by a block of identical dimensions, the background counting rate was observed as a function of the angular position of the movable counter. With the collimator in position, the counter was swept across the radiation beam and the counting rate recorded for each position. The counting rates, corrected for background, were plotted against the appropriate angles. Of course, it was assumed that both crystals of the coincidence spectrometer were equally efficient for the detection of gamma radiation. If this were not so, separate measurements would have to be made for each crystal.

The resolution curves, $\epsilon(\alpha)$, for several gamma ray energies are shown in Figs. 15 a) b) c) d) and e). The J_{2k} of equations (41) were evaluated numerically with the aid of a planimeter. The numerical results together with the details of the gamma rays used are listed in Table I. The values of Q_2/Q_o and Q_4/Q_o tabulated are to be used only if both counters detect radiations of the same energy. If this is not the case, equations (40) must be used to evaluate the corrections. The entries J_2/J_o and J_4/J_o for 511 kev radiation were calculated from the results obtained using Church's formulae (equations (38)), by taking the square root of Q_2/Q_o and Q_4/Q_o respectively.

The degree of collimation used undoubtedly leaves much to

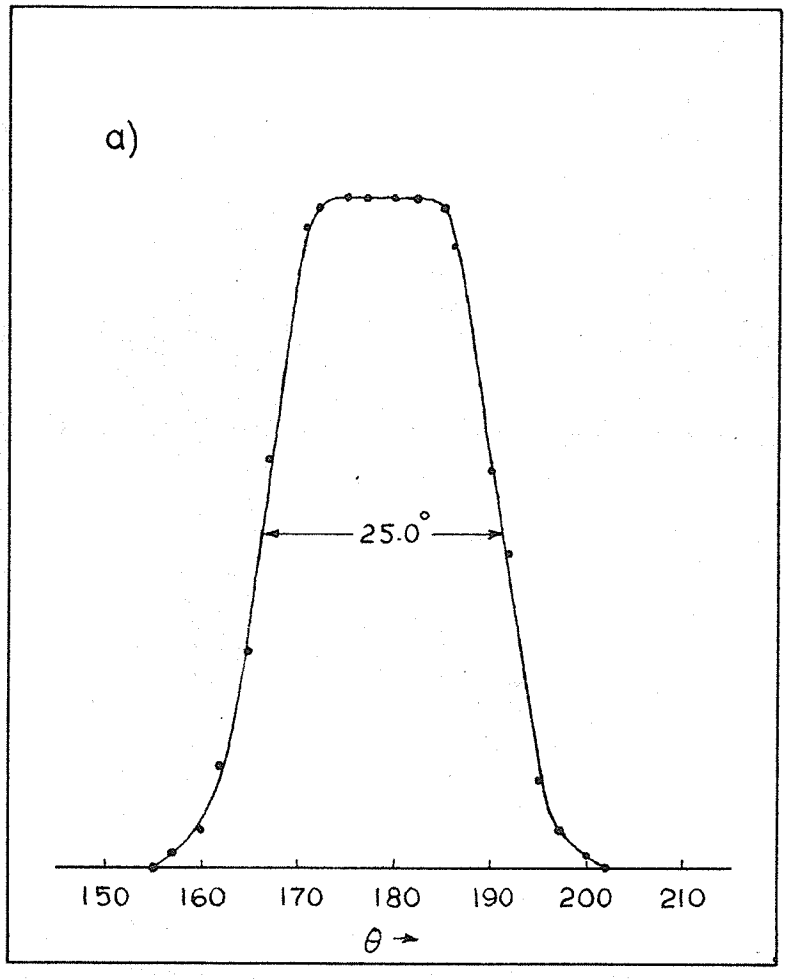

Fig. 15. Angular resolution curves for

a) 312 kev photoelectron line (Ir^{192})
b) 662 kev " " (Cs^{137})
c) 1114 kev " " (Zn^{65})
d) 1332 kev " " (Co^{60})
e) 1690kev " " (Sb^{124})

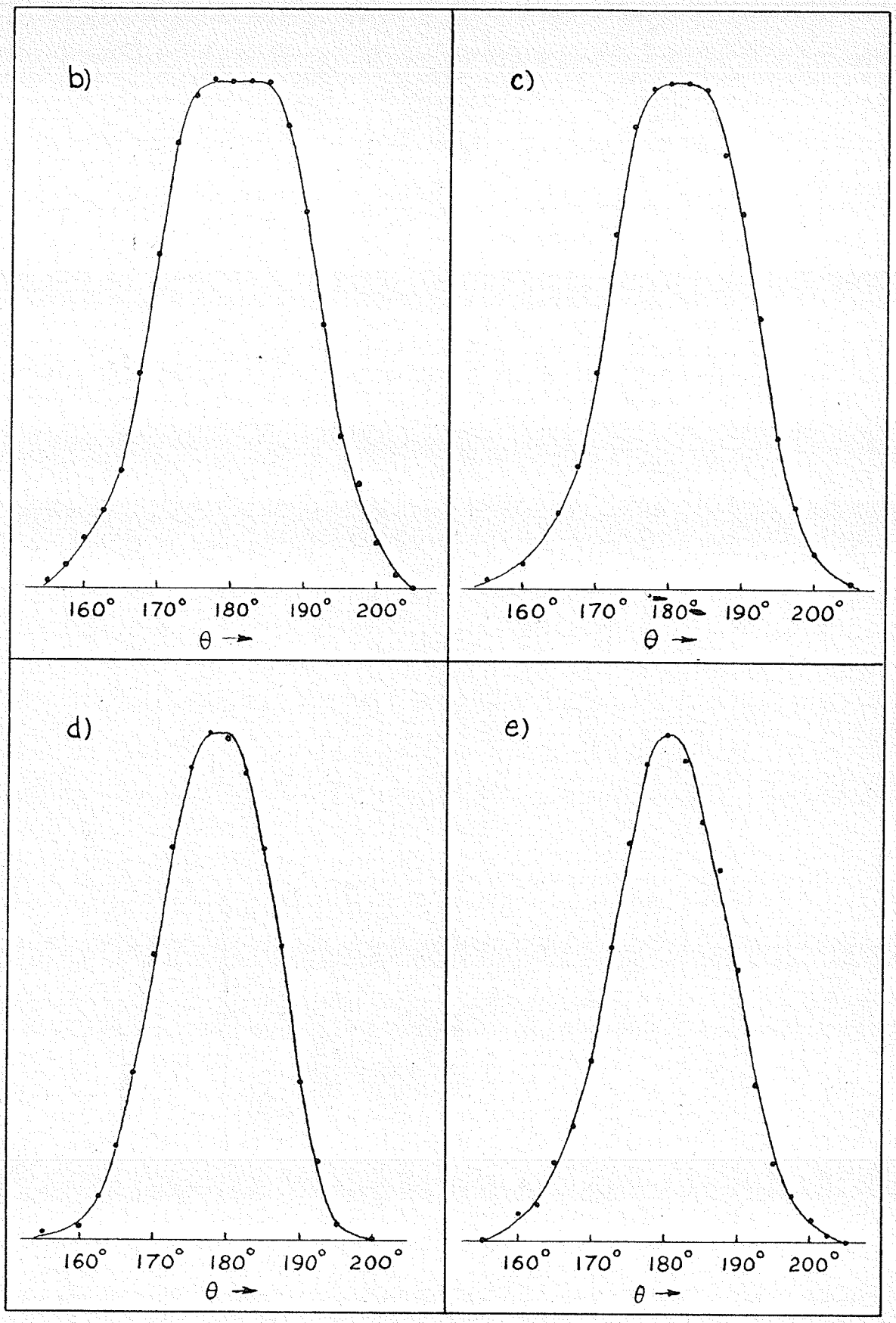
b)
160° 170° 180° 190° 200°
θ →
c)
160° 170° 180° 190° 200°
θ →
d)
160° 170° 180° 190° 200°
θ →
e)
160° 170° 180° 190° 200°
θ →

Fig. 15 cont'd

	γ -Ray Energy	Source	$\frac{J_2}{J_o}$	$\frac{J_4}{J_o}$	$\frac{Q_2}{Q_o}$	$\frac{Q_4}{Q_o}$
,a	312 kev	Ir^{192}	.942	.833	.887	.695
b	662 kev	Cs^{137}	.943	.820	.890	.672
c	1114 kev	Zn^{65}	.950	.825	.902	.680
d	1332 kev	Co^{60}	.942	.852	.887	.726
e	1690 kev	Sb^{124}	.930	.822	.865	.675
f	511 kev	β^+-Zn^{65}	(.957)	(.865)	.917	.747

Table I. - Angular resolution correction terms for several monoenergetic gamma rays.

be desired. Since only weak sources were available, however, a compromise had to be accepted between beam definition and the statistical accuracy of the points on the resolution curves. This was particularly important in the case of the lower energy gamma rays (312 kev and 662 kev). Here the background in the laboratory was exceedingly troublesome, being comparable in magnitude to the beam intensity. A thicker collimator would undoubtedly have resulted in better beam definition but it would have been excessively difficult to obtain the results. Due to a lack of very small crystals suitable for studying the beam shape, it was not possible to correct for the finite width of the gamma ray beam. (See reference 19).

As far as was possible, monoenergetic sources were used for the resolution curves. In the case of (e) and (a), however, the photoelectron lines contained more than one component. For the former, an interfering transition in Sb^{124} at 2090 kev contributed to the counting rate. It was estimated, however, that $\leq$ 10% of the counts were due to this transition. The situation was more favorable in the case of (a). The Compton maximum of a strong 468 kev gamma ray interferes with the line at 312 kev which was used in the measurement. But only $\sim$ 4% of the counts were due to the interfering transition; the shape of the curve was due primarily to the line at 312 kev.

In spite of the two minor flaws mentioned above, the technique was felt to be satisfactory on the whole. The appropriateness of the correction terms obtained will be illustrated in succeeding sections.

The shapes of the resolution curves show, qualitatively, how the product of the detection and photo-peak efficiencies for a scintillation counter varies with energy. The narrowness of the high energy curves indicates that the portions of the crystal which are near the cylindrical

surface are relatively inefficient when it comes to giving pulses corresponding to the full gamma ray energy. On the other hand, the breadth of the low energy curves suggests that the converse is true for softer radiations. In addition, it demonstrates that the detection efficiency across the crystal is approximately constant for low energy gamma rays. The curves obtained by Lawson and Frauenfelder (19) for the Co^{60} gamma rays (1172 and 1332 kev) showed a remarkable lack of symmetry. This presumably was due in part to a lack of homogeneity in the crystals used. No evidence of this effect was found in the present investigation.

d) Directional Correlation in Nickel - 60

It is customary to test directional correlation apparatus by means of so-called "well-established" gamma ray cascades. Of these, the two component cascade of Ni^{60} is perhaps the simplest and best-known to nuclear physicists. However, as Frauenfelder (45) has pointed out, it is sometimes unwise to check apparatus by studying well-known isotopes, for often they turn out to be not so well-known as we think. In correlation measurements, this was demonstrated recently by a Swiss group (46). Their experimental result for the cascade in Ni^{60} was 11% lower than the theoretical value and could not be accounted for in terms of experimental errors. Although this cast some doubt on the accepted results for Ni^{60}, subsequent work by Klema and McGowan (8) mentioned on P. 4 seems to have confirmed that theory and experiment are consistent for this case. Having thoroughly investigated the literature on Ni^{60}, the author felt that the directional correlation was sufficiently well-established to permit the use of the isotope for the testing of the present coincidence spectrometer. The results of directional measurements with Ni^{60} will consequently form the subject matter of this section.

The properties of those levels in Ni^{60} which are excited by negatron emission in Co^{60} have been given in detail by Keister and Schmidt (47). They are shown in Fig. 16. The gamma ray energies have been accurately measured by Lind et al. (48) with a curved crystal spectrometer; the values are 1171.5 ± 1.0 and 1331.6 ± 1.0 kev. (The values 1172 and 1332 kev are used in this thesis.) In addition, the conversion coefficients of the gamma rays have been determined (49); they indicate that both transitions are electric quadrupole (E2). Several directional correlation studies have been carried out for Ni^{60}. (For details as to what has been accomplished to date, reference 5 is cited.) With the exception of that of the Swiss paper (46), all the evidence points to the E2 assignment for both transitions. Since Ni^{60} is an even-even nucleus, it is usual to assign a spin of 0 and even parity to its ground state (50). Since both radiations are quadrupole, the assignment of a spin of 2 to the first excited state and of 4 to the second excited state is indicated. The electric character of the radiations implies that there is no parity change in either transition. (Refer to the table on P. 8). These assignments are shown in Fig. 16.

The study of the directional correlation between the two gamma rays of Ni^{60} was undertaken in order to 1) test the coincidence spectrometer and 2) enable the author to gain experience with the technique. A small metallic pellet of Co^{60} with a strength of about 0.1 mc was used in the experiment. The source was supplied by Atomic Energy of Canada Ltd. It was formed by pile irradiation of cobalt metal; the reaction is $Co^{59}(n, \gamma)\ Co^{60}$. The gamma ray spectrum of Co^{60} was obtained with spectrometer #2, using a 0.5 volt gate; it is shown in Fig. 17. The two photoelectron lines, the associated Compton maxima (C), and the backscattered line are all prominently displayed. With the gate of each discriminator set on a different photoelectron line, the arrange-

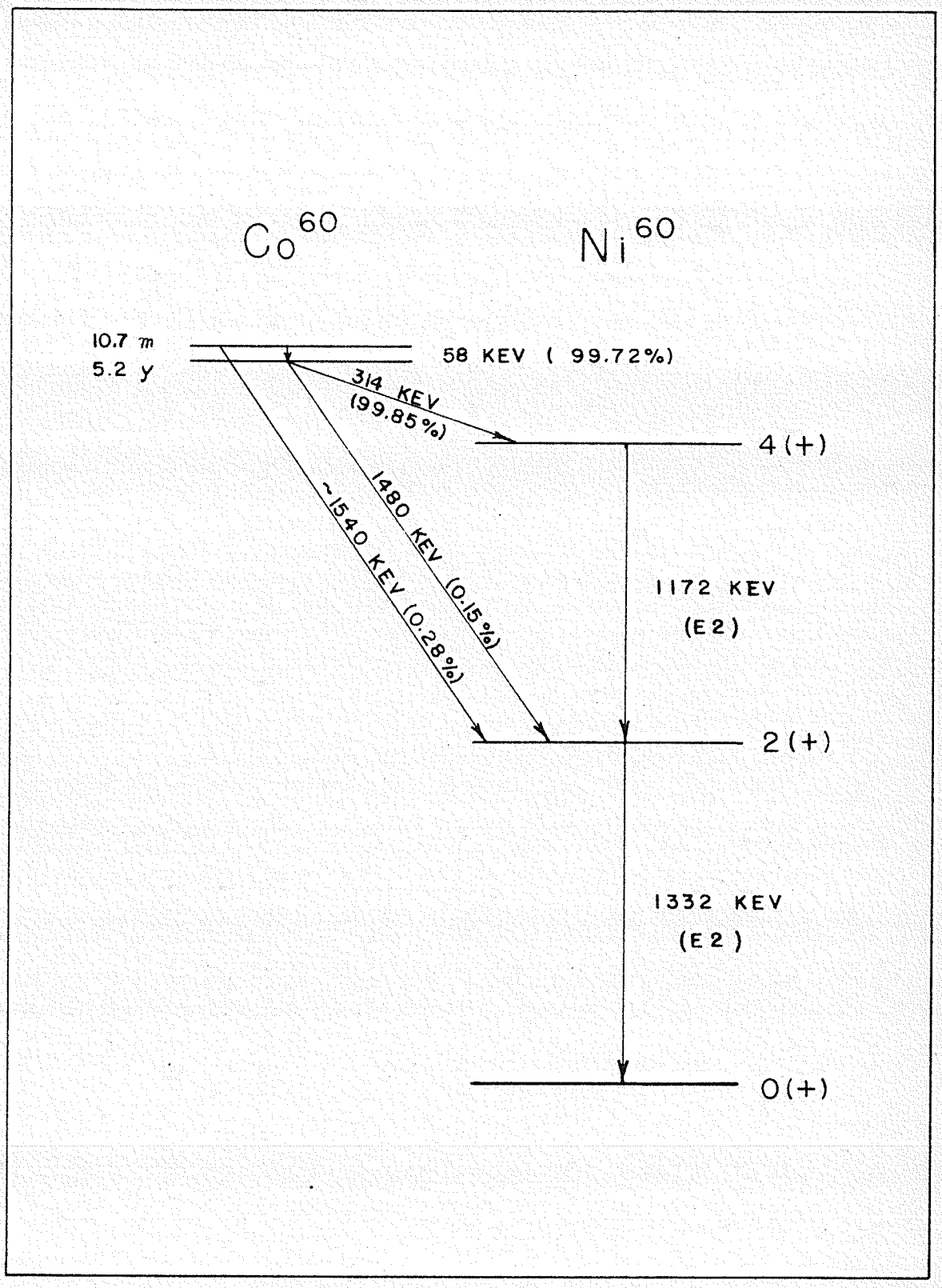

Fig. 16. Decay scheme of Co^{60} (following Keister et al.)

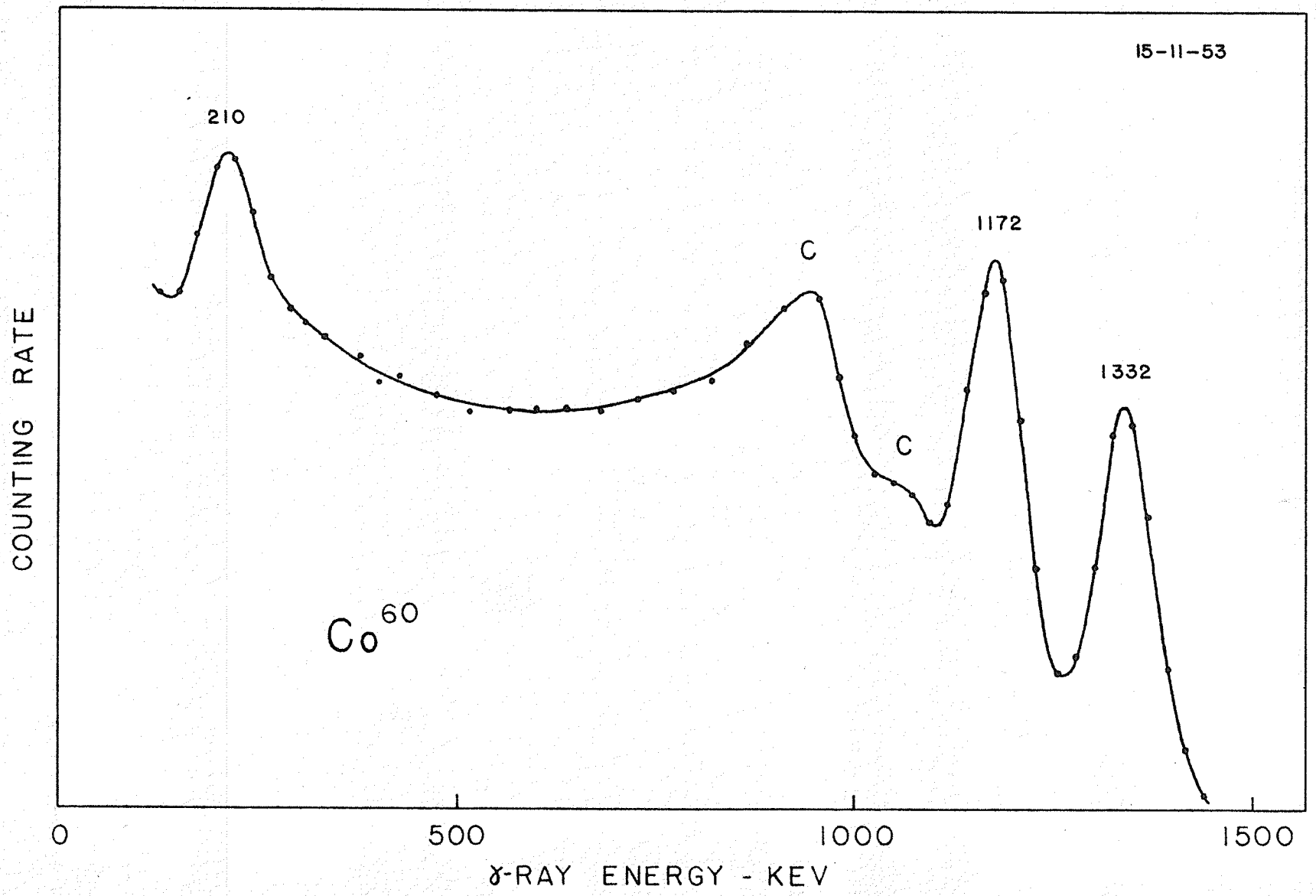

Fig. 17. Spectrum of gamma radiation following negatron emission in Co^{60}. The peak at 210 kev is due to backscattering of the two primary gamma rays.

ment of Fig. 11 gave a net coincidence rate of about 15 counts per min., of which $\sim$ 6 were accidental. (A better genuine-to-accidental coincidence ratio could have been obtained with a weaker source, but none was available.) Of course, the outer circular surfaces of both crystals were protected by the usual 2 mm thick lead plates.

The following technique was used to collect the coincidence data in this and subsequent directional investigations. At the commencement of a run, the gamma ray spectrum was scanned with both differential discriminators. The gate of each was then widened and placed on the appropriate energy region or feature. The resolving time of the coincidence unit was measured next, as follows. The pulses from one counter were delayed by 1 microsecond so that no genuine coincidences would occur. (The assumption has been made that no metastable states exist in the cascades concerned.) The single and coincidence counting rates were recorded until several hundred coincidences had been counted. Equation (32) was then used to calculate τ. The coincidence unit was reset to its normal operating condition and the movable counter rotated until the angle between the counter axes was 90°. The single and coincidence counting rates were then measured at that position; usually 30 or 40-minute counting intervals were used. Next, the movable counter was moved to the position θ, $90^\circ \leqslant \theta \leqslant 180^\circ$, and a similar count taken. It was then returned to the 90° position and the entire procedure repeated. A run usually took from 4 to 6 hours. The resolving time τ was measured several times during this period, the average value being used to calculate the accidental rate at 90° and θ°. The difference between the net and accidental coincidence rates gave the genuine coincidence rate. The average coincidence rate for the entire run was determined at 90°, and divided

by the product of the average single counting rates of each detector. This compensated for any small asymmetry in the positioning of the source. The data at θ were handled in the same fashion. If N_θ and N_{90° denote the average normalized genuine coincidence rates at θ and 90° respectively, then from the data collected the ratio N_θ/N_{90° could be calculated. This gave one estimate of the asymmetry in the coincidence rate at θ, and one estimate of the corresponding point on the correlation curve. Usually four such determinations were made and the average value plotted at the position θ. The root-mean-square error on each point on the curve was estimated prior to mathematical analysis. Data were obtained at 120°, 140°, 160° and 180°, giving five points on the correlation function. A function W of the form $W = \sum_k A_{2k} P_{2k} (\cos \theta) = \sum_k a_{2k} \cos^{2k} \theta$ was fitted to the points using the method of least squares (refer to sections d) and g) of Chapter I). The coefficients A_{2k} and a_{2k} so determined were corrected for the finite angular resolution of the detectors, and the corrected form of W compared to theoretical shapes for various spin assignments to the levels concerned.

The curve which resulted from carrying out the above procedure with Ni^{60} is shown in Fig. 18. (In the figure the function W - 1 has been plotted.) The full curve was obtained by fitting $W - 1 = A_2' P_2 (\cos \theta) + A_4' P_4 (\cos \theta)$ to the experimental points by least squares analysis. To correct the coefficients A_{2k}' the correction factors for 1114 and 1332 kev radiations were used (See Table I). (The former energy is very close to the energy of the Co^{60} gamma ray at 1172 kev.) Since each counter detected one gamma ray only, the net correction factors were $Q_2/Q_o = .895$, and $Q_4/Q_o = .703$. The corrected and uncorrected values of the A_{2k} and a_{2k} are compared with theoretical predictions in Table II.

	a_2	a_4	A_2	A_4	180° Asymmetry
uncorrected	.1040	.0410	.0888	.0090	.144
corrected	.1055	.0586	.0992 $\pm$.0450	.0128 $\pm$.0117	.164 $\pm$ .012
theory	.1250	.0416	.1020	.0091	.1667

Table II.

The points - ⊗ - in Fig. 18 lie on the theoretical correlation curve for a 4 (E2) 2 (E2) 0 spin assignment for the levels of Ni^{60} shown in Fig. 16. It can be seen that the corrected experimental curve is in excellent agreement with the theoretical curve corresponding to the above assignment.

Of course, in this analysis the assumption has been made that the transitions involve only pure multipoles; this appears to be completely justified by the experimental facts.

There seems to be little likelihood of a perturbation of the correlation function by the electronic shells of the nickel atom. The criterion for the existence of such a perturbation is that the lifetime of the intermediate state (at 1332 kev in this case) be $> 10^{-11}$ sec. (45). Aeppli et al. (46) have estimated the upper limit to the lifetime of the intermediate state in Ni^{60} as $\leq 10^{-11}$ sec. This suggests that the directional correlation is independent of electronic interactions. The use of a metallic source also eliminates any possible perturbation of the nuclear state by inhomogeneous electric fields such as exist in crystals and molecules. For these to occur, the lifetime of the inter-

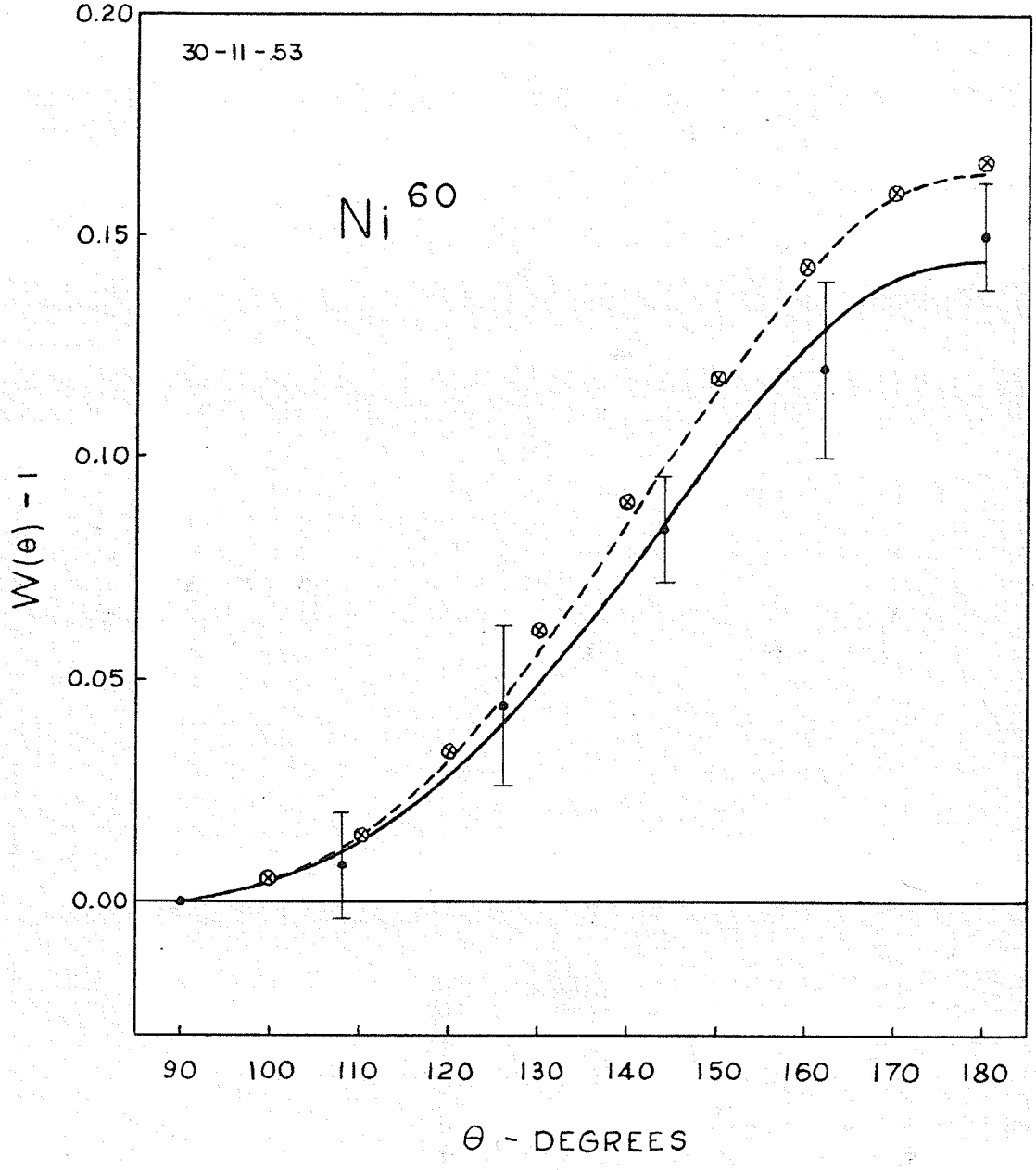

Fig. 18. Directional correlation function for Ni^{60}. The solid curve was obtained by a least square fitting to the experimental points. The dashed curve is the least square curve corrected for the finite angular resolution of the detectors. The points ⊗ lie on the theoretical curve for a $2^2 - 2^2$ basic correlation.

mediate state would have to be $\sim 10^{-4}$ seconds (45). This is at variance with the estimated lifetime of the state in Ni^{60}. Seome evidence has been presented (8) to show that perturbations do occur when cobalt salts are used as sources.

The total asymmetry (at 180°) of .164 ± .012 agrees very well with the theoretical value of .1667. This is due largely to the use of appropriate corrections. If the data are corrected using Church's formulae for annihilation radiation, the resulting asymmetry (.157) disagrees with the predicted value. Many discrepancies between theory and experiment which have been reported have been due to the lack of proper corrections to the data. When suitable angular resolution curves are obtained, however, the agreement with theory is usually found to be most satisfactory, at least for the pure radiation cases.

The results obtained with Ni^{60} were so encouraging that the spectrometer was immediately put to use studying more complex problems. No further technical changes were made in its design. The following four sections will present the results of these investigations.

e) Directional Correlation in Arsenic - 75

The low-lying levels of As^{75} can be excited either by negatron emission in Ge^{75} or K-capture in Se^{75}. In this section, the levels excited by the latter mode of decay only will be discussed. K-capture in 128-day Se^{75} is followed by the emission of some ten gamma rays. Since 1945, several attempts have been made to place these radiations in a level scheme, but only two recent contributions to the literature will be discussed in detail here. The reader is referred to one of these - a paper by Jensen et al. (51) - for a complete review of the literature.

In addition to Jensen's paper, some coincidence work by Schardt (52) will be considered.

The decay scheme of Fig. 19 is due to Schardt (52). (A discussion of the spin assignments will be given later.) It agrees closely with that given by Jensen except for the order of the gamma rays in the 203 - 65 kev cascade and several discrepancies concerning intensities. Additional evidence from the decay of Ge^{75} indicates that the ordering of the levels in As^{75} should be as given in Fig. 19. The following table shows the relative intensities of the gamma rays according to each author.

γ - Ray Energy (kev)	Relative Intensity	
	Schardt*	Jensen
67	~ .012	-
76	< .002	0.20
98	~ .036	~ 0.01
124	.84	~ 0.03
138		0.3
203	~ .021	-
269	1.00	1.00
281		~ 0.07
405	0.17	0.2

The most serious discrepancy is in the intensity of the 138 kev gamma ray; this forms part of the principal cascade of Fig. 19 (marked with an asterisk). Even though Schardt estimated the intensity of the 124 - 138 kev transitions combined, his result differs from Jensen's by a factor of 2.8. Therefore, before undertaking directional studies,

* measured with a scintillation spectrometer

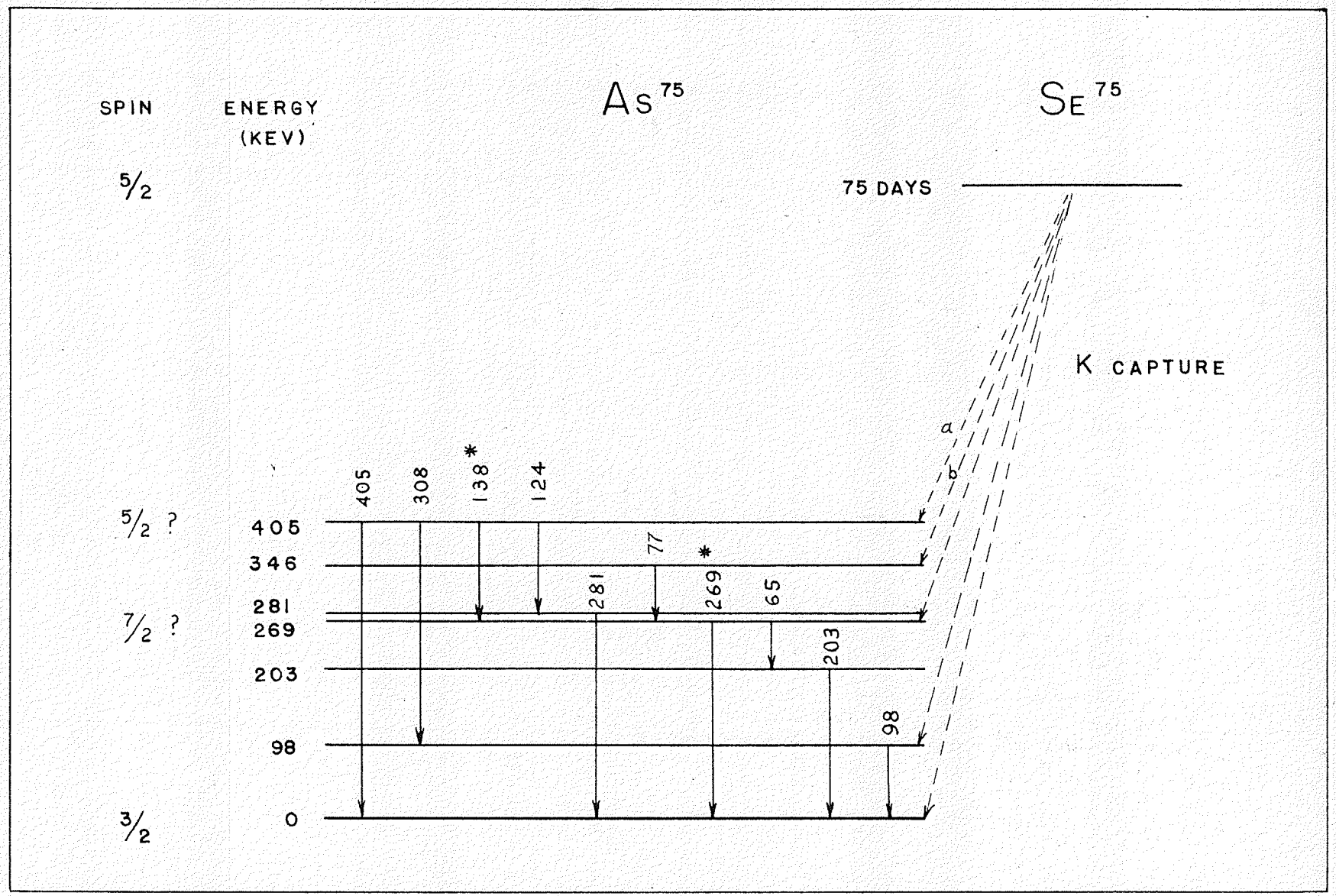

Fig. 19. Decay scheme of Se^{75}. The gamma rays involved in directional correlation studies are marked with an asterisk (*). See text for discussion of spin assignments.

it was decided to check this measurement of Schardt's and either confirm or reject it.

The Se^{75} source was a small metallic pellet with a strength of about .05 mc. Pure metallic selenium was irradiated in the Oak Ridge pile to form Se^{75}; the reaction is $Se^{74}(n, \gamma)\ Se^{75}$. The gamma ray spectrum was scanned using spectrometer #2, employing a 0.5 volt gate. The result is shown in Fig. 20. The photoelectron lines at 138 and 269 kev are slightly asymmetrical; the former contains the 124 kev radiation and the latter the line at 281 kev. The small degree of asymmetry suggests that both these transitions are weak however. (This will be discussed later.) This tends to support Jensen's conclusions based on β -ray work. After correcting for the asymmetry using Fig. 3 c), the intensities of the 138 and 269 kev gamma rays were found to be 0.8 and 1.0 respectively, in good agreement with Schardt's result. This implies that most of the transitions from the ground state of Se^{75} go to the 405 kev level in As^{75}. This conclusion was reached independently by Schardt. Before discussing this matter of intensities further, however, it might be well to present the results of the correlation studies.

The directional correlation between the photoelectron lines at 138 and 269 kev was studied assuming that the contribution to the coincidence rate from the 124 - 281 kev cascade was small. (We shall return to this point later.) To reduce the effects of backscattering of the 405 kev gamma ray, a 1 mm thick lead absorber was placed on counter #1, and a 2 mm. lead absorber on counter #2. (The latter detected the 269 kev radiation only.) The half value thickness in lead for the backscattered quanta from a 405 kev gamma ray is about 1 mm; this, coupled

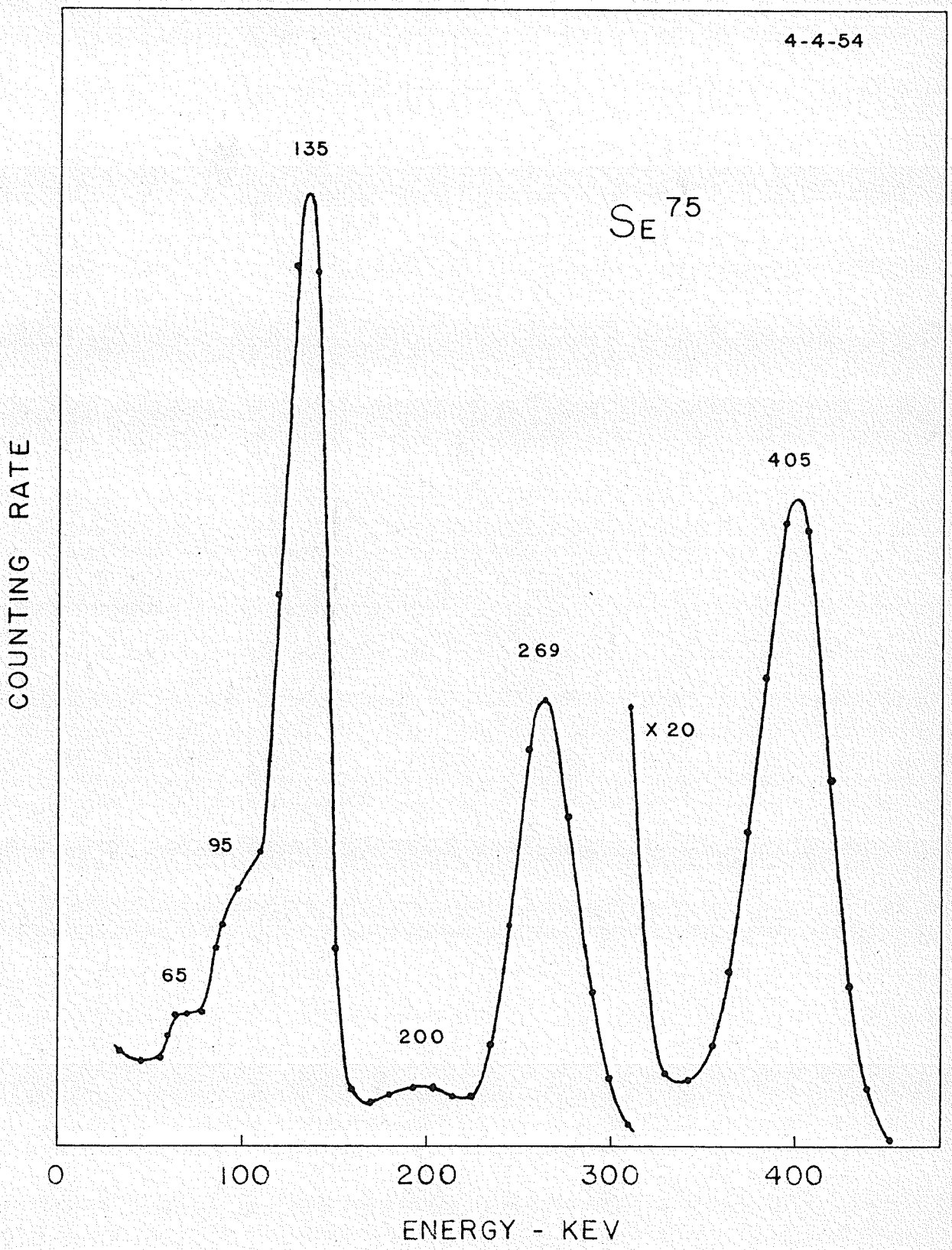

Fig. 20. Spectrum of gamma radiation following K-capture in Se^{75}.

with the low intensity of the crossover transition (405 kev), suggests that backscattering was almost completely eliminated by the absorbers used. With this arrangement, the net coincidence rate was found to be about 22 counts per minute, of which 10 were accidental. The experimental points with their root-mean-square errors are shown in Fig. 21. The correction factors for 312 kev gamma radiation were used in lieu of those for 138 and 269 kev which were unobtainable due to the high background. Their values were .887 and .695. The equation $W - 1 = \sum A_{2k} P_{2k} (\cos \theta)$ was least squares fitted to the experimental points for two different cases: 1) $A_{2k} = 0$, $k \geqslant 2$ and 2) $A_{2k} = 0$, $k \geqslant 3$ ($k = 1, 2, 3$ etc.). These will be discussed separately. Four additional pieces of information must be considered at the same time, however; they are listed below.

a) The spin of the ground state of As^{75} is known to be 3/2 (53).

b) The spin of the ground state of Se^{75} has been measured by Townes at Columbia University; the value is 5/2 (54).

c) The crossover transition (405 kev) is observed and has a reasonable intensity.

d) The conversion coefficients for the 405 and 269 kev gamma rays have been measured (54). They indicate that the multipole characters of the transitions are M1 and E2 respectively.

Case (1) $W(\theta) - 1 = A_2 P_2 (\cos \theta)$

Fig. 21 shows the curves corresponding to this case. The full line is the uncorrected least squares fit to the experimental points; the dashed curve is the corrected form. If pure radiations are assumed, it is found that the observed correlation is almost identical with the theoretical prediction for a basic dipole-quadrupole correlation. The points ⊗ indicate the shape of this theoretical curve. The observed coefficient $A_2 = -.070 \pm .005$ agrees closely with the value of -.0714

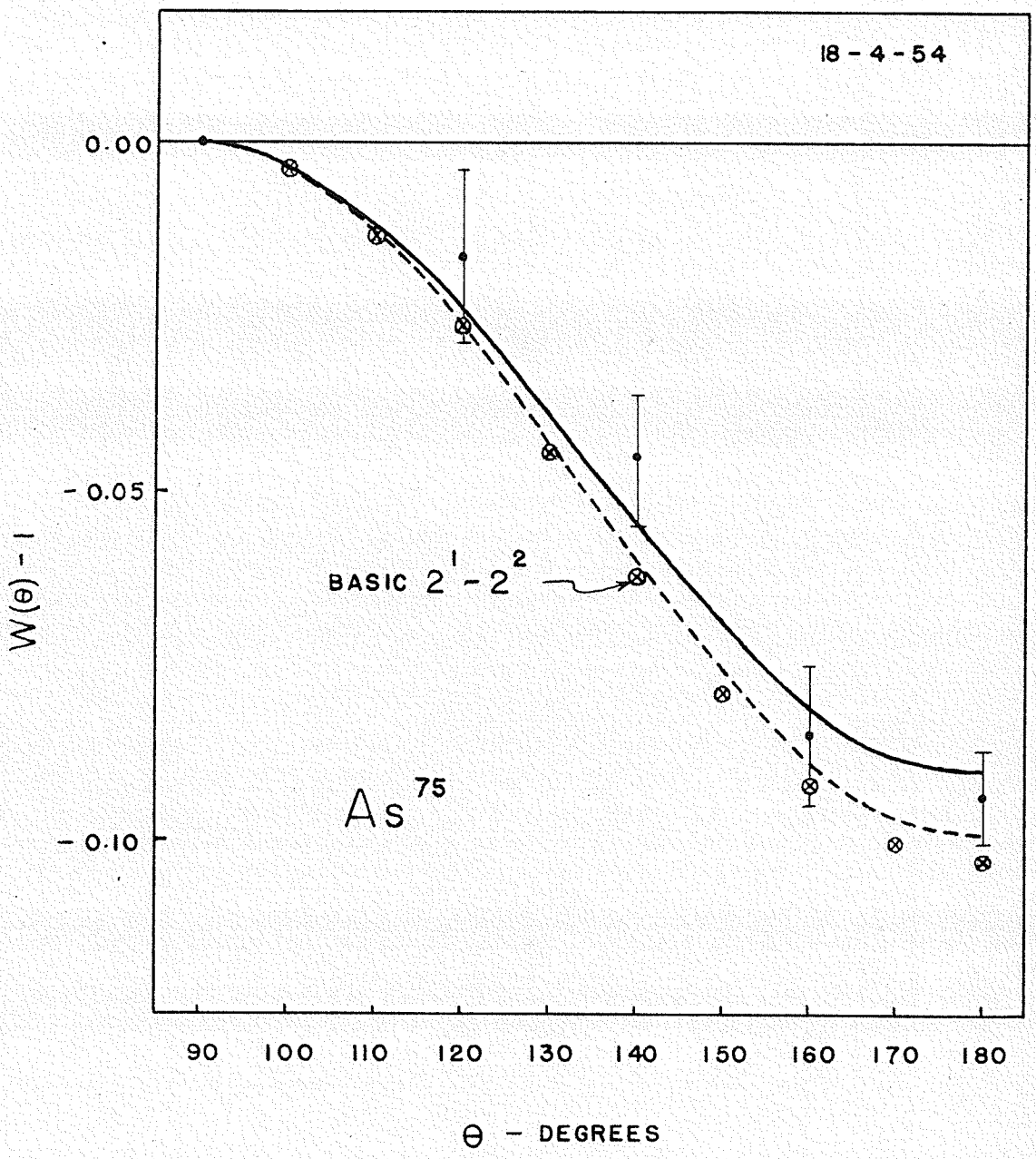

Fig. 21. Directional correlation function for the principal cascade in As^{75}. The full curve is a least squares fit to the experimental points; the dashed curve is the corrected curve; the points ⊗ lie on the theoretical curve for a 9/2(D) 7/2 (Q) 3/2 basic correlation.

taken from Lloyd's tables (14). The only possible spin assignment for this case is 9/2 (D) 7/2 (Q) 3/2. This is at variance with remarks (b) and (c) quoted above, however, and is highly unlikely. On the other hand, Schardt's work points quite definitely to spins of 5/2 and 3/2 for the levels at 405 and 0 kev respectively. Thus, the only other assignment possible is 5/2 (D) 7/2 (Q) 3/2 ($W(\theta) - 1 = -.153\ P_2(\cos\theta)$). Unfortunately, the correlation function in this case does not agree with experiment if the radiations have pure multipolarities.

If the intensity measurements due to Jensen are assumed to be valid (that is, if the ratio of the intensities of the 138 and 124 kev transitions is 10 : 1), an interference by the 124 - 281 kev cascade might alter the correlation for the $5/2 \rightarrow 7/2 \rightarrow 3/2$ spin assignment. To check this, the total asymmetry at 180° was calculated for the case of a mixture of the two cascades concerned. Intensity ratios of 10 : 1 and 5 : 1 were used for the 138 and 124 kev transitions. The results are tabulated below for 4 possible spin assignments for the 124 - 281 kev cascade. All the radiations are assumed to be pure multipoles.

	Spin Sequence for 124-281 kev Cascade	Asymmetry at 180°		Observed Asymmetry at 180°
		Int. Ratio 10:1	Int. Ratio 5:1	
a	$5/2 \rightarrow 1/2 \rightarrow 3/2$	-.192	-.170	
b	$5/2 \rightarrow 3/2 \rightarrow 3/2$	-.198	-.182	
c	$5/2 \rightarrow 5/2 \rightarrow 3/2$	-.214	-.214	-.1015
d	$5/2 \rightarrow 9/2 \rightarrow 3/2$	-.135	-.056	

For j = 1/2 (case (a)), the weak cascade would contribute nothing to the observed correlation because the radiations concerned would be emitted isotropically. In the case of b) and c) no reasonable intensity ratio will yield the observed correlation. Case d) is more promising, however; the correlation function for the weaker cascade is $W(\theta) - 1 = .3274\ P_2(\cos\theta) - .0344\ P_4(\cos\theta)$, which is positive from 90° to 180°. If 14% of the coincidences at 90° were due to the 124 - 281 kev cascade, the observed correlation could be justified. In spite of the good agreement with the observed intensities, there are two serious objections to this assignment: (1) It is difficult to reconcile a spin change of 3 units with the intensity suggested here for the 281 kev gamma ray; (2) The second transition could have the following multipolarities:- parity favored - E3 or M4, parity unfavored - E4 or M3. For a 280 kev transition involving any one (or a mixture) of these multipoles, the lifetime of the 281 kev level would be of the order of 2 to 3 seconds (55). This would completely destroy any correlation, or for that matter, any contribution to the coincidence rate.

Before drawing any conclusions from these arguments, further consideration of the gamma ray spectrum of Fig. 20 will prove profitable. Making no allowance for the asymmetry of the lines, the energy resolution was calculated for the two prominent features of the spectrum. The results were 19% and 14.7% for the 138 and 269 kev transitions respectively, after correcting for the gate width. These compare favorably with the values 19% and 13% obtained from the resolution - energy curve of Fig. 3 c). The implication is that the 124 - 281 kev cascade is considerably weaker than the main cascade. If this were not the case, one would expect a pronounced broadening of the lines, particularly in the case of the low energy line.

After careful consideration of the work of Schardt, Jensen and the author, the conclusion was reached that the 124 - 281 kev cascade can be disregarded as far as directional measurements are concerned. Until more accurate intensity measurements are available, the author feels unjustified in reaching any other conclusion. With this assumption, the observed correlation was assumed to be due primarily to the 138 - 269 kev cascade and re-examined, as outlined below.

Case (2) $W(\theta) - 1 = A_2 P_2 (\cos \theta) + A_4 P_4 (\cos \theta)$.

Of the two components of the principal cascade, only the 138 kev component is entirely unidentified with regard to multipolarity. From the preceding discussion, it is apparent that the 138 kev transition must involve a multipole mixture. Since $j_1 - j = 1$, an M1 + E2 multipole mixture was assumed to be the case.

Taking the form of W given above and the $5/2 \rightarrow 7/2 \rightarrow 3/2$ spin sequences, the least squares fitting to the experimental data gave the coefficients $A_2 = -.0617$ and $A_4 = -.0108$. For the mathematical analysis, the general form of W (equation (11)) was used. The functions W_I, W_{II} and W_{III} were evaluated using both Sharp's tables (13) and those of Biedenharn and Rose (7). They were found to be:

dipole - quadrupole:	$W_I = 8 - 1.224 P_2$
quadrupole-quadrupole:	$W_{II} = 8 + .2915 P_2 - 1.825 P_4$
mixed:	$W_{III} = 3.535 P_2$

Substitution of these equations into equation (11) and normalization of A_o to unity yields:

$$W(\theta) = 1 + \left\{ \frac{0.292 \delta^2 + 7.070 \delta - 1.224}{8 \delta^2 + 8} \right\} P_2 + \left\{ \frac{- 1.825 \delta^2}{8 \delta^2 + 8} \right\} P_4$$

where $\delta^2 = \dfrac{\text{intensity of E2 radiation}}{\text{intensity of M1 radiation}}$

The functions W_I, W_{II} and W_{III} are shown in Fig. 22. An examination of the form of the curves suggests that some mixture of the three could modify curve a) to agree with the observed correlation. The theoretical coefficients A_2 and A_4 were plotted as functions of δ as shown in Fig. 23. The line marked 1 indicates where the experimental value of A_2 lies on the curve $A_2(\delta)$. The line marked 2 indicates the equivalent position for A_4. For the quadratic mixing assumed here, it was found that no value of δ between the limits set by points 1 and 2 gave coefficients A_2 and A_4 in complete agreement with experiment. However, since δ is obviously small, the linear approximation due to Lloyd (14) (see equation (21)) was tried. For this case the expansion $W(\theta) - 1 = A_2 P_2 (\cos \theta)$ was again used. The dashed line of Fig. 23 shows a plot of $A_2(\delta)$ in this approximation. The value of δ consistent with the observed correlation was found to be $\pm .094$. Thus, of the transitions from the 405 to the 269 kev level, only .88% are electric quadrupole; the remainder are magnetic dipole. Following convention, the phase angle between the radiations is taken as 0°. The complete spin assignment for the principal cascade can now be written as 5/2 (99.12% M1, .88% E2)7/2(E2)3/2. This multipole mixture has the directional correlation found experimentally.

It is not necessary to reiterate in complete detail the conditions under which the above analysis was carried out. If the interfering cascade is weak and the spins of the ground states of Se^{75} and As^{75} are truly 5/2 and 3/2 respectively, the above analysis explains the observed correlation quite adequately. If this is not the case, further correlation experiments and analyses will have to await better intensity measurements. Of course, the possibility that both transitions are mixed cannot be conclusively ruled out by what has been done here, but this case has such a high degree of arbitrariness associated with it, that no further consideration will be given to it at this time.

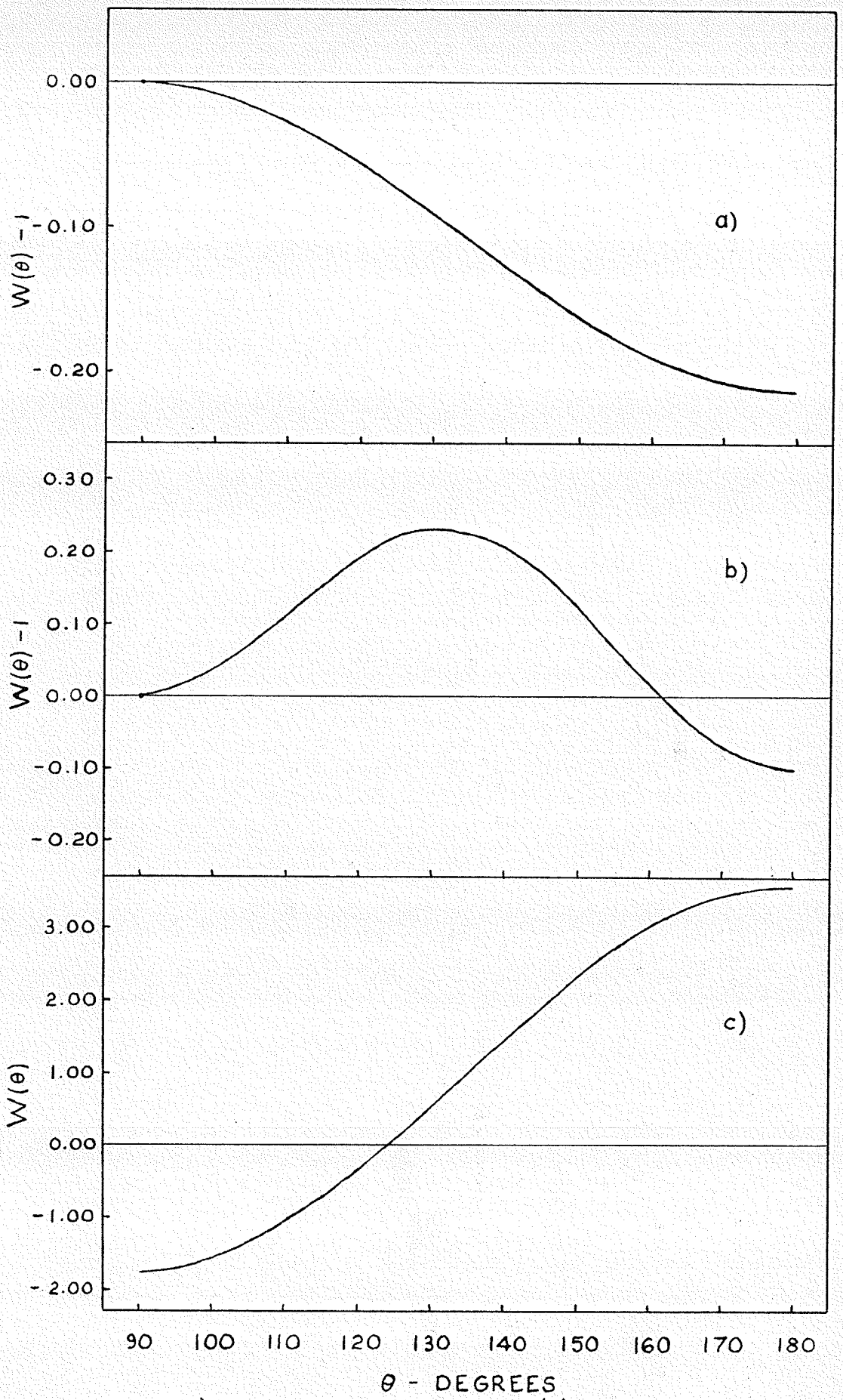

Fig.22 a) Plot of the D-Q function $W(\theta)-1 = -.153\ P_2$
b) " " " Q-Q function $W(\theta)-1 = .0365\ P_2 - .2285\ P_4$
c) " " " mixing function $W(\theta) = 3.535\ P_2$

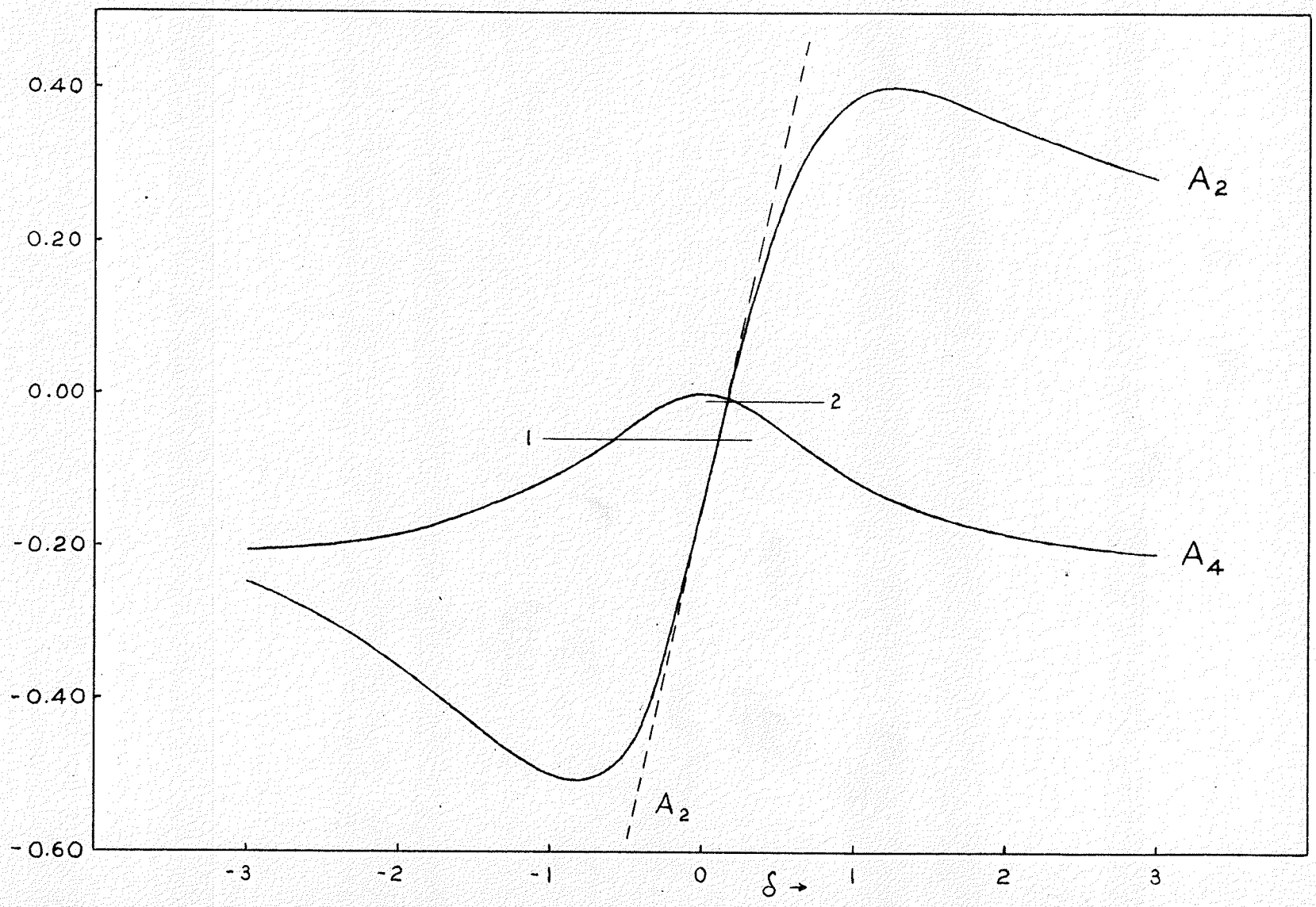

Fig. 23. The coefficients A_2 and A_4 as functions of δ for the assignment 5/2 (D,Q) 7/2 (Q) 3/2.

f) The Decay Scheme of Antimony -124; Directional Correlation in Tellurium - 124

This decay scheme has received much attention in recent years because of its importance to the theory of β -decay. A variety of experiments using β -ray, scintillation and coincidence spectrometers have been performed. However, rather than tabulate all the references to the early work here, a paper by Langer, Lazar and Moffatt (56) is cited which will supply the reader with a complete bibliography. In this section, reference will be made only to the more recent contributions to the literature.

The accepted level scheme for Te^{124} is shown in Fig. 24. (Note that the energy values of the gamma rays agree with those of the levels to within $\pm$ 15 kev.) The absence of the ground-to-ground β -transition, results in a very high intensity for the 600 kev gamma radiation. The triple cascade (642, 715 and 600 kev gamma rays) has been discussed by several workers (56, 57). Langer (58) has given the results of a triple coincidence experiment which established conclusively the order of the three radiations concerned. Coincidence studies with the 1690 - 600 kev, and 2090 - 600 kev gamma ray cascades have also been carried out (56, 59). These have not been completely satisfactory in the author's estimation, for the line at 2090 kev in the coincidence spectrum was not resolved distinctly. (This has been accomplished in the present work, however, as will be shown later.) The transitions between the1315 kev level and those at 2290 and 2690 kev have been detected by Lazar (60) and the author. In addition, a gamma ray at 120 kev has been reported once (61) but has not been found in subsequent investigations. The spin assignments of Fig. 24 will be discussed in detail later.

Prior to undertaking directional measurements, it was decided

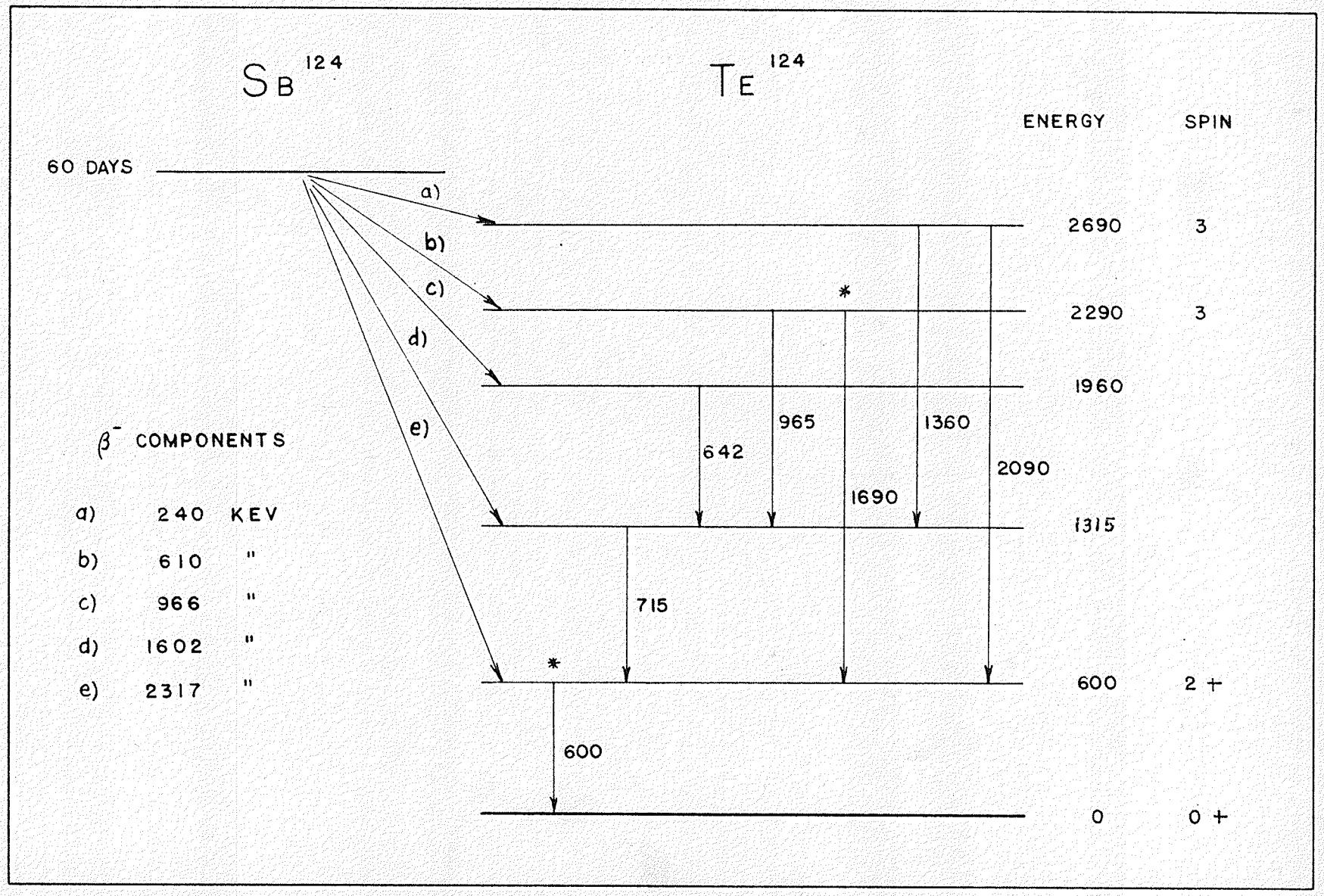

Fig. 24. Levels in Te^{124} following negatron emission in Sb^{124}.

to re-investigate the entire gamma ray spectrum in an effort to clear up some of the minor difficulties e.g. the absence of gamma rays at 965 and 1360 kev, the lack of good resolution in earlier coincidence experiments, and the doubtful existence of the 120 kev gamma ray.

The Sb^{124} source was supplied by Atomic Energy of Canada Ltd. Pure antimony metal was irradiated with slow neutrons in the pile, forming Sb^{124} through the reaction Sb^{123} (n, γ) Sb^{124}. The source strength was estimated to be .005 mc. Its physical form was a column 3 mm in diam. x 7 mm in height, of very small irregular pieces sealed into a plastic cup with paraffin. Since the greater dimension was vertical, the source possessed adequate symmetry for directional measurements in a horizontal plane.

The gamma ray spectrum was studied using spectrometer #2 with a 0.5 volt gate. The bulk spectrum above 200 kev is shown in Fig. 25. The photoelectron line at 600 kev is composite, containing, as it does, the strong 600 kev gamma ray and the weaker one at 645 kev. On the high energy side of this line, some evidence for the 715 kev gamma ray can be seen. The high energy radiations at 1690 $\pm$ 10 and 2090 $\pm$ 10 are in evidence at the end of the spectrum. The energies of these several lines were determined using the well-known gamma rays of Cs^{137} (662 kev), Zn^{65} (1114 kev) and Co^{60} (1172, 1332 kev).

In Fig. 26, the results of a more detailed examination of the spectrum are displayed. (Note: The counting rates in the figures have not been normalized.) Fig. 26 a) shows the backscattered line at 190 kev (due to all the radiations above 600 kev), the Compton edge of the 600 kev line and a smaller line at 110 kev. The photoelectron lines of Se^{75} at

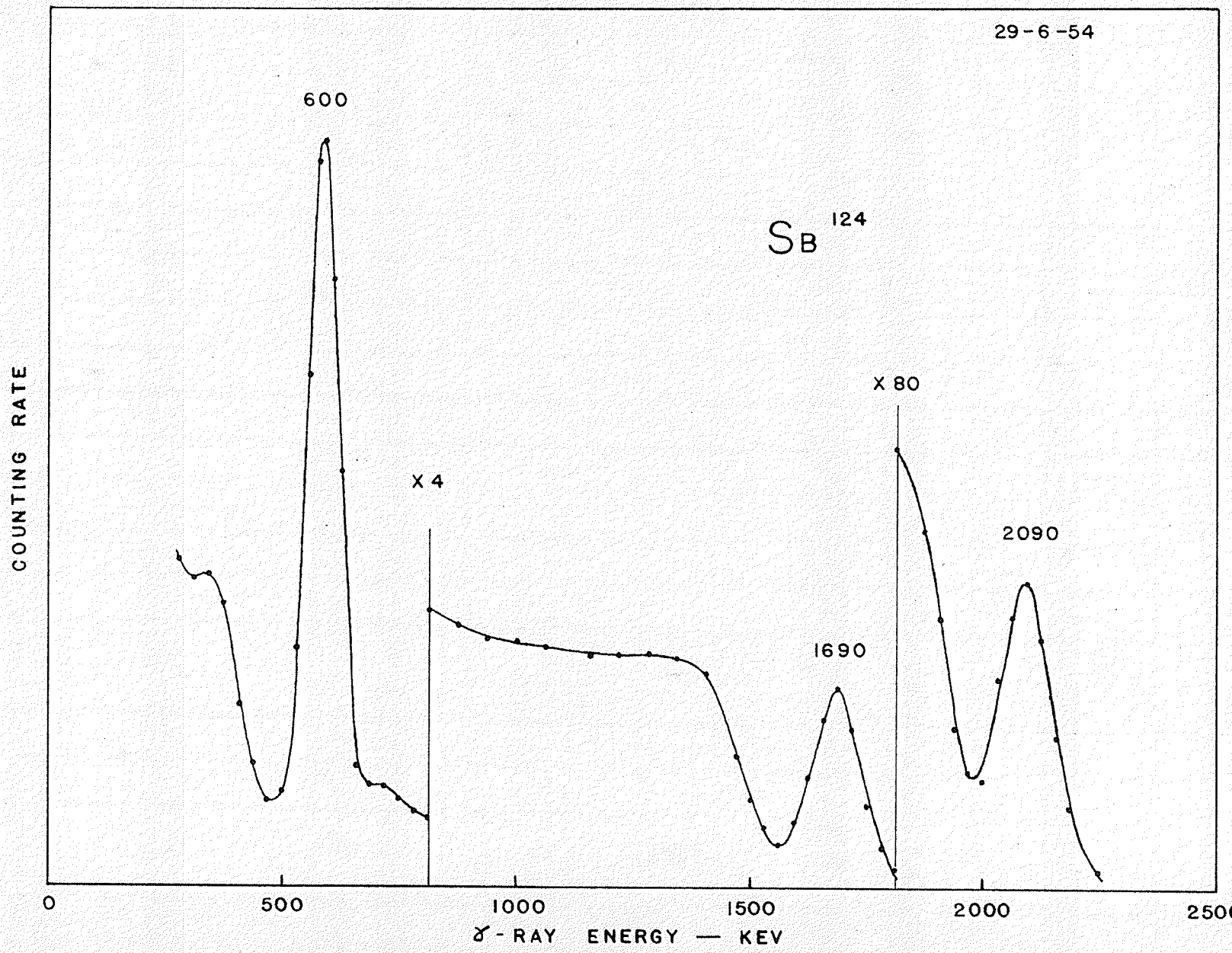

Fig. 25. Bulk gamma ray spectrum of Sb^{124} above 200 kev.

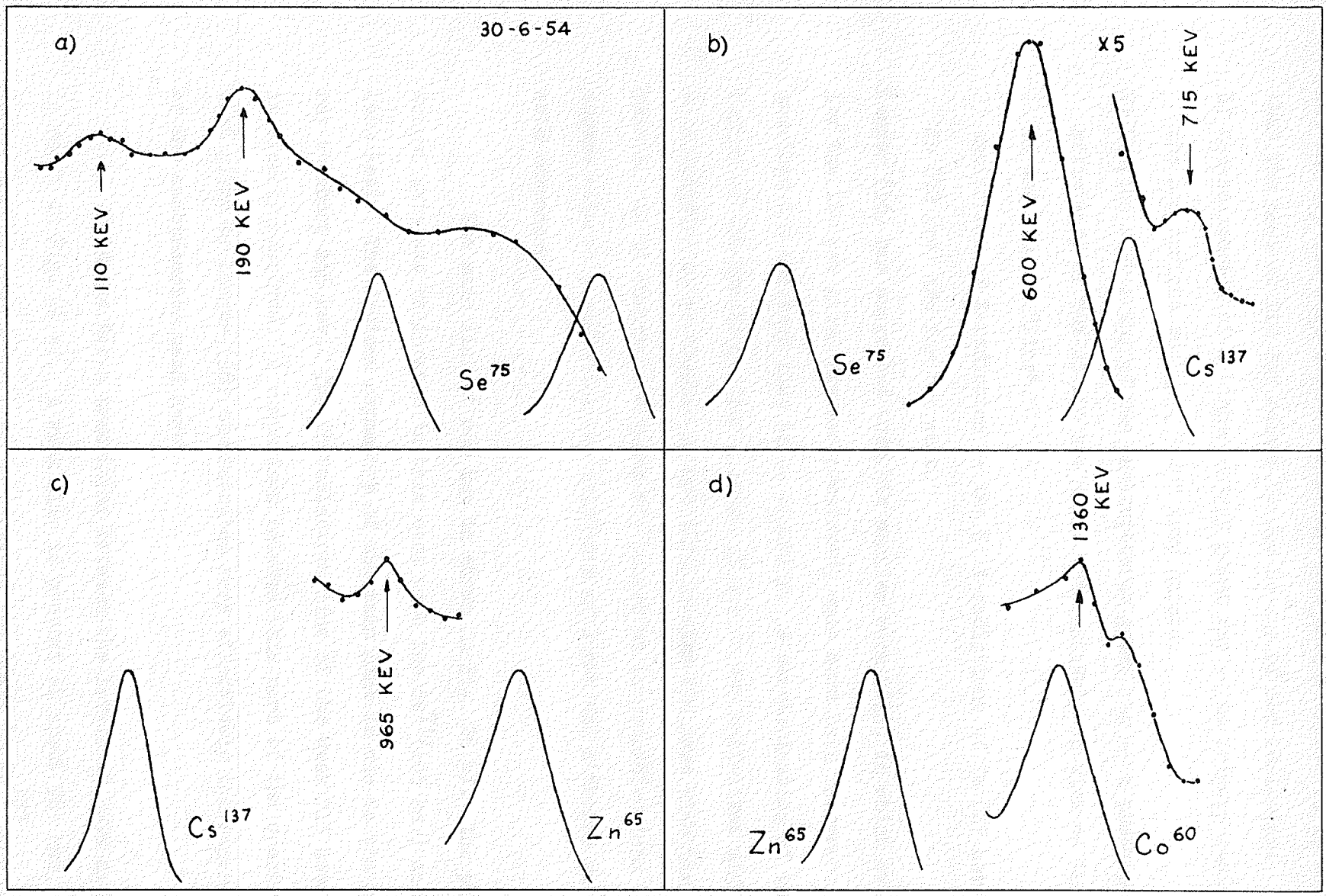

Fig. 26. Details of the gamma ray spectrum following negatron emission in Sb^{124}. See text for the details on the gamma ray standards used.

269 and 405 kev were used to calibrate the energy axis. It is concluded that the peak at 110 kev cannot be due to any of the following:

1) backscattering of a higher energy gamma ray — no primary radiation of the appropriate energy (~ 200 kev) exists.
2) Compton scattering of the backscattered gamma ray -- a photo-peak efficiency of 90% at 200 kev makes this unlikely in view of the intensity of the 110 kev "line".
3) excitation of X-radiation -- the K X-radiations of Te (27 kev) and of Pb (72 kev) are far too soft.

Langer (56) has suggested that his earlier work (61), in which evidence for the 120 kev gamma ray was presented, must have been in error. He ascribed the observed line to an impurity. A re-examination of this region of the spectrum after a lapse of one or two half-lives might lead to a decision as to whether or not this is also the case with the present source. As it stands, the gamma ray cannot be incorporated into the decay scheme without postulating the existence of a new and hitherto unreported beta component.

The main line at 600 kev is shown in Fig. 26 b). The pulse height axis was calibrated in this case with the Se^{75}(405 kev) and Cs^{137} (662 kev). The decided asymmetry of the main line is due to the gamma ray at about 645 kev. The photoelectron line of the weak 715 kev radiation is clearly resolved. A comparison between this part of the spectrum with that given by Langer (56) demonstrates very effectively the superiority of the spectrometer used here.

Evidence for a transition between the levels at 2290 and 1315 is shown in Fig. 26 c). A weak line is present at about 965 kev, the energy having been determined in terms of the lines in Cs^{137} and Zn^{65}

(1114 kev). Since it cannot be a pair line due to one of the high energy components, it was taken to be the photoelectron line of an unreported gamma ray.

Fig. 26 d) shows the result of a detailed study of the region near 1360 kev. The 'step' in the Compton edge, though small, was reproducible. The peak of lower energy was taken to be the photoelectron line due to a 1360 kev gamma ray; such a radiation fits the decay scheme quite well. The Compton maximum of the 1690 kev gamma ray has an energy of about 1460 kev, which is in good agreement with the energy of the 'step' - 1450 kev. The energy determinations in this case were made in terms of Zn^{65} and Co^{60}(1332 kev).

During the course of this investigation, a paper by Lazar (60) appeared which substantiated the present conclusions, although somewhat different energies were quoted for several of the transitions.

The coincidence work mentioned earlier was checked with the spectrometer, taking full advantage of its superior resolution. The detectors were placed at 180° with respect to one another and brought up close to the source. Both were shielded with 2 mm lead plates. Spectrometer #1 was set to detect the photoelectron line at 600 kev; the gate of the second spectrometer was widened to 1 volt and swept across the high energy region. Fig. 27 a) and b) exhibits the results of the experiment. a) shows the two high energy lines when scanned with spectrometer #2 only, using a one volt gate; b) shows the high energy end of the spectrum as determined with the coincidence spectrometer. The correspondence between the two runs is remarkably good. The line at 2090 kev is quite distinct in b). Using a similar arrangement, Langer (56) reproduced the high energy

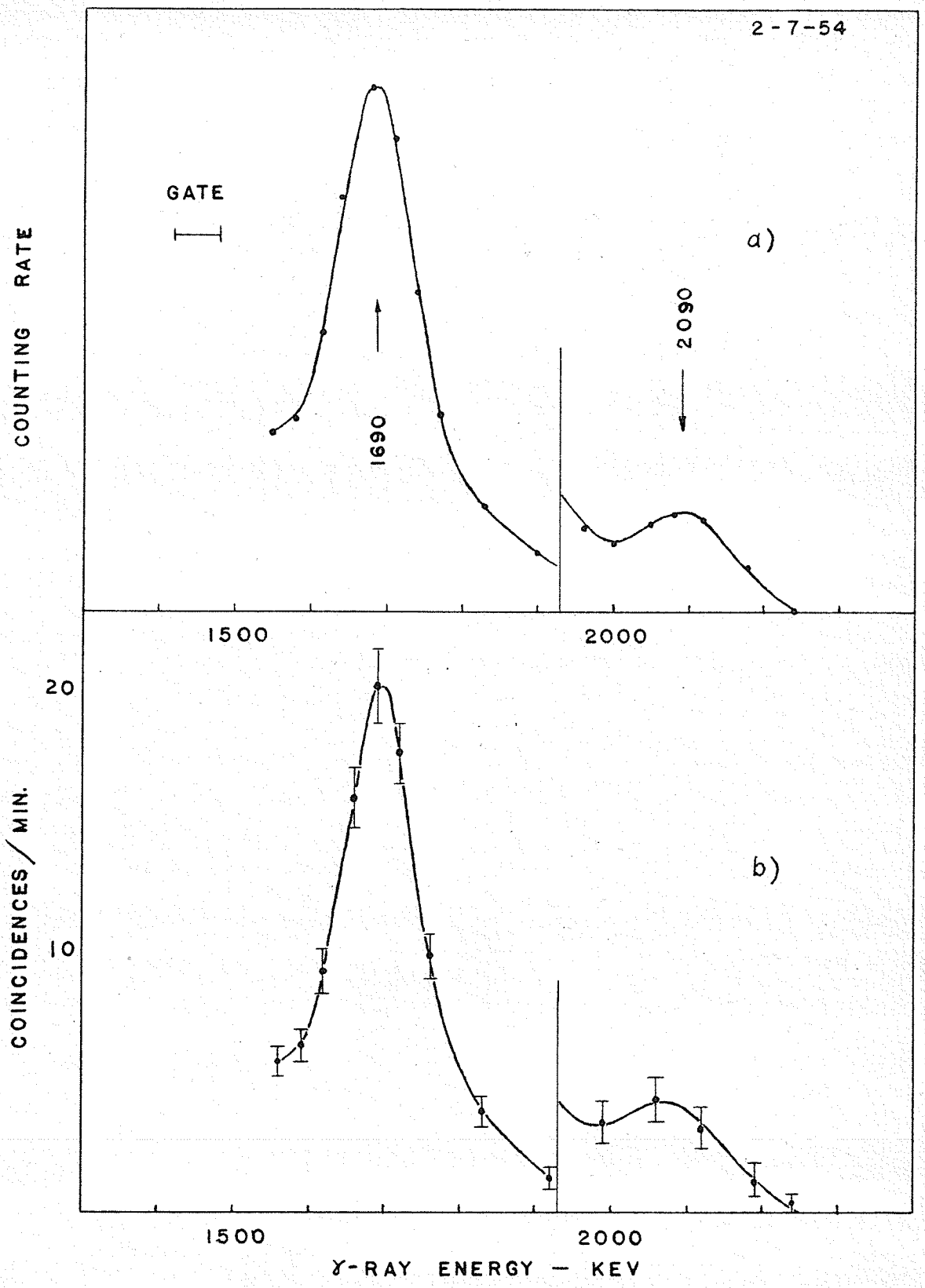

Fig. 27 a) Photoelectron lines due to gamma rays at 1690 and 2090 kev (gate width: 1 volt).
b) Spectrum of coincidences between the line at 600 kev and the high energy end of the spectrum (same gate width).

end of the ordinary spectrum in his coincidence spectrum, but was unable to resolve either line distinctly. The present investigation eliminates the need for any qualitative discussion of the coincidence spectrum; both lines are completely resolved.

The decay scheme of Fig. 24 now appears to be well founded on experiment, the only anomaly being the 110 kev radiation. In view of this, we shall now direct our attention to the spin assignments for the levels in Te^{124}.

Metzger (62) has measured the K-conversion coefficient for the 600 kev gamma transition in Te^{124}. His result agrees closely with the theoretical value for E2 radiation as given by Rose et al. (63). (This furnishes another example of the validity of the empirical rules for even-even nuclei.) Some $\beta - \gamma$ correlation experiments have been performed which tend to confirm this result. Stevenson and Deutsch (64) and Darby (65) have measured the $\beta - \gamma$ correlation for the 2317 kev beta component and the 600 kev gamma ray. Their results agree with either of the spin assignments $1 \rightarrow 1 \rightarrow 0$ or $3 \rightarrow 2 \rightarrow 0$ (the first number in a sequence in this case denotes the spin of the Sb^{124} ground state.) An examination of the correlation functions suggests that above 1600 kev where the electrons are due to the highest energy beta component only, the results are in somewhat better agreement with the latter spin assignment. However, since the asymmetries at 180° differ by only 17% for the two sequences, and the experimental errors are very large, it is difficult to reach an unambiguous conclusion. Of course, one is inclined to accept the $3 \rightarrow 2 \rightarrow 0$ assignment in view of Metzger's work.

Further evidence for the spin assignment of Fig. 24 has been obtained from gamma-gamma directional correlation studies. Early experi-

ments (66) with Sb^{124} suggested that the radiation was isotropic, but the lack of energy selectivity invalidates this conclusion. Some asymmetry was found by Kraushaar and Goldhaber (67), but their work contained two serious flaws - 1) the angular corrections for 511 kev radiation were used even though all the gamma rays involved had energies in excess of 600 kev, and 2) integral biasing was used on the counters (one was set to detect radiations above .1 Mev and the other those above .7 Mev). The principal contribution to the coincidence rate was assumed to be due to the 1690 - 600 kev cascade. It was found that the 180° asymmetry was 25% less than that predicted by theory for a $3 \rightarrow 2 \rightarrow 0$ spin sequence assuming pure radiations. An M1 - E2 mixture was assumed for the first component of the cascade (1690 kev) and the mixing ratio estimated.

Metzger (68) repeated the experiment shortly afterwards and arrived at a somewhat different conclusion. He used differential discriminators for energy selectivity, but he employed the same inappropriate angular resolution correction in his analysis. For a superposition of the 1690 - 600 kev and 2090 - 600 kev cascades, he found $a_2 = -.094 \pm .010$, after correcting for angular resolution. (The theoretical value is .1032 if the spins of the 2290 and 2690 kev levels are the same.) Using Lloyd's linear mixing approximation, it is not difficult to show, as Metzger did, that the first transition in the cascade contains at the most .001 parts E2 to one part M1. On the basis of the magnitude of the mixing ratios which have been observed to date, Metzger rejects the possibility of such a mixture in this case. From the measured intensities of the 600 and 1690 kev gamma rays, and the observed numbers of conversion electrons due to each (the latter determined by a group at Princeton University (68)), Metzger arrives at a value of 2.6×10^{-4} for the conversion coefficient of the 1690 kev radiation. If one uses the Princeton

data and the intensities given by Lazar (60), however, the coefficient becomes 3.3×10^{-4}, and with the author's intensity measurements, $\sim 3 \times 10^{-4}$. Metzger quotes the theoretical value for an E1 transition as 2.2×10^{-4} and for an M1 + .001 E2 transition as 5.8×10^{-4}. On this basis he assumes the 1690 kev radiation is E1 and assigns a negative parity to the 2290 and 2690 kev levels.

It is interesting to note that Hutchinson and Wiedenbeck (69) in an earlier investigation were unable to detect conversion electrons for the 1690 kev transition. They set an upper limit of 5×10^{-4} on the conversion coefficient and ruled out E3 and M4 as possible multipolarities for the gamma ray.

Although Metzger's results look good, they conflict seriously with some theoretical work done by Morita and Yamada (70). These authors can explain the observed beta-gamma correlation assuming that (a) the spin and parity assignment is $(3-) \rightarrow (2+) \rightarrow (0+)$ and (b) the 2317 kev beta component is first forbidden (see reference (69)). They reject the $(4+) \rightarrow (2+) \rightarrow (0+)$ sequence, because it is in complete disagreement with the observed beta-gamma correlation. If one calculates the log ft values for the 240 and 610 kev beta transitions, one gets 7.1 and 7.8 respectively, in good agreement with the empirical value for the first forbidden class of transitions. However, if the ground state of Sb^{124}, and the 2290 and 2690 kev levels in Te^{124} all have spin of 3 and odd parity, these two beta transitions should be allowed. In order to avoid this complication, Metzger suggests the assignment 4+ for the ground state of Sb^{124} but, of course, this conflicts with both the beta-gamma correlation measurements and their theoretical interpretation.

As far as gamma-gamma directional measurements are concerned,

Metzger's results are the only reliable ones available in the literature. However, it was decided to re-examine the 1690 - 600 kev cascade for two reasons: 1) the factor used by Metzger to correct his data was inappropriate, and 2) it was found possible to isolate the cascade in question.

The source described above was used in the experiments. The counters were protected from scattered radiation by the usual conical shields and 2mm thick lead plates. With the counters in the usual position for directional studies, one discriminator set to accept pulses in the 600 kev line and the other, pulses in the 1690 kev line, it was found that the net coincidence rate was about 5 counts per minute, of which 0.5 were accidental. Moving the second discriminator to the 2090 kev line resulted in a negligible genuine coincidence rate. This was due to the small solid angles subtended by the detectors and the extremely low intensity of this transition. It was assumed, then, that all the coincidences detected in the previous run were due to the 1690 - 600 kev cascade. The observed correlation function is shown in Fig. 28. As usual, the dashed curve is the corrected least squares fit to the experimental points. The form of the function was assumed to be $W(\theta) - 1 = A_2 P_2 (\cos \theta) = a_2 \cos^2 \theta$. ($A_2 = -.0712 \pm .006$, $a_2 = -.1030 \pm .008$). The correction factors, J_2/J_o for 1690 and 662 kev radiations were used (see Table I). The points - ⊗ - lie on the theoretical curve for a basic dipole - quadrupole correlation. Since the transition from the 2290 kev level to the ground state of Te^{124} is not observed, the only possible spin sequence for the levels concerned is $3 \rightarrow 2 \rightarrow 0$. Of course, the experiment is parity insensitive and so a definite parity assignment cannot be made. However, in view of the discrepancy between the conversion measurements of Hutchinson and the Princeton group mentioned by Metzger, the author feels that an independent determination of the relative parity of the 600 and 2290 kev levels is

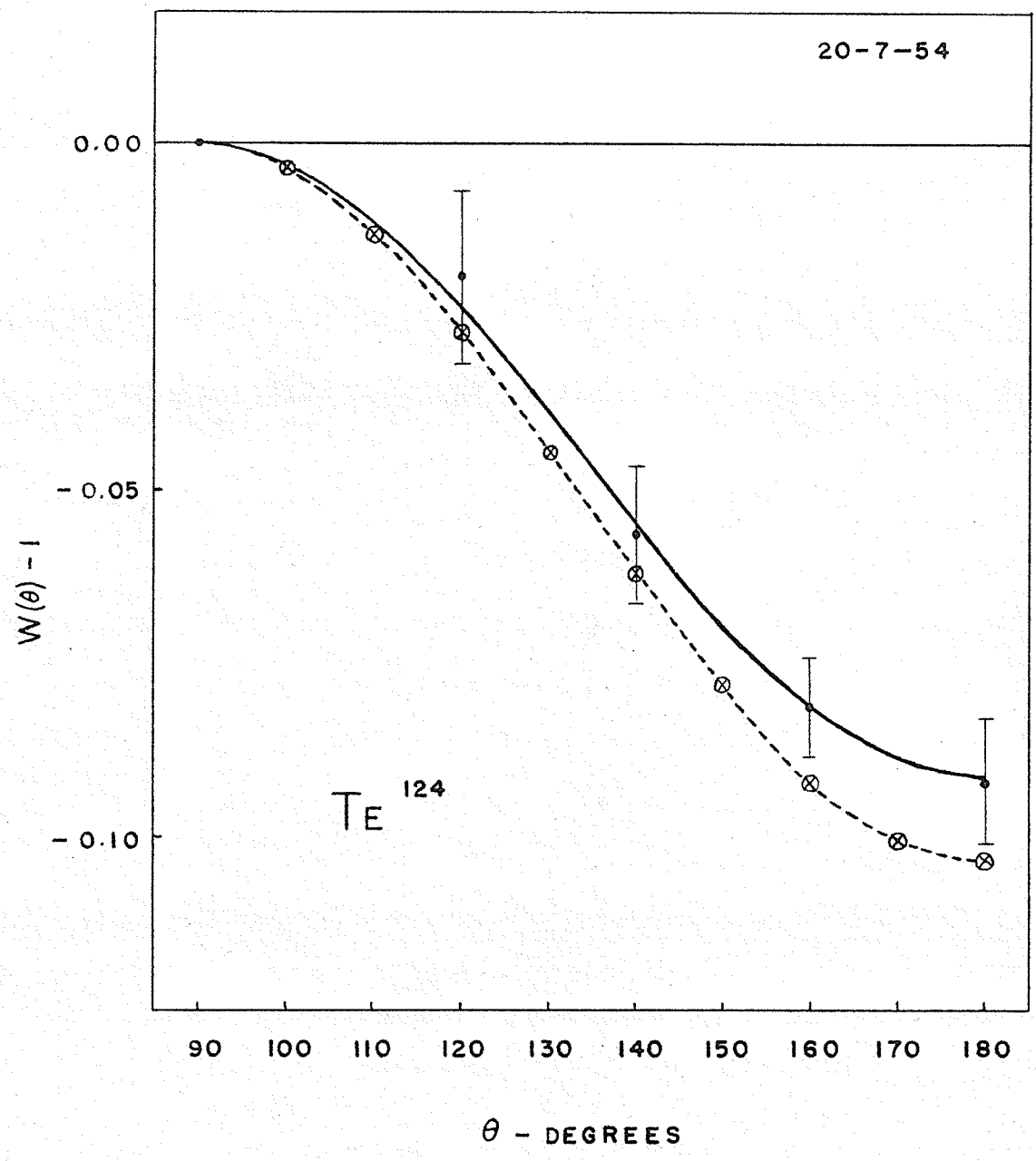

Fig. 28. Directional correlation for the 1690 - 600 kev gamma ray cascade in Te^{124}. The full curve is a least squares fit to the experimental points. The dashed curve is the least squares fit corrected for the effect of finite angular resolution. The points ⊗ lie on the basic correlation for the spin assignment 3 - 2 - 0.

necessary. If the log f t value of the 610 kev beta-transition is regarded as having no significance when it comes to determination of the degree of forbiddenness, then the assignment (3-) to the ground state of Sb^{124} and the 2290 kev level of Te^{124} is valid, and the 610 kev beta transition is allowed. Metzger must feel that it is necessary to retain the first forbidden character of this beta component, however, for he ascribes the assignment (4+) to the ground state of Sb^{124}. This, of course, is at variance with Morita's conclusions on the beta-gamma correlation. (The reader is referred to Morita's paper (70) for an excellent discussion of the (4+) → (2+) → (0+) assignment for the beta-gamma cascade.)

The present investigation has removed any possibility of the 1690 kev transition being mixed. The data indicate a pure dipole transition, whether magnetic or electric. It appears, then, as though the problem can be resolved only by 1) a re-evaluation of the conversion coefficient for the 1690 kev transition, or 2) a gamma-gamma polarization-direction experiment. Further work with the beta-gamma correlation might be profitable also. Many improvements in technique have been made since the early work was done.

To summarize the situation, the following remarks are appended. The assignment of spin 3 to the level at 2290 kev (and probably to that at 2690 kev if Metzger's results are accepted) has been established by a directional correlation experiment. Odd parity has been assigned to the levels by Metzger on the basis of intensity and conversion measurements. The net result disagrees with the observed log ft values for the beta-transitions concerned. On the other hand, if even parity is assigned to the levels, the result is in agreement with the observed value of log ft but not with internal conversion measurements (68). Unless theformer is

to be completely ignored, the parity assignment to the 2290 kev level in Te^{124} must be regarded as still in doubt. It is suggested that a polarization-direction experiment might resolve the difficulty.

In addition to the experiments described above, an attempt to detect the triple directional correlation due to the 642 - 715 - 600 kev cascade was made. Each discriminator was set to detect all three gamma rays. An asymmetry of about $\pm$ .1 was obtained at 180° after correction for the background coincidences due to several overlapping correlations. In view of the exceedingly large errors involved in the work, however, the investigation was discontinued after the 180° asymmetry had been measured. It was felt that the chance of securing unambiguous results from so complex a situation was rather remote. No interpretation of the result quoted is attempted here.

g) Directional Correlation in Tungsten - 182

The gamma ray spectrum associated with the beta-activity in Ta^{182} is one of the most complicated known, containing as it does some 27 radiations. The gamma rays fall into two main groups - one with several components all of whose energies are less than 300 kev, and the other with three strong components with energies in excess of 1000 kev. Cork et al. (71, 72) and Pearce and Mann (73) have studied the gamma rays using beta-ray spectrometers. Muller et al. (74) have carried out very accurate energy determinations as have Boehm et al. (75). Both groups used curved crystal spectrometers. Mihelich (76) has reported some coincidence work which was undertaken to determine the order of the levels in W^{182}. Fowler et al. (77) have recently presented a level scheme which incorporates all the intense radiations and which agrees very well with that given by Boehm. Both groups have presented possible spin assignments

which differ from one another quite markedly for the higher levels - that is, for levels above 1200 kev. They agree that, being an even-even nucleus, the ground and first excited states of W^{182} should have spins 0 and 2 respectively and even parity. From that point, however, the two assignments diverge.

The level scheme of Fig. 29 is due to Fowler. The spin assignments shown on the left were determined from conversion data. Evidence for a level at 680 $\pm$ 5 kev, predicted by the collective model of the nucleus, is mentioned by Fowler, but no details are given in the paper. (It is interesting to note that the location of the level at 1222 kev is correctly predicted by this model.) The expected spin for the 1222 kev level is 8, which is in complete disagreement with the assignment quoted. On the other hand, Boehm et al. assign spin 2 and even parity to this state, and spin 2, odd parity to the level at 1289 kev. The experiment to be described here was performed in an effort to resolve this discrepancy.

The reader might well ask why these particular levels were chosen for investigation by the author.. There are two reasons for the choice:

1) The levels concerned are the only two in the scheme to which spins have been assigned by two independent groups. The assignments in this case are at variance with one another. It might be possible to prove one of these incorrect. In addition, since the collective model predicts a spin of 8 for one of these (1222 kev), there is the added opportunity of checking a theoretical prediction.
2) The transitions from these levels to the ground and first excited states are intense, as is the transition between the levels. In a scheme as complex as that of W^{182}, the only chance of getting

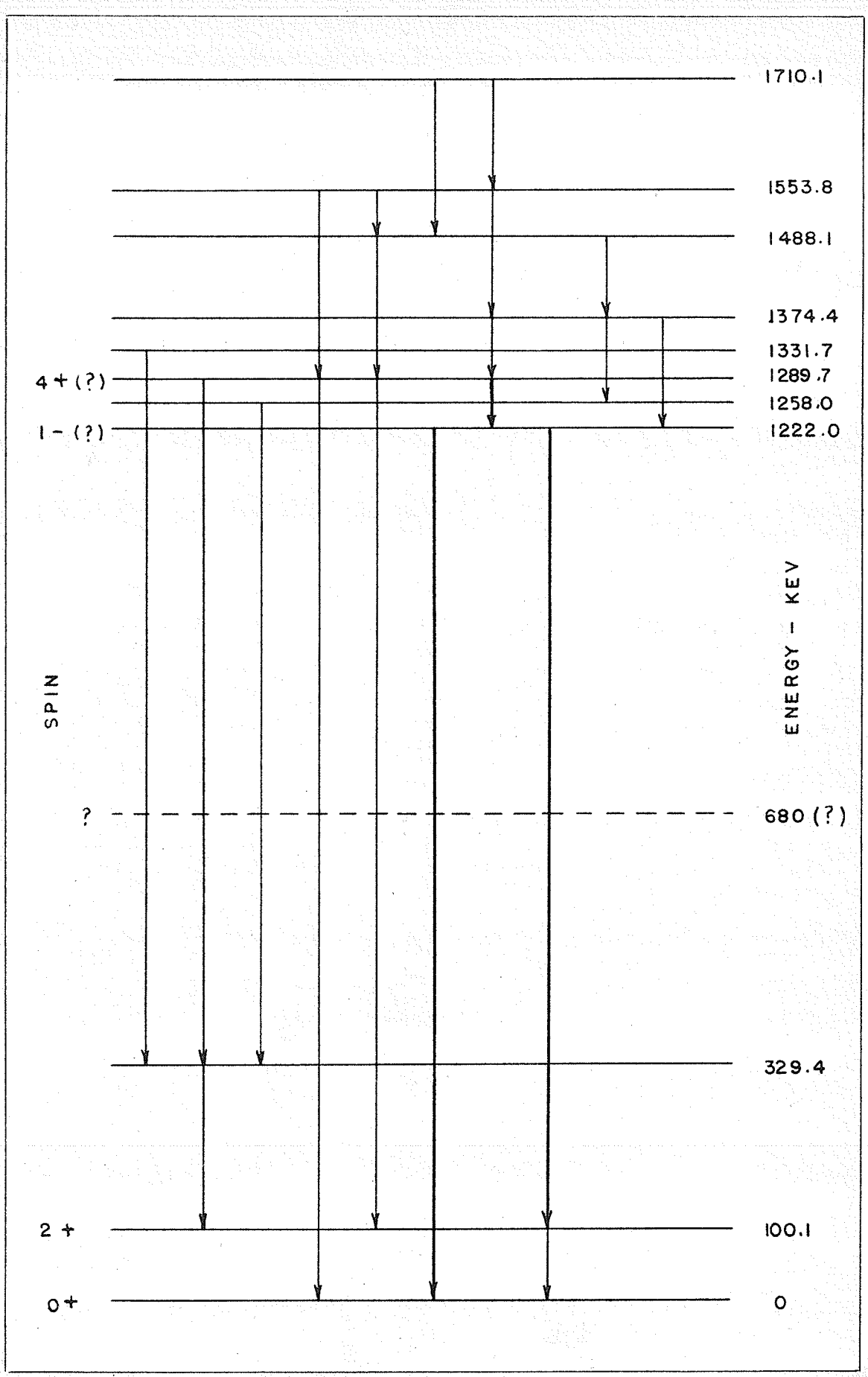

Fig. 29. Energy levels in W^{182} (Fowler et al.(77)). Directional correlation experiments performed with boldface transitions.

unambiguous results is to work with the intense transitions. This point is, perhaps, more easily appreciated after a consideration of the gamma ray spectrum which will now be discussed.

The Ta^{182} source was prepared by irradiation with slow neutrons of pure tantalum metal. The irradiation was carried out in the Chalk River pile. The reaction involved is $Ta^{181}(n, \gamma)\ Ta^{182}$. The source had a strength of only .01 mc. Its physical form was a 1/8" diam. spherical pellet. This was regarded as well suited to directional experiments. Of course, as in previous work, it was assumed that the use of a metallic source would eliminate any possibility of perturbations of the nuclear system by the electronic shells of the atom.

The gamma ray spectrum associated with the decay of Ta^{182} is shown in Fig. 30. It was obtained with spectrometer #2 using a 0.5 volt gate. The two main groups of radiations are easily identified. Each line of the spectrum is composite to some extent, of course. In the case of the line at 65 kev, the only interfering radiation is 11 times weaker than the 67.7 kev transition. The latter occurs between the levels at 1289 and 1222 kev. The high energy group contains lines at 1121, 1189 and 1222 kev, with relative intensities 120, 56 and 115 respectively. (The 67.7 kev transition is assumed to have an intensity of 100.) The pulse height axis for this spectrum was calibrated using the strong lines in Se^{75}, Cs^{137}, Zn^{65} and Co^{60}. A search was made for the ground state transition from the proposed level at 680 kev, but no evidence for its existence was found. The result suggests that either this level is not excited by beta-decay in Ta^{182}, or the transition to the ground state is highly forbidden. Of course, the 'background' due to the high energy gamma rays made the experiment difficult to perform.

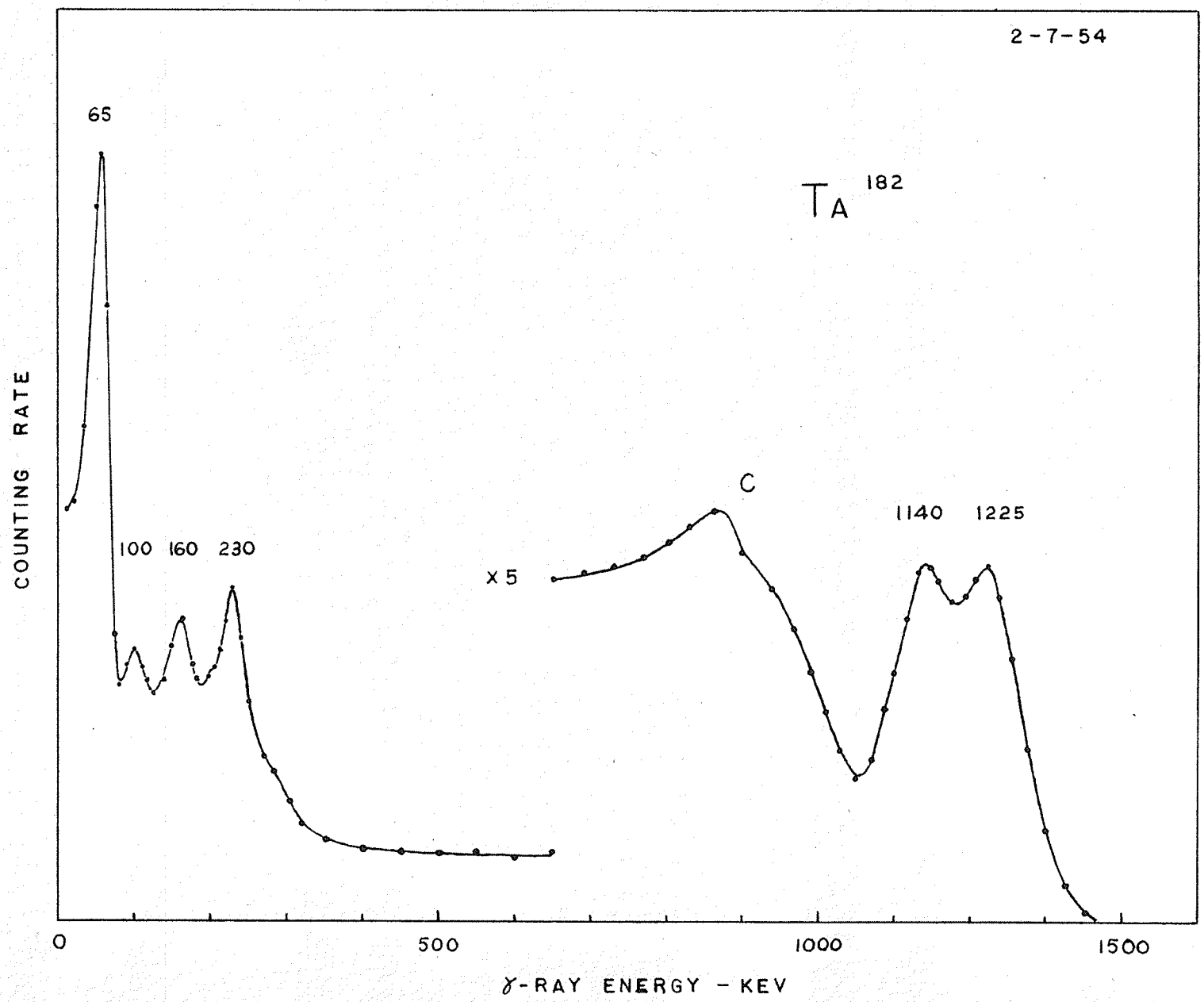

Fig. 30. Spectrum of gamma radiation following negatron emission in Ta^{182}.

Before discussing the correlation measurements, some consideration should be given to the possible correlations which might be detected. We shall consider Fowler's assignment first. Throughout the discussion, it will be assumed that only pure multipoles are involved in the transitions.

If the 67 - 1222 kev cascade has a spin sequence $4 \rightarrow 1 \rightarrow 0$, the associated correlation function is $W(\theta) - 1 = -.125\ P_2 (\cos \theta)$. On the other hand, if the 67 - 1122 kev cascade has a spin sequence $4 \rightarrow 1 \rightarrow 2$, its correlation function is $W(\theta) - 1 = -.0125\ P_2 (\cos \theta)$. Since the 1122 and 1222 kev gamma rays are very nearly of the same intensity, a simple calculation shows that if these two correlations are observed simultaneously, the asymmetry at 180° will be about -.090, uncorrected for angular resolution. In view of what was accomplished with Se^{75} and Sb^{124}, it was felt that such an asymmetry could be detected without too much difficulty. If, however, the spin of the 1222 kev level is 3, then the expected asymmetry at 180° is -.038.

Should the spin of the level at 1222 kev be an even integer (0, 2 or 4) different conclusions must be drawn. For the case $j = 0$, the 1222 kev transition becomes absolutely forbidden, which contradicts the experimental results. If $j = 2$ or 4, the combined cascades will exhibit a positive correlation.

If Boehm's spin assignments are correct, the correlation function for the 67 - 1222 kev cascade $(2 \rightarrow 2 \rightarrow 0)$ is $W(\theta) - 1 = + .250\ P_2 (\cos \theta)$. For the other cascade, assuming a) pure radiations and b) minimum multipole orders consistent with the selection rules of P. 8, $W(\theta) - 1 = .175\ P_2 (\cos \theta)$. The net correlation for this case would be a positive one. We shall return to this point later.

To measure the asymmetry due to the combined cascades, the gate of discriminator #1 was set on the low energy side of the 65 kev line, while discriminator #2 was set on the broad line at the high energy end of the spectrum. The high energy lines are in coincidence with the 100 and 152 kev gamma rays, also. Fortunately, at these low energies, the photo-peak efficiencies are 100% and 98% respectively, so that the 'low energy gate' would not detect pulses due to these radiations. Even for the 230 kev line, the interference would be negligible, since the photo-peak efficiency for this case is 83% and the remaining 17% of the pulses are distributed over a fairly wide energy range.

It was found necessary to remove the lead shielding from the low energy detector to minimize the excitation of the K X-radiation of lead. This X-radiation would not only mask the line at 65 kev, but also increase the accidental coincidence rate. The frontal lead absorber on the high energy counter was increased to a thickness of 5 mm, however, to compensate for the lack of lead on the other detector. It was felt that this thickness of lead would reduce the occurrence of backscattered coincidences to negligible proportions. The coincidence rate with the arrangement described was found to be about 32 counts per minute, of which 20 were accidental. The high background made it necessary to measure the resolving time - τ - more often than was done in previous experiments. In view of the large error associated with the determination of a point, it was decided to measure the asymmetry at 145° and 180° only, rather than obtain a complete correlation curve.

The observed asymmetries are shown in the accompanying table.

Angle	$N_{\theta}/N_{90^{\circ}}$	Asymmetry
0°	1.000	0
145°	.934	-.066
180°	.950	-.050

The results seem to suggest that backscattering at the 180° position was contributing to the genuine coincidence rate.

The observed asymmetries could not be corrected for angular resolution without a knowledge of the correlation coefficients A_{2k}. However, some qualitative remarks can be made about the results.

It is apparent that any correction for angular resolution will increase the asymmetry. If this is kept in mind, then for Fowler's decay scheme, the assignment of spin 3 to the 1222 kev level would be inconsistent with the experimental facts. On the other hand, the assignment of a spin of 1 to the state is not in complete agreement with the observed asymmetry either. Of course, if the effect of backscattering is large, which it may well be, good agreement between experiment and theory could not be expected.

As was mentioned above, the assignments of Boehm, assuming pure radiations, etc., lead to a net positive correlation. However, in his paper, Boehm claims that the 1122 kev transition is a mixture of M1 and E2 radiations. The 67.7 and 1222 kev transitions are taken to be pure E1 and E2 respectively. Using these multipolarities and the intensities quoted by Boehm, an attempt was made to fit the observed asymmetry at

180° to the theoretical form for the expected correlation. This was found to be impossible; the net correlation was essentially positive for all possible mixing ratios for the 1122 kev transition. If the correlation data given above are correct, then either the spin or multipole assignments of Boehm must be in error. Of course, since the multipolarities were determined from conversion data, the chance of an incorrect assignment is relatively large.

To draw an unambiguous result from the above discussion is not possible. Fowler's spin assignment is approximately consistent with the observed correlation, but any mixing of the radiations concerned would invalidate even this conclusion. The multipole assignments of Boehm appear to be inconsistent with the observed asymmetries, but due to the rather incomplete knowledge of the conversion coefficients for the gamma rays involved, further arguments on this point would indeed be superfluous. The predictions of the collective model for the high energy states can definitely be ruled out, however.

h) Directional Correlation in Platinum - 192

Ir^{192} decays by negatron emission to Pt^{192} and by K-capture to Os^{192}. The gamma rays following the decay have been investigated with beta-ray spectrometers by Cork et al. (78), Kyles (79), Sablo and Johns (80), Wolfson (81), and Bashilov (82). Accurate energy determinations have been carried out by Muller et al. (74) using a curved crystal spectrometer. A scintillation spectrometer has been used by Pringle et al. (83) for this work, with particular attention paid to those radiations whose energies were in excess of 700 kev. In this investigation, we shall be concerned with the gamma ray transitions in the Pt^{192} nucleus only. For the ordering of the levels in Os^{192}, reference (83) is cited.

The beta-ray spectrum of Ir^{192} is complex, consisting of some five components (79). The ordering of the levels of the Pt^{192} nucleus, however, seems reasonably well established in spite of this complexity. Fig. 31 shows the level scheme as given by Pringle et al. (83). The high energy crossover transitions were originally found by these authors. However, Sablo (80) has recently presented confirming evidence for their existence. In addition to this, he has presented evidence for a new level at 1160 kev, just 40 kev lower than the fifth excited state shown in Fig. 31. If this is correct, the photoelectron line at 1210 kev in the gamma ray spectrum found by Pringle should have been considerably broader than it was, and of course the energy would have been somewhat lower. The resolution was found to be about 5.5%, in good agreement with the expected value for this energy. The other features of the decay scheme seem well established, however, and no doubt further work will clarify the situation with regard to the 1201 kev level.

The gamma ray spectrum mentioned above is shown in Fig. 32. (Note the logarithmic ordinate axis.) The most prominent features of the spectrum are the grouping of three lines at 312 kev and the grouping of two more at 471 kev. The former is due to gamma rays with energies 296, 308 and 316 kev, the latter to radiations with energies 468 and 484 kev. It is known (79) that the 468 kev gamma ray is in coincidence with the 316 kev component of the main line but with neither of the other two. The several other lines in the spectrum did not enter into the coincidence work to be described here, and will not be discussed further. The reader is referred to the papers by Pringle (83) for details concerning these features.

In an effort to determine some of the spins of the levels in

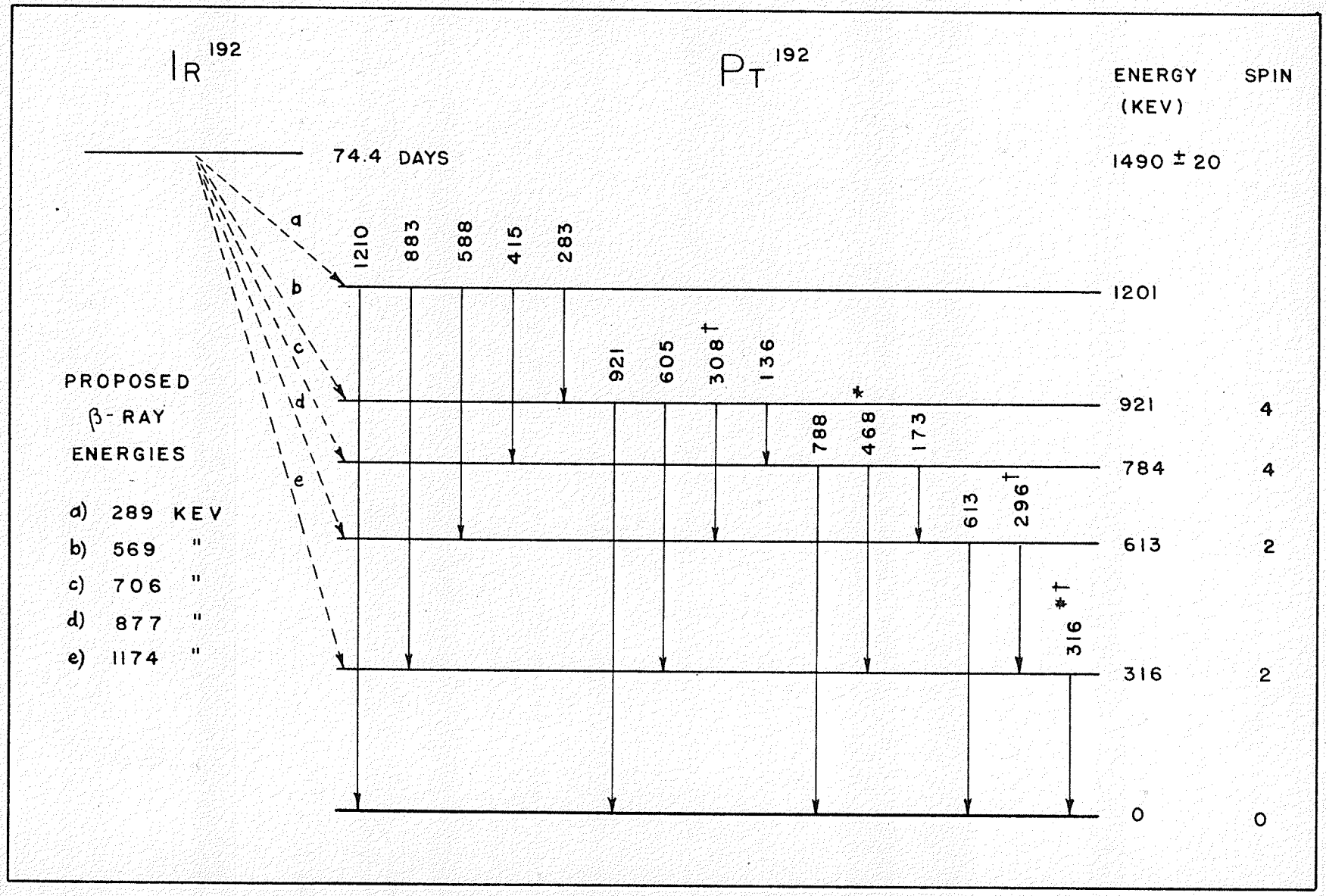

Fig. 31. Energy levels in Pt^{192}. The directional correlations of the transitions * and † have been studied.

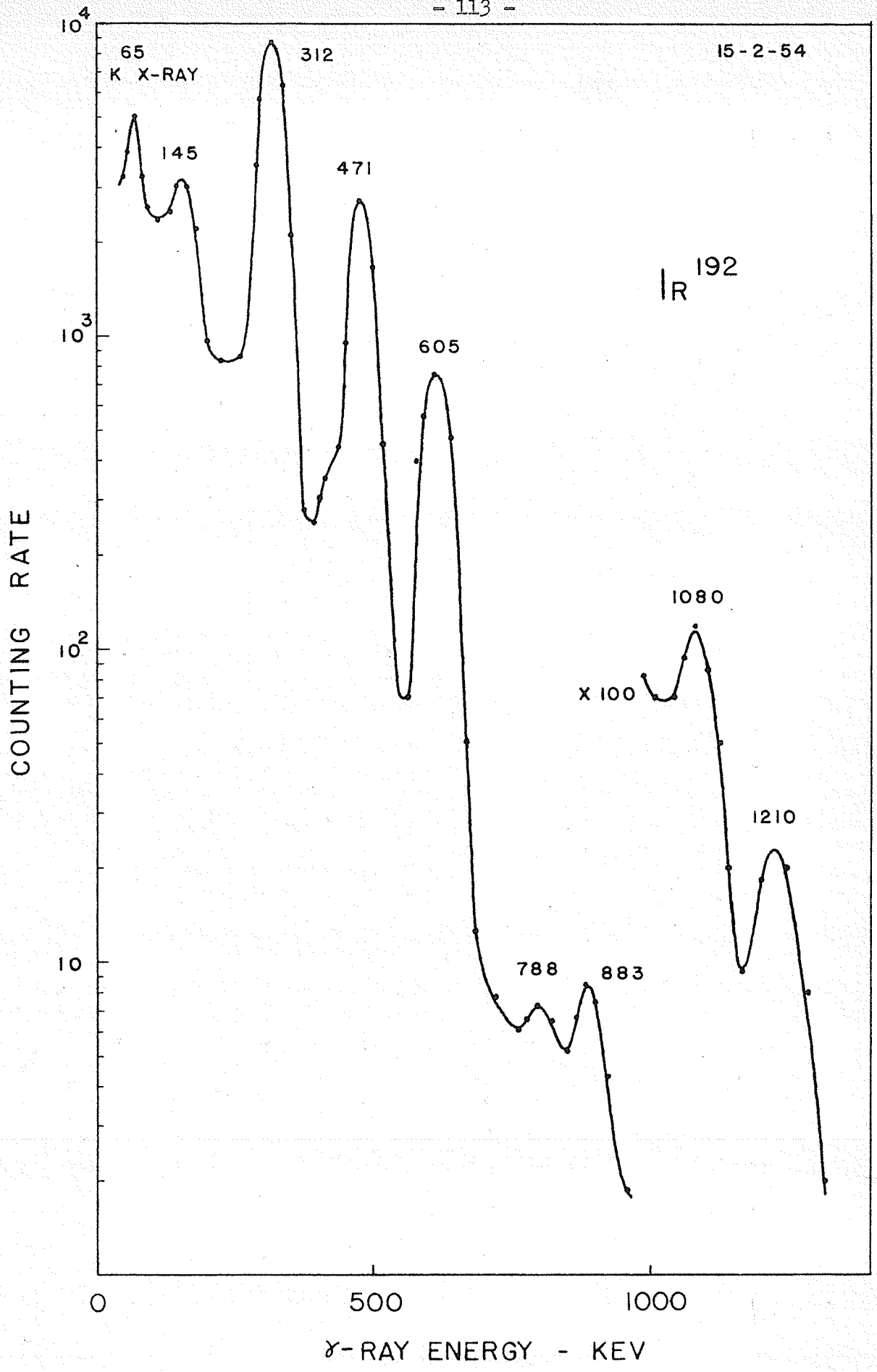

Fig. 32. Spectrum of gamma radiation following negatron emission and K-capture in Ir^{192}.

Pt^{192}, the decay scheme of Fig. 31 was examined for promising cascades. After several trial-and-error experiments with a number of cascades, it was decided that the coincidence rates were suitable for two cases only: 1) the 316 - 468 kev cascade, and 2) the triple cascade whose components form the photoelectron line at 312 kev.

An Ir^{192} source was obtained through the irradiation of iridium metal in the Chalk River pile. The isotope Ir^{191} has an abundance of 38.5% and permits the formation of Ir^{192} through the reaction $Ir^{191}(n, \gamma)$ Ir^{192}. The primary source had a strength of 1 mc. For the coincidence work, the source consisted of a few minute filings taken from the original pellet. These were sealed into a plastic cup with paraffin. The strength of this secondary source was estimated to be of the order of .01 mc. It was found that the arrangement possessed adequate symmetry to permit directional studies to be undertaken.

The data were collected using the technique described earlier; the usual lead shielding was used. For the 316 - 468 kev cascade, the net coincidence rate was about 16 counts per minute, of which 2 per minute were accidental. (The rates for the triple cascade will be discussed later.) The directional correlation function for this cascade is shown in Fig. 33. Once again, the full line represents the least squares fit to the experimental points assuming an expansion of the form $W(\theta) - 1 = A_2 P_2 (\cos \theta) + A_4 P_4 (\cos \theta)$. The dashed curve is the experimental result after corrections were applied for angular resolution. The correction factors J_{2k}/J_o for 312 kev gamma radiation were used for the softer component of the cascade (See Table I). For the 468 kev transition, the corrections were obtained by taking the square root of the Q_{2k}/Q_o for annihilation radiation. The net result was the following: $Q_2/Q_o = .906$ and $Q_4/Q_o = .730$. The accompanying

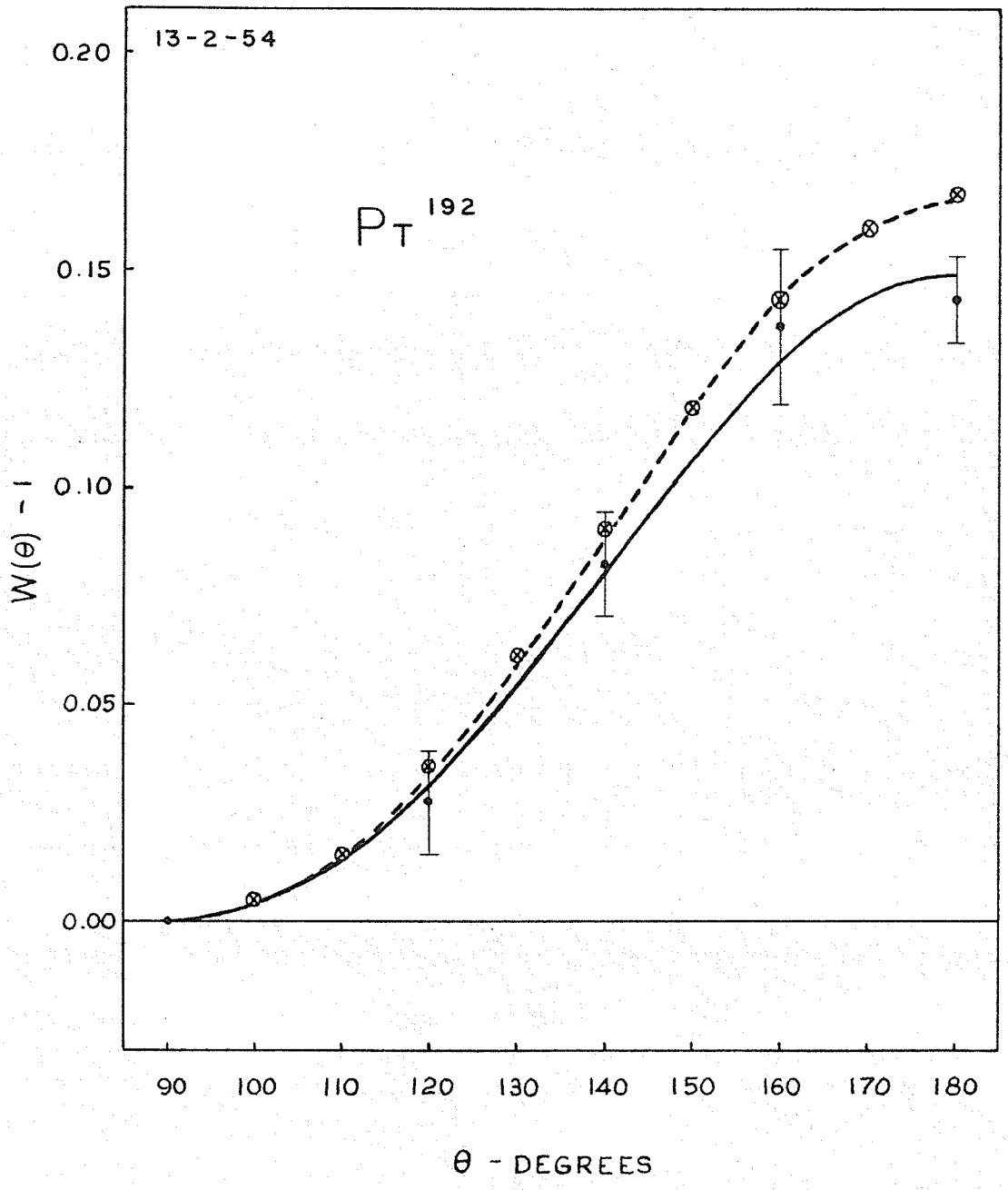

Fig. 33. Directional correlation between the 316 and 468 kev gamma rays following negatron emission in Ir^{192}. The dashed curve is a corrected least squares fit to the experimental points. The points ⊗ lie on the theoretical curve for a 4 - 2 - 0 spin assignment.

table contains the corrected and uncorrected coefficients obtained from the least squares analysis. The theoretical coefficients are those for the spin sequence $4 \rightarrow 2 \rightarrow 0$, with both radiations pure electric quadrupole.

	a_2	a_4	A_2	A_4	180° Asymmetry
uncorrected	.1086	.0398	.0912	.0087	
corrected	.1116	.0546	.1005 ± .038	.0119 ± .047	.166 ± .010
theory	.1250	.0416	.1020	.0091	.1667

The excellent agreement between theory and experiment, coupled with a knowledge of the rules for even-even nuclei, leaves no doubt as to the correctness of the above assignment in this case. This is borne out by the shape of the dashed curve of Fig. 33.

To the author's knowledge, the conversion coefficient for the 316 kev radiation has not been mentioned in the literature to date. The result, when obtained, would be expected to confirm the E2 assignment given above. It is interesting to note, also, that a spin of 4 for the 784 kev level is consistent, qualitatively, with the low intensity of the ground state transition from this level, as observed by Pringle et al. (83). Since the above experiment was parity insensitive, definite parity assignments are not possible. It is likely, however, from a consideration of the systematics of even-even nuclei, that the levels concerned have even parity.

As mentioned above, the strong triple gamma ray cascade in Ir^{192} contains gamma rays with energies 296, 308 and 316 kev. The energies have been measured accurately by Muller (74), but the relative intensities

are not so well established, as shown in the table below.

Energy	Muller (74)	Sablo (80)	Wolfson(81)
295.94 kev	39	35	50
308.45 kev	38	38	50
316.46 kev	100	100	100

The measurements of Sablo and Muller, which are the more recent, agree reasonably well. It is probable that they are close to the true values.

Since it was not possible to resolve the individual components of the main line, the gate of each spectrometer was set to accept the entire photoelectron line at 312 kev. With the same arrangement as described above, the genuine coincidence rate was found to be about 15 counts per minute, the accidental rate about .2 counts per minute. Fig. 34 a) - full curve - shows the least squares fit to the experimental points assuming the functional form $W(\theta) - 1 = A_2 P_2 (\cos \theta) + A_4 P_4 (\cos \theta)$. The dashed curve is the least squares fit corrected for the presence of coincidences from the 316 - 468 kev cascade. This correction was carried out as follows.

An examination of the decay scheme and the spectrum indicated that the observed coincidence rate was due to the triple and 316 - 468 kev cascades only. The theoretical shape of the pulse height distribution for a 510 kev gamma ray, as given by Maeder (31), was used to approximate that due to the 468 kev radiation. From this, an estimate was made of what percentage of the coincidences at 90° was due to the presence in the gates of part of the Compton distribution of the 468 kev gamma ray. The coincidence rate at

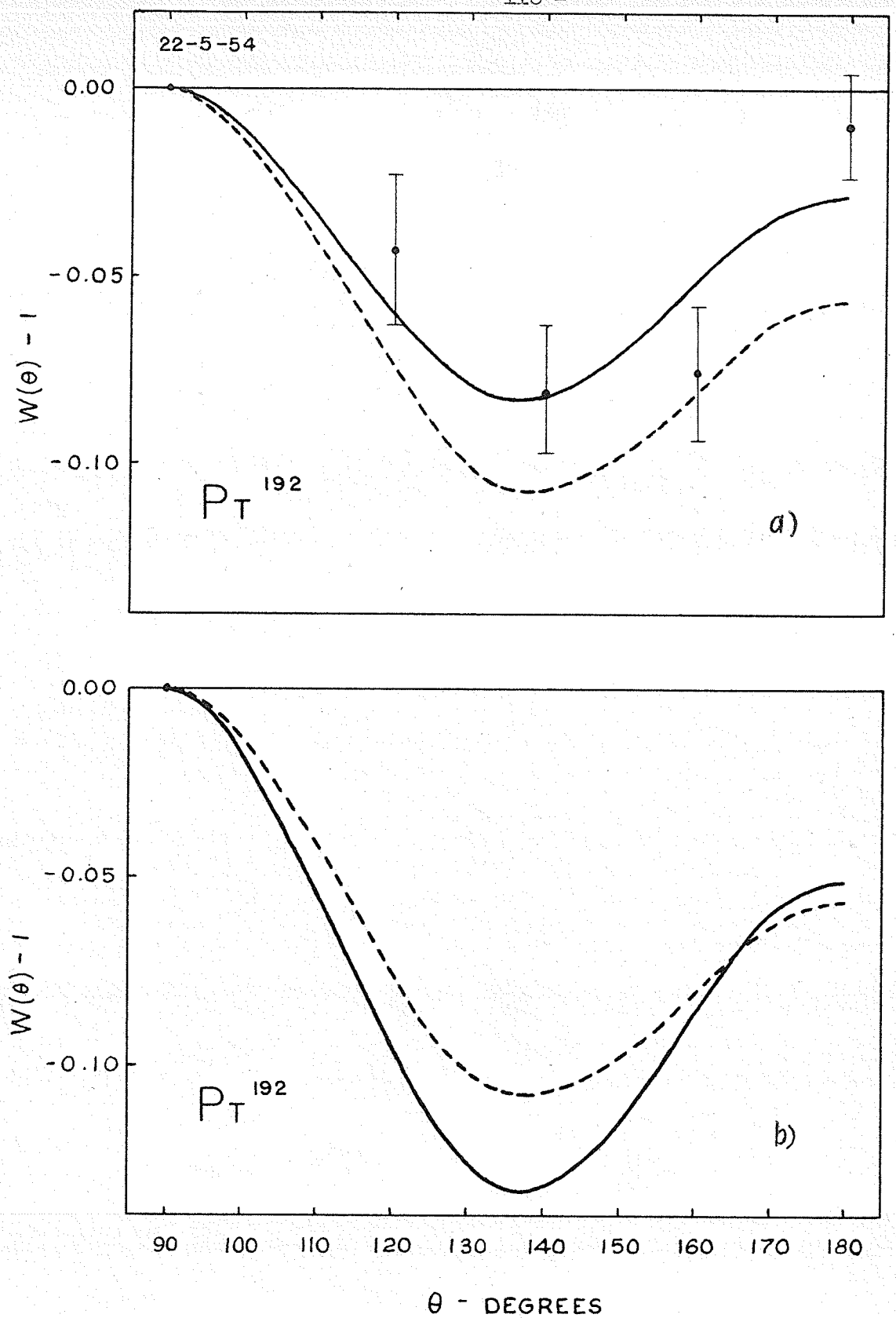

Fig. 34 a) Full curve - least squares fit to the experimental points assuming $W(\theta)-1 = A_2P_2(\cos\theta) + A_4P_4(\cos\theta)$. Dashed curve - least squares fit corrected for coincidences due to the 468-316 kev cascade.
b) Dashed curve - same as for a). Full curve - least squares fit after correcting for finite angular resolution.

90° was corrected by this amount; the rates at other angular positions were corrected using the observed angular correlation for the interfering cascade (Fig. 33, full line). The corrected result is the dashed curve of Fig. 34 a).

The correction factors for 312 kev radiation - $Q_2/Q_o = .887$, $Q_4/Q_o = ,693$ - were used to further correct the result. The curves of Fig. 34 b) show the changes involved. The full curve is, of course, the final result which must be explained theoretically.

The table given below contains the coefficients in the expansion $W(\theta) - 1 = A_2 P_2 (\cos \theta) + A_4 P_4 (\cos \theta)$ for the various curves of Figs. 34 a) and b).

	a_2	a_4	A_2	A_4	180° Asymmetry
uncorrected	-.299	+.270	-.0472	+.0647	-.029
corrected for 316-468 cascade	-.356	+.297	-.0713	+.0722	-.057
Further corrected for ang. res.	-.473	+.422	-.0803 $\pm$ .058	+.1040 $\pm$ .065	-.051 $\pm$ .014

In order to compare the observed correlation with a theoretical formula, it is necessary to calculate the function corresponding to a superposition of three double correlations - those due to the 308 - 296,

296 - 316 and 308 - 316 kev cascades. (The last cascade yields an example of the first-third correlation mentioned on P. 20.) The intensity measurements given by Sablo (80) were used in carrying out these calculations. His data permit one to calculate the appropriate weights, which determine the contribution of each cascade to the observed correlation function. The following figures are the relative intensities as quoted by this author for the radiations concerned:

296	kev	-ray	66.7
308	"	"	72.2
316	"	"	190.
613	"	"	7.8

The spins of the ground and first excited states were determined with some certainty by the preceding experiment. Since the 921 kev radiation was found to be exceedingly weak (83), it is reasonable to assume that the spin of the 921 kev level is either 3 or 4. Using j to denote the spin of the second excited state, we get the two general spin sequences $3 \rightarrow j \rightarrow 2 \rightarrow 0$ and $4 \rightarrow j \rightarrow 2 \rightarrow 0$. Using values of j from 1 to 4 inclusive gives eight possible spin assignments. None of these gives A_2 correlation function in good agreement with experiment when all the radiations are assumed to be pure. Hence, for the final comparison between theory and experiment, one of the three transitions was always taken to be a multipole mixture. The choice of which gamma ray was to be mixed was determined solely by the

the spin assignment and the empirical results which have appeared in the literature. For example, in the case $3 \rightarrow 1 \rightarrow 2 \rightarrow 0$, the $1 \rightarrow 2$ transition was assumed to be a dipole-quadrupole mixture, while for the sequence $4 \rightarrow 4 \rightarrow 1 \rightarrow 0$, the $4 \rightarrow 4$ transition was taken as mixed. Of course, some of the possibilities could be rejected on the basis of intensity considerations, but as a final check, formal calculations were carried out for all sequences.

Of the eight correlation functions obtained, one (that for the sequence $3 \rightarrow 2 \rightarrow 2 \rightarrow 0$) contained terms up to P_2 only. Of the remainder, all but one had A_4 coefficients that gave imaginary values for δ. The only spin sequence which gave a result in reasonable agreement with experiment was 4(Q) 2 (D, Q) 2 (Q) 0. For this case, the following correlation functions were found:

308 - 296 kev radiations:

$$W(\theta) = 1 + \left\{\frac{-.0218\,\delta^2 + .2088\,\delta + .0714}{1 + \delta^2}\right\} P_2 + \left\{\frac{.0026\,\delta^2}{1 + \delta^2}\right\} P_4$$

296 - 316 kev radiations:

$$W(\theta) = 1 + \left\{\frac{-.0766\,\delta^2 + .7320\,\delta + .2500}{1 + \delta^2}\right\} P_2 + \left\{\frac{.3266\,\delta^2}{1 + \delta^2}\right\} P_4$$

308 - 316 kev radiations:

$$W(\theta) = 1 + \left\{\frac{-.0219\,\delta^2 + .0510}{1 + \delta^2}\right\} P_2 + \left\{\frac{.0026\,\delta^2 - .0060}{1 + \delta^2}\right\} P_4$$

The function corresponding to a superposition of these equations, weighted according to the known intensities of the gamma rays involved, was found to be:

$$W(\theta) = 1 + \left\{\frac{-.0405\ \delta^2 + .3180\ \delta + .1254}{1 + \delta^2}\right\} P_2 + \left\{\frac{.1129\ \delta^2 - .0020}{1 + \delta^2}\right\} P_4$$

where δ^2 = $\frac{\text{intensity of E2 radiation in intermediate transition}}{\text{intensity of M1 radiation in same transition}}$

The coefficients A_2 and A_4 of the above equation have been plotted as functions of δ, as shown in Fig. 35. It should be noted that since both $A_2(\delta)$ and $A_4(\delta)$ are slowly varying functions of δ for $\delta < -1$, the determination of the most satisfactory value of δ can be accomplished only by trial and error. Using this technique, it was found that the best fit to the experimental data could be obtained with $\delta = -6.2$. For this value, $A_2 = -.0863$ ($\sim 7.5\%$ lower than the measured value), and $A_4 = +.1100$ ($\sim$ 5.4% higher than the measured value). Since δ is negative, the two radiations have a relative phase of 180°. The calculated correlation function (dashed curve) for this value of δ, together with the experimental one (full curve) are shown in Fig. 36. The agreement between the two is most satisfactory in view of the possible error in the estimation of the contribution of the 468 - 316 kev cascade to the coincidence rate.

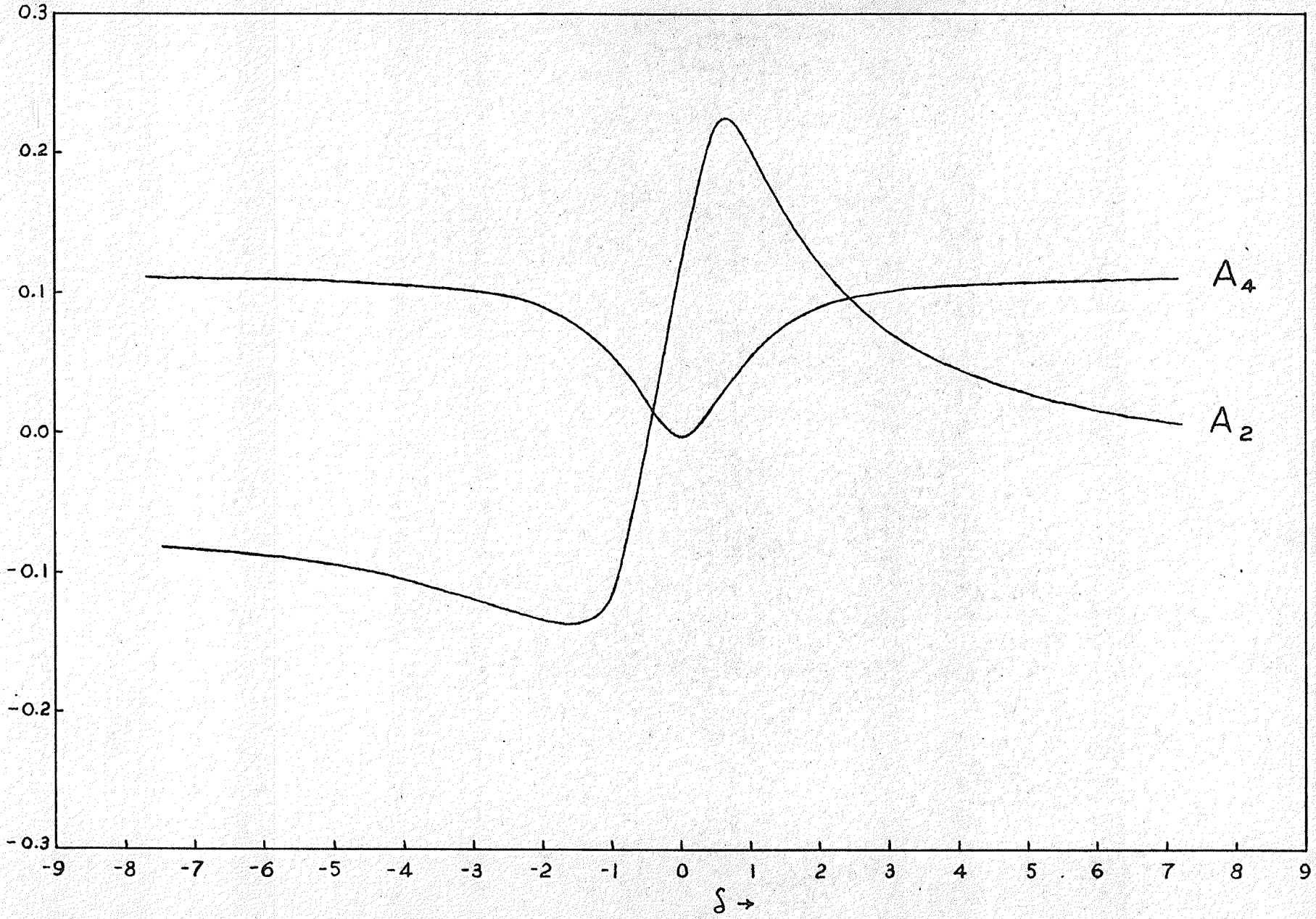

Fig. 35. A_2 and A_4 as functions of δ for the triple correlation function.

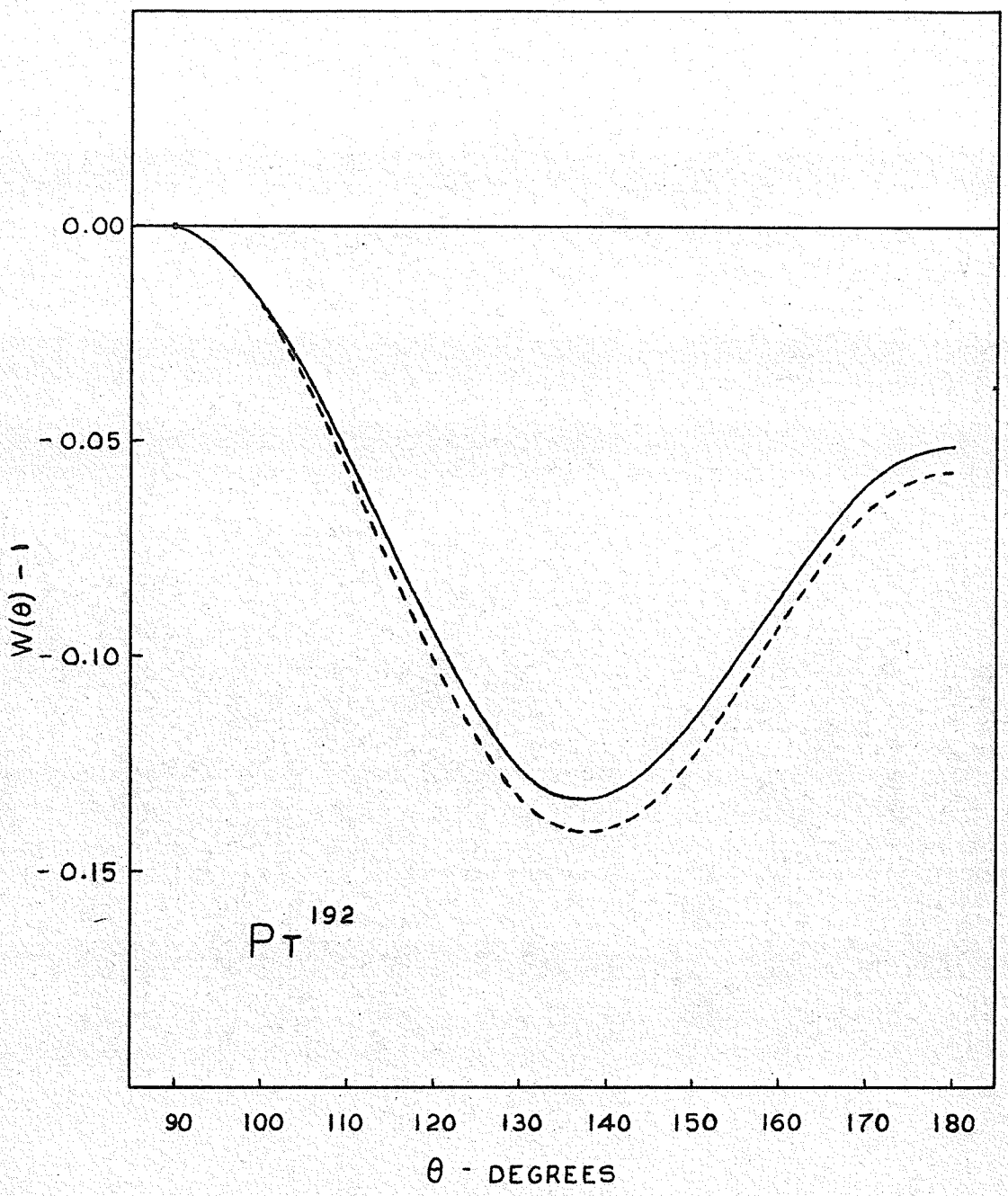

Fig. 36. Full curve - experimental triple correlation function.

Dashed curve - theoretical triple correlation function for the assignment
4(E2) 2 (2.5% M1, 97.5% E2) 2 (E2) 0.

The value of δ used above corresponds to an E2 intensity of 97.5% for the intermediate transition. That this transition is mixed and not pure quadrupole is obvious from the fact that as $\delta \to \infty$ (E2 intensity of 100%) $A_2 \longrightarrow -.0405$ and $A_4 \longrightarrow .1129$. The first coefficient then differs from the experimental value by a factor of 2 and hence this case is inadmissible.

Several large E2 admixtures have been observed by other workers (84, 85). Schiff (85) has pointed this out for the following isotopes which contain a $2 \to 2 \to 0$ spin sequence - Hg^{198}(60% E2), Te^{122} (80% E2), Pt^{196} (95% E2). To these may now be added the case of Pt^{192} with 97.5% E2. Unfortunately, the number of known cases for which the E2 admixture is large in a $2 \to 2$ transition is small, so that no conclusions can be drawn regarding possible regularities with Z, A, etc. When this situation has been remedied, however, nuclear shell structure might be able to supply an explanation.

By way of review, the following remarks are made. The $4 \to 2 \to 0$ spin sequence has been established for the 784, 316 and 0 kev levels. The radiations seem to be pure electric quadrupole in character. The strong triple cascade has been shown to possess a directional correlation consistent with the net spin assignment 4(E2) 2 (2.5% M1, 97.5% E2) 2 (E2) 0 for the levels at 921, 613, 316 and 0 kev. (The spins are shown in the decay scheme - Fig. 31.) The spins in this case were established by 1) the results of the first correlation experiment, and 2) the elimination of all

alternative assignments. Of course, it is not unlikely that the observed correlation could be explained by a different spin assignment for the 921 and 613 kev levels if both the first and second transitions in the triple cascade were assumed to be mixed. In view of the excellent agreement obtained here, however, this possibility was not investigated by the author. The conclusions which have been reached appear to be consistent with all the experimental facts, and they contain the minimum number of assumptions. The fact that Kyles (79) has also suggested this assignment on the basis of intensity and conversion measurements gives additional support to the conclusions.

In connection with the spin of the fifth excited state, coincidences between the 588 and 613 kev gamma rays were sought in the hope that the directional correlation between these two radiations might be studied. It was found that due to the high accidental rate, changes in the genuine rate with θ (the angle between the counters) were completely masked. The strong components of the 605 kev line - at 613 and 615 kev - (see Figs. 31 and 32) gave this high accidental coincidence rate which swamped any genuine coincidences between the 588 and 613 kev components. Kyles (79) has suggested a spin of 6 for the 1201 kev level on the basis of intensity measurements. This seems difficult to reconcile with the observed intensity of the ground state transition from this level (see Fig. 32 and ref. 83). Confirmation or rejection of this assignment might be possible by means of a directional correlation experiment if the background

could be substantially reduced through the use of a very much shorter coincidence resolving time. Unfortunately, the use of the commercial coincidence unit mentioned earlier would not permit this modification in the present spectrometer.

CHAPTER IV

SUMMARY AND CONCLUSIONS.

The coincidence spectrometer described in the early sections of this thesis has proven to be satisfactory for directional correlation studies, although some improvement in stability could be realized. Drifting in the present spectrometer made it necessary to use a laborious but nevertheless reliable technique for collecting experimental data. The high energy selectivity obtained through the use of lead absorbers and differential discriminators permitted the isolation of single cascades in complex decay schemes.

Through the use of time resolution experiments and ordinary coincidence techniques, the decay scheme of Zn^{65} has been clarified. No evidence for an additional positron component or second gamma ray cascade was found. Delayed coincidence measurements indicated that asymmetrical time resolution curves can result from intrinsic time delays in the equipment itself.

The angular resolution corrections discussed in Chapter I were determined for several gamma ray energies. It was found that a pronounced change in the shape of the resolution curve occurred as the energy of the radiation was increased. The correction factors for 312, 662, 1114, 1332 and 1690 kev gamma rays were tabulated. The correction factors found through the use of annihilation radiation were evaluated also, and their use for radiations whose energies are very different from 500 kev was discussed.

The well-known directional correlation in Ni^{60} has been

investigated with the spectrometer. The observed correlation was found to be in good agreement with the spin assignment 4(E2) 2 (E2) 0. The use of the Ni^{60} cascade as a laboratory 'standard' for the testing of directional correlation apparatus was discussed in the light of recent experiments with the cascade.

The directional correlation of the principal cascade in As^{75} has been investigated on the assumption that an interfering cascade is weak. It was found that the observed correlation could be explained by the spin assignment 5/2 (99.12% M1; .88% E2) 7/2 (E2) 3/2. Of course, this does not preclude a pure dipole-quadrupole assignment if the additional cascade mentioned above contributes a significant number of coincidences to the observed coincidence rate. A discussion of the possible asymmetries assuming a composite correlation was given, but no definite conclusions could be drawn. Until more accurate intensity measurements are forthcoming, a final decision on the spins is not possible.

A thorough study of the gamma ray spectrum of Sb^{124} was carried out using a single channel spectrometer. Two new gamma rays were found and the energies of the principal features of the spectrum measured. The ordering of the levels at 600, 2290, and 2690 kev was checked by means of a coincidence experiment. In this case, the spectrometer permitted the resolution of the details of the coincidence spectrum. This was followed by a study of the directional correlation of the 1690 - 600 kev cascade, which was found to be in agreement with the spin sequence 3 (D) 2 (Q) 0. The $3 \rightarrow 2$ (1690 kev) transition is certain ly pure dipole radiation. A discussion of the parity assignment for the 2290 kev level was given. The author has suggested that a polarization-direction experiment would resolve the ambiguity in the parity of this state.

The theoretical implications of such a measurement make it of considerable interest to the experimentalist and theorist alike. It could lead to an increase in our knowledge of the 'scattering' of log ft values for allowed transitions.

A rather difficult problem in W^{182} was encountered. Since the level scheme of W^{182} is one of the most complex known, it was not possible to isolate a single cascade for correlation studies. However, a superposition of two intense cascades was examined and the results compared with two spin assignments which have appeared in the literature. Although the results favored one of these over the other, definite conclusions were not possible. A discussion was given of possible spin assignments and the asymmetries to be expected for them. If the spectrometer had been stable enough to permit the use of narrow gates on the discriminators, it would not have been difficult to isolate a single cascade and study its correlation. It is anticipated that further improvements in stability will permit these studies to be undertaken in the future.

In the case of Pt^{192}, it was possible to assign to five out of six levels, spins which are in agreement with all the known experimental evidence. This was accomplished using 1) the systematics for even-even nuclei, 2) intensity considerations, and 3) directional correlation measurements. A large E2 admixture in a $2 \rightarrow 2$ transition similar to several others which have been reported in the literature was found. The agreement between the experimental results and the calculated form of the correlation for the intense triple cascade indicates that the study of triple cascades can yield important data. The spin assignment for the first four excited states of Pt^{192} is in fair agreement with the results of conversion measurements reported privately by an Edinburgh group.

With regard to the correlation technique as a whole, the following comments are made. A perusal of the literature on correlation experiments indicates that most of the simple problems have been studied, and in many cases, solved. In future, experimentalists using this technique will have to focus their attention on the more complex decay schemes. From the present work, the author has drawn 2 major conclusions regarding such investigations: 1) It is possible to get valuable information from a study of two cascades simultaneously provided that the gamma ray intensities are known with some certainty; 2) The study of triple-component cascades can lead to spin and multipolarity assignments provided that there is some supplementary evidence to guide the experimentalist in his choice of spins.

There is little doubt that the study of angular correlations has already become one of the standard techniques of the nuclear physics laboratory. It is with keen anticipation that we should look forward to the innovations in this technique which will probably appear within the next few years.

ACKNOWLEDGMENTS

The author wishes to express his thanks to Dr. R. W. Pringle for his encouragement and interest in this project from the date of its inception. The award of a Studentship (1952-53) and a Fellowship (1953-54) by the National Research Council of Canada is gratefully acknowledged. Finally, the author would like to thank his wife for her patience in the proofreading and the typing of the manuscript.

REFERENCES

(1) Hamilton , Phys. Rev. 58, 122 (1940).

(2)Dunworth, Rev. Sci. Inst. 11, 167 (1940).

(3) Goertzel, Phys. Rev. 70, 897 (1946).

(4) Kikuchi, Watase and Itoh, Zeit. fur Physik 119, 185 (1942).
Beringer, Phys. Rev. 63, 23 (1943).

(5) Brady and Deutsch, Phys. Rev. 72, 870 (1947); 74, 1541 (1948).

(6) Brady and Deutsch, Phys. Rev. 78, 558 (1950).

(7) Biedenharn and Rose, Rev. Mod. Phys. 25, 729 (1953).

(8) Klema and McGowan, Phys. Rev. 91, 616 (1953).

(9) Blatt and Weisskopf "Theoretical Nuclear Physics" P. 583, John Wiley and Sons.

(10) Lipmann, Phys. Rev. 81, 162 (1951).

(11) Condon and Shortley "Theory of Atomic Spectra", Cambridge Press.

(12) Biedenharn, Blatt and Rose, Rev. Mod. Phys. 24, 249 (1952).
Biedenharn, Oak Ridge National Laboratory Report No. 1098.

(13) Sharp, Kennedy, Sears and Hoyle, "Tables of Coefficients for Angular Distribution Analysis", AECL Report No. 97, Dec. 1953.

Kennedy, Sears and Sharp "Tables of X Coefficients" AECL No. 106, May, 1954.

(14) Lloyd, Phys. Rev. 83, 716 (1951); this paper contains references to other papers by the same author.

(15) See for example Lapp and Andrews "Nuclear Radiation Physics", Prentice-Hall Co.

(16) Jarrett "Statistical Methods used in the Measurement of Radioactivity", AECU - 262.

(17) Chatterjee and Saha, Phys. Rev. 91, 200 (1953).
Zeit. fur Physik, 135, 141 (1953).

(18) Church and Kraushaar, Phys. Rev. 88, 419 (1952).

(19) Lawson and Frauenfelder, Phys. Rev. 91, 649 (1953).

(20) Rose, Phys. Rev. 91, 610 (1953).

(21) Breitenberger, Proc. Phys. Soc. (London) A66, 846 (1953).

(22) Sokolnikoff "Higher Mathematics for Engineers and Physicists" P. 536, McGraw-Hill Co.

(23) Van Name, Phys. Rev. 75, 100 (1949).

(24) Binder, Phys. Rev. 76, 856 (1949).

(25) Bay, Phys. Rev. 77, 419 (1950).

(26) Newton, Phys. Rev. 78, 490 (1950).

(27) e.g. Graham and Bell, Can. Jour. of Physics 31, 377 (1953).

(28) Roulston, Ph.D. Thesis, University of Manitoba, 1952.

(29) McGowan, Phys. Rev. 93, 163 (1954).

(30) Klema and McGowan, Phys. Rev. 92, 1469 (1953).

(31) Maeder, Muller and Wintersteiger, Helv. Physica Acta 27, 3 (1954).

(32) F. K. McGowan - Private communication.

(33) W. E. Kreger - Private communication.

(34) Roulston, Nucleonics 7, 27 (1950).

(35) Birks "Scintillation Counters", McGraw-Hill Co. Ltd.
Curran "Luminescence and the Scintillation Counter", Academic Press.

(36) Pringle, Taylor and Roulston, Phys. Rev. 87, 1016 (1952).

(37) Cohn and Kurbatov, Phys. Rev. 78, 318 A (1950).

(38) Bouchez, Physica 18, 1171 (1952).

(39) Mann, Rankin and Daykin, Phys. Rev. 76, 1719 (1949).

(40) Yuasa, Compt. Rend. 235, 366 (1952).
Physica 18, 1267 (1952).

(41) Sakai and Hubert, C. R. Acad. Sci. (Paris) 236, 1249 (1953).

(42) Perrin, J. Phys. Radium 14, 273 (1953).

(43) Perkins and Haynes, Phys. Rev. 92, 687 (1953).

(44) M. Sakai, Ohio State University - Private communication.

(45) Frauenfelder "Annual Review of Nuclear Science" Vol. II (1953).

(46) Aeppli, Frauenfelder, Heer and Riietschi, Phys. Rev. 87, 379 (1952).

(47) Keister and Schmidt, Phys. Rev. 93, 140 (1954).

(48) Lind, Brown and DuMond, Phys. Rev. 76, 1838 (1949).

(49) Chang-Yun Fan, Phys. Rev. 87, 252 (1952).

(50) Scharff-Goldhaber, Phys. Rev. 90, 587 (1953).

(51) Jensen, Laslett, Martin, Hughes and Pratt, Phys. Rev. 90, 557 (1953).

(52) Schardt and Welkor, Phys. Rev. 93, 916 A (1954).

(53) Wigner "The j-j Coupling Shell Model for Nuclei" - Notes privately circulated.

(54) A. W. Schardt - Private communication.

(55) Goldhaber and Sunyar, Phys. Rev. 83, 906 (1951).

(56) Langer, Lazar and Moffatt, Phys. Rev. 91, 338 (1953).

(57) E. P. Tomlinson, Indiana Conference on Nuclear Spectroscopy and the Shell Model; Technical Report (1953).

(58) Langer and Starner, Phys. Rev. 93, 253 (1954).

(59) Johansson and Almquist, Arkiv Fur Fysik 5, 427 (1952).

(60) Lazar, Phys. Rev. 95, 292 (1954).

(61) Cook and Langer, Phys. Rev. 73, 1149 (1948).

(62) Metzger, Phys. Rev. 86, 435 (1952).

(63) Rose, Goertzel, Spinard, Harr and Strong, Phys. Rev. 83, 79 (1951).

(64) Stevenson and Deutsch, Phys. Rev. 83, 1202 (1951).

(65) Darby, Can. Jour. of Physics 29, 569 (1951); Phys. Rev. 83, 676 (1951).

(66) Kloepper, Lennox and Wiedenbeck, Phys. Rev. 88, 695 (1952).

(67) Kraushaar and Goldhaber, Phys. Rev. 89, 1081 (1953).

(68) Metzger, Phys. Rev. 90, 328 (1953) and private communication.

(69) Hutchinson and Wiedenbeck, Phys. Rev. 88, 699 (1952).

(70) Morita and Yamada, Prog. Theor. Physics 10, 111; 10, 641 (1953).

(71) Cork, Keller, Rutledge and Stoddard, Phys. Rev. 78, 95 (1950).

(72) Cork, Childs, Branyan, Rutledge and Stoddard, Phys. Rev. 81, 642 (1951).

(73) Pearce and Mann, Can. Jour. of Physics 31, 592 (1953).

(74) Muller, Hoyt, Klein and DuMond, Phys. Rev. 88, 775 (1952).

(75) Boehm, Marmier and DuMond, Phys. Rev. 95, 864 (1954).

(76) Mihelich, Phys. Rev. 95, 626 A (1954).

(77) Fowler, Kruse, Keshishian, Klotz and Mellor, Phys. Rev. 94, 1082 (1954).

(78) Cork, LeBlanc, Stoddard, Childs, Branyan and Martin, Phys. Rev. 82, 258 (1951).

(79) Kyles, Edinburgh University - Private communication.

(80) Sablo and Johns - Presented at C. A. P. meeting, May, 1954.

(81) Wolfson, Proc. Royal Soc. Canada 44, 193 A (1950).

(82) Bashilov, Anton'eva and Dzhelepov, Izvest. Akad. Nauk. Ser. Fiz. S.S.S.R. 16, 264 (1952).

(83) Pringle, Turchinetz and Taylor, Phys. Rev. 95, 115 (1954). also Pringle and Roulston, Phys. Rev. 87, 930 (1952).

(84) Schrader, Phys. Rev. 92, 928 (1953).

(85) Schiff and Metzger, Phys. Rev. 90, 849 (1953).